To the Graduate Council:

I am submitting herewith a thesis written by George N. Georgiades entitled "Spectroscopic Studies of the Effects of Bee Venom Melittin on Model Phospholipid Membranes." I have examined the final copy of this thesis for form and content and recommend that it be accepted in partial fulfillment of the requirements for the degree of Master of Science, with a major in Physics.

Solon Georghiou, Major Professor

We have read this thesis
and recommend its acceptance:

Accepted for the Council

Vice Chancellor
Graduate Studies and Research

SPECTROSCOPIC STUDIES OF THE EFFECTS OF BEE VENOM MELITTIN ON MODEL PHOSPHOLIPID MEMBRANES

A Thesis

Presented for the

Master of Science

Degree

The University of Tennessee, Knoxville

George N. Georgiades

August 1982

3063076

Στή σύζυγο μου Ρίτα
καί τά παιδιά μου
Ξένια καί Νεοκλή.

To my wife Rita
and my children
Xenia and Neoklis.

ACKNOWLEDGEMENTS

I express my graditude to my major professor Dr. S. Georghiou. His efforts made my graduate studies possible in the first place. Later, in every step of my work, the invaluable assistance of both the dedicated scientist and the good friend was always there, encouraging and advising.

I am very grateful to Dr. Ajay Mukhopadhyay for his help in many aspects of this work, especially with the preparation of the liposomes in the first steps of this study.

I, also, want to extend my sincere thanks to Dr. Jorge Churchich and Dr. Leaf Huang of the Department of Biochemistry for making their laboratory facilities available.

ABSTRACT

The enhancement of the 0-0 vibronic transition in the fluorescence spectrum of pyrene, which is a measure of the polarity of the microenvironment of the probe, and the formation of intramolecular excimers by 1, 3-bis (1-pyrene) propane, (PC_3P), have been employed for investigating the effects of bee venom melittin on distearoylphosphatidylcholine, (DSPC), bilayer liposomes. For melittin-to-lipid molar ratios > 1:165 melittin has been found to induce a pronounced increase in the enhancement in the vicinity of the phase transition temperature, T_t, of the phospholipid; this implies that the protein causes structural rearrangements in the bilayer that result in an increase in its packing density with a concomitant dislocation of the probe toward the direction of the polar head groups. Alternatively, on the basis of the concept of lipid cluster formation, the protein reduces the probability of formation of such clusters; the resulting reduction in the number of mismatches between gel and liquid domains impedes the penetration of the probe into the bilayer. Apparent activation energies of the order of RT have been obtained from the enhancement profiles. The observed increase in the T_t in the presence of the protein is in line with these interpretations.

Nanosecond time-resolved measurements have shown that the long-wavelength emission by PC_3P, that peaks at ~ 480 nm, is an excited-state process with very little contribution from ground-state complex formation.

Plots of log (q_e/q_m) against 1/T, where q_e and q_m are fluorescence quantum yields of excimer and monomer, respectively, have been found to be linear in the two phases of the phospholipid but to exhibit a break in the adjoining region. Such plots allowed the determination of the energies of activation, of the differences in the free energies of activation and of the entropies of activation for excimer formation in the two phases. The PC_3P molecules are in a less favorable conformation for excimer formation in the crystalline phase than in the liquid-crystalline phase. The protein is found not to affect significantly the excimer-forming ability of the probe below T_t but to impede it above it. In the fluid state melittin is found to increase the entropy of activation relative to that in the crystalline phase. This implies an induced disorganization of the conformations of the two pyrene moieties of PC_3P and, by extension, of the lipid structure. Furthermore, the protein causes a decrease in the free energy of activation in that phase relative to that in the crystalline phase, which implies enhancement of the fluidity of the bilayer.

The results of both studies show that melittin exerts its most pronounced effect when liquid domains of the lipid are present by altering both the fluidity and the organization of the lipid.

TABLE OF CONTENTS

CHAPTER		PAGE
I.	INTRODUCTION	1
	I.1. Enhancement of the o-o vibronic transition of pyrene	4
	I.2. Intramolecular excimer formation by PC_3P	8
II.	MATERIALS AND METHODS	12
III.	RESULTS	23
IV.	DISCUSSION	56
	IV.1. Enhancement of the o-o vibronic transition of pyrene embedded in DSPC liposomes	56
	IV.2. Intramolecular excimer formation by PC_3P	77
V.	CONCLUSION	85
LIST OF REFERENCES		87
VITA		91

LIST OF TABLES

TABLE PAGE

1. Transition temperatures T_t of DSPC bilayer liposomes for different melittin-to-lipid molar ratios determined from plots of the enhancement ratio R as a function of temperature 32

2. Width ΔT of the transition of DSPC liposomes for different melittin-to-lipid molar ratios determined from plots of the enhancement ratio R as a function of temperature 33

3. Activation energies for intramolecular excimer formation by PC_3P in DSPC bilayer liposomes for different melittin-to-lipid molar ratios in the crystalline phase, E_{cr}, and in the liquid-crystalline (fluid) phase E_{fl} 43

4. Discontinuies Δ_f, differences of free energies of activation $\Delta G^{\ddagger}_{cr} - \Delta G^{\ddagger}_{fl}$, differences of activation entropies $\Delta S^{\ddagger}_{cr} - \Delta S^{\ddagger}_{fl}$, transition temperatures T_t, temperatures of onset of liquid-crystalline phase T_f, and width of transition $T_f - T_{cr}$ (where T_{cr} is the temperature of the onset of transition) for intramolecular excimer formation by PC_3P embedded in DSPC liposomes in the presence of different melittin-to-lipid molar ratios 46

5. Apparent activation energies obtained from the log R against 1/T plots 75

LIST OF FIGURES

FIGURE		PAGE
1.	Block diagram of the spectrofluorometer	16
2.	Fluorescence spectrum of PC_3P embedded in DSPC liposomes at 1°C being representative of the monomer spectrum . . .	19
3.	Fluoresence spectrum of PC_3P embedded in DSPC liposomes at 45°C	20
4.	Fluoresence spectrum of PC_3P embedded in DSPC liposomes at 45°C in the presence of a melittin-to-lipid molar ratio of 1:100	21
5.	Enhancement of the o-o vibronic transition of pyrene embedded in DSPC liposomes as a function of temperature .	24
6.	Enhancement of the o-o vibronic transition of pyrene embedded in DSPC liposomes as a function of temperature. (1) In the absence of melittin; (2) in the presence of 1:5 mellitin-to-lipid molar ratio; and (3) in the presence of 1:10 melittin-to-lipid molar ratio	25
7.	Enhancement of the o-o vibronic transition of pyrene embedded in DSPC liposomes as a function of temperature. (1) In the absence of melittin; (2) in the presence of melittin with 1:20 melittin-to-lipid molar ratio; and (3) in the presence of 1:40 melittin-to-lipid molar ratio	26
8.	Enhancement of the o-o vibronic transition of pyrene embedded in DSPC liposomes as a function of temperature. (1) In the absence of melittin; (2) in the presence of 1:80 molar ratio; and (3) in the presence of 1:100 melittin-to-lipid molar ratio	27
9.	Enhancement of the o-o vibronic transition of pyrene embedded in DSPC liposomes as a function of temperature. (1) In the absence of melittin; (2) in the presence of 1:120 molar ratio; and (3) in the presence of 1:165 melittin-to-lipid molar ratio	28
10.	Enhancement of the o-o vibronic transition of pyrene embedded in DSPC liposomes as a function of temperature. (1) In the absence of melittin; (2) in the presence of 1:200 molar ratio; and (3) in the presence of 1:300 melittin-to-lipid molar ratio	29

FIGURE PAGE

11. Enhancement of the o-o vibronic transition of pyrene embedded in DSPC liposomes as a function of temperature. (1) In the absence of melittin; and (2) in the presence of 1:500 melittin-to-lipid molar ratio 30

12. Fluoresence spectra of PC_3P embedded in DSPC liposomes . 35

13. Fluoresence spectra of PC_3P embedded in DSPC bilayer liposomes for a melittin-to-lipid molar ratio of 1:40 . . 36

14. Logarithm of the ratio of the fluorescence quantum yield of the excimer to that of the monomer for PC_3P embedded in DSPC liposomes as a function of 1/temperature 37

15. Logarithm of the ratio of the fluorescence quantum yield of the excimer to that of the monomer for PC_3P embedded in DSPC liposomes as a function of 1/temperature in the presence of 1:500 melittin-to-lipid molar ratio 38

16. Logarithm of the ratio of the fluorescence quantum yield of the excimer to that of the monomer for PC_3P embedded in DSPC liposomes as a function of 1/temperature in the presence of 1:300 melittin-to-lipid molar ratio 39

17. Logarithm of the ratio of the fluorescence quantum yield of the excimer to that of the monomer for PC_3P embedded in DSPC liposomes as a function of 1/temperature in the presence of 1:100 mellitin-to-lipid molar ratio 40

18. Logarithm of the ratio of the fluorescence quantum yield of the excimer to that of the monomer for PC_3P embedded in DSPC liposomes as a function of 1/temperature in the presence of 1:10 melittin-to-lipid molar ratio 41

19. Time-resolved spectra of PC_3P embedded in DSPC liposomes at 45°C, for the following times relative to the peak of the exciting light pulse. (1) 0 ns; (2) 10.4 ns; (3) 30.4 ns; (4) 39.1 ns; (5) 47.8 ns; (6) 69.6 ns; and (7) 87 ns. 47

20. Time-resolved fluorescence spectra of PC_3P embedded in DSPC liposomes in the presence of melittin at a melittin-to-lipid molar ratio of 1:500 at 45°C for the following times 48

21. Time-resolved fluorescence spectra of PC_3P embedded in DSPC liposomes in the presence of melittin at a melittin-to-lipid molar ratio of 1:100 at 45°C for the following times 49

FIGURE PAGE

22. Time-resolved fluorescence spectra of PC_3P embedded in DSPC liposomes in the presence of melittin at a melittin-to-lipid molar ratio of 1:40 at 45°C for the following times 50

23. Time-resolved fluorescence spectra of PC_3P embedded in DSPC liposomes at 67°C, for the following times relative to the peak of the exciting light pulse 52

24. Time-resolved fluorescence spectra of PC_3P embedded in DSPC liposomes in the presence of melittin at a melittin-to-lipid molar ratio of 1:500 at 67°C for the following times 53

25. Time-resolved fluorescence spectra of PC_3P embedded in DSPC liposomes in the presence of melittin at a melittin-to-lipid molar ratio of 1:100 at 67°C for the following times 54

26. Time-resolved fluorescence spectra of PC_3P embedded in DSPC liposomes in the presence of melittin at a melittin-to-lipid molar ratio of 1:40 at 67°C for the following times 55

27. Plot of the enhancement ratio as a function of the melittin-to-lipid molar ratio (expressed as a fraction) . 59

28. Logarithm of the enhancement ratio of the o-o vibronic transition of pyrene embedded in DSPC liposomes as a function of 1/temperature 63

29. Logarithm of the enhancement ratio of the o-o vibronic transition of pyrene embedded in DSPC liposomes in the presence of 1:500 melittin-to-lipid molar ratio, as a function of 1/temperature 64

30. Logarithm of the enhancement ratio of the o-o vibronic transition of pyrene embedded in DSPC liposomes in the presence of 1:300 melittin-to-lipid molar ratio, as a function of 1/temperature 65

31. Logarithm of the enhancement ratio of the o-o vibronic transition of pyrene embedded in DSPC liposomes in the presence of 1:200 melittin-to-lipid molar ratio, as a function of 1/temperature 66

32. Logarithm of the enhancement ratio of the o-o vibronic transition of pyrene embedded in DSPC liposomes in the presence of 1:165 melittin-to-lipid molar ratio, as a function of 1/temperature 67

FIGURE PAGE

33. Logarithm of the enhancement ratio of the o-o vibronic transition of pyrene embedded in DSPC liposomes in the presence of 1:120 melittin-to-lipid molar ratio, as a function of 1/temperature 68

34. Logarithm of the enhancement ratio of the o-o vibronic transition of pyrene embedded in DSPC liposomes in the presence of 1:100 melittin-to-lipid molar ratio, as a function of 1/temperature 69

35. Logarithm of the enhancement ratio of the o-o vibronic transition of pyrene embedded in DSPC liposomes in the presence of 1:80 melittin-to-lipid molar ratio, as a function of 1/temperature 70

36. Logarithm of the enhancement ratio of the o-o vibronic transition of pyrene embedded in DSPC liposomes in the presence of 1:40 melittin-to-lipid molar ratio, as a function of 1/temperature 71

37. Logarithm of the enhancement ratio of the o-o vibronic transition of pyrene embedded in DSPC liposomes in the presence of 1:20 melittin-to-lipid molar ratio, as a function of 1/temperature 72

38. Logarithm of the enhancement ratio of the o-o vibronic transition of pyrene embedded in DSPC liposomes in the presence of 1:10 melittin-to-lipid molar ratio, as a function of 1/temperature 73

39. Logarithm of the enhancement ratio of the o-o vibronic transition of pyrene embedded in DSPC liposomes in the presence of 1:5 melittin-to-lipid molar ratio, as a function of 1/temperature 74

40. Light scattering, measured as absorbance at 360 nm for PC_3P embedded in DSPC liposome as a function of temperature 83

CHAPTER I

INTRODUCTION

Extensive use has been made in recent years of liposomes which are lipid assemblies possessing a bilayer structure that resembles that found in natural membranes (Singer and Nicolson, 1972). Fluorescent probes can yield a wealth of information on the structure and dynamics of bilayers. They report on: the fluidity and the effective polarity of the region of the bilayer in their immediate vicinity, structural changes undergone by the lipid during its phase transition, effects of proteins, cholesterol, ions and drugs, accessibility of their binding sites to molecules that have the property to quench their fluorescence, proximity of functional sites of proteins embedded in lipid bilayers, surface potential and fusion of bilayers.

Of particular interest are lipid-protein interactions that play a crucial role in the structure and function of natural membranes. A rather simple model of such associations is offered by melittin, the major protein component of bee venom. It lyses model and natural membranes at high concentrations (Haberman 1972; Sessa et al., 1969), whereas low concentrations activate phospholipase A_2 by affecting the organization of bilayers (Mollay and Kreil, 1974; Mollay et al., 1976; Yunes et al., 1977).

Early studies (Mollay et al., 1976; Mollay and Kreil 1973; Dufourcg and Faucon, 1977) reported a blue shift of about 15 nm in

the fluorescence spectral maximum of the single tryptophan residue of melittin upon binding to phospholipids relative to that in aqueous solution. On the basis of that observation, those workers inferred that the residue penetrated deeply into the hydrophobic core of the bilayer. Use of fluoresence spectral shifts to estimate the polarity of the microenvironment of a fluorescent probe, however, can be adversely affected by restricted relaxation of neighboring polar groups during the lifetime of the excited state of the probe (Azzi, 1975). Eftink and Ghiron (1976) demonstrated that a reliable method for determining the degree of exposure of the tryptophan residue of proteins to the solvent is that of quenching of its fluorescence by acrylamide, a polar, nonionic quencher. That method was used for melittin bound to egg phosphatidylcholine (EPC) and distearoylphosphatidylcholine (DSPC) and it was found that the second-order rate constant, kq, of fluorescence quenching is about 1×10^9 $M^{-1}S^{-1}$ (Georghiou et al., 1982a, Georghiou et al., 1982b). Since the polar quencher is rather unlikely to penetrate into the bilayer, the relatively high magnitude of kq suggests the occurrence of rather frequent encounters between the hydrophilic acrylamide molecules and the residue during the time span of light emission. On the basis of that observation it was inferred that the tryptophan residue of melittin does not penetrate deeply into the phospholipid bilayer. Another interesting finding was that melittin binds to phospholipid in an aggregated form.

From the available evidence the following picture emerges regarding the mode of melittin-phospholipid interaction (Georghiou

et al., 1981, Georghiou et al., 1982a, Georghiou et al., 1982b). The initial step appears to involve electrostatic attraction (Dufourcq and Faucon, 1977; Dawson et al., 1978) between the lipid phosphate group and basic amino acid residues (lysine or argenine of the C-terminal part of the protein). The importance of polar interactions is suggested by the observation of a differential scanning calorimetry study (Mollay, 1976) that the hydrophlic fragment 21-26 decreases the heat of the phase transition, mimicking the intact melittin, whereas the hydrophobic fragment 1-20 is ineffective in that respect. The protein-lipid electrostatic attraction will cause partial neutralization of the protein positive charge and diminish protein-protein electrostatic repulsion, which, in turn, will facilitate hydrophobic interactions leading to aggregation. In the second step of the interaction the predominantly hydrophobic part of protein may penetrate into the bilayer to some extent giving rise to further stabilization of the protein-lipid complex. The model of Dawson et al. (1978) proposes that the depth of melittin penetration is less than 10 Å.

Spectroscopic studies have addressed the question of the structural changes induced by melittin when it binds to phospholipids. Two ESR studies presented evidence that melittin causes disordering of the acyl chains (Williams and Bell, 1972; Verma et al., 1976). This is consistent with the enhancement of the permeability to ions and molecules observed upon binding of melittin to phospholipids (Sessa et al., 1969). Very recently, a Raman study reported lowering of the transition temperature, T_t, of DMPC liposomes by

melittin (Lavialle et al., 1980). This contradicts the findings of Verma and Wallach (1970) who had earlier also used the Raman method at comparable melittin-to-lipid molar ratios and reported that melittin raises the T_t of DMPC. This matter, therefore, remains to be settled.

In the present study we have used the enhancement of the 0-0 vibronic transition of pyrene and the phenomenon of intramolecular excimer formation by 1, 3-bis (1-pyrene) propane, PC_3P, for investigating further the effects of melittin on the dynamics and structure of distearoylphosphatidylcholine (DSPC) bilayer liposomes. A brief description of these approaches is presented below.

1. Enhancement of the o-o Vibronic Transition of Pyrene

The o-o vibronic transition in the fluorescence spectrum of pyrene (at about 373 nm), which is very weak in inert solvents (e.g heptane), is enhanced considerably when pyrene is dissolved in polar solvents, such as butanol, methanol, pyridine, dimethyl formamide, or water (Lianos and Georghiou 1979; Nakajima 1971). By employing IR and nanosecond fluorometric techniques, it was demonstrated (Lianos and Georghiou 1979a; Lianos and Georghiou 1979b) that the enhancement effect is the result of ground-state molecular complex formation between pyrene and polar solvent groups, which reduces the symmetry of the pyrene molecule giving rise, in turn, to the enhancement of weakly allowed vibronic transitions. The IR studies involved the effect of pyrene on the -OH fundamental stretching vibration of alcohols in the region 3500-3700 cm^{-1} and the induction

by polar solvents of the appearance of a new band in the IR spectrum of pyrene at ~ 1625 cm^{-1} where an IR-forbidden band in invert solvents is known to exist. A statistical analysis of the fluorescence decay data was also carried out (Lianos and Georghiou, 1979a; Lianos and Georghiou, 1979b) by the method of nonlinear least-squares and presented further evidence for complexation: two components were detected with decay times corresponding to those of free and complexed pyrene. In a subsequent study (Mukhopadhyay and Georghiou, 1980) it was reported that 1, 12-benzoperylene and naphthalene, two other symmetric aromatic hydrocarbons, also exhibit the enhancement effect. Those studies established: (a) the origin of the enhancement as involving ground-state complexation with neighboring polar groups; and (b) that the degree of enhancement is a measure of the effective polarity of the microenvironment of the fluorophore.

It is of interest to compare the enhancement method for obtaining information on the polarity of the microenvironment of a fluorescent probe with that utilizing fluorescent spectral shifts (probes of the ANS type have been used extensively in the literature in such studies). The accuracy of polarity determinations by the latter method can be adversely affected by restricted relaxation of neighboring polar groups during the lifetime of the excited state (Azzi, 1975). The enhancement method, on the other hand, does not suffer from such an uncertainty, as the emission monitored is from a probe–polar group molecular complex, formed in the ground electronic state of the probe, whose association constant does not

change appreciably upon excitation; that inference is reached on the basis of the very small shifts of the o-o vibronic band in polar environments relative to that in inert solvents according to the analysis of Pimentel (1957). After elucidating the photophysics of the enhancement, it was used for determining the approximate location of pyrene employed as a fluorescent probe of liposomes. It was found (Lianos et al, 1980) that for pyrene incorporated into EPC bilayer liposomes the degree of enhancement of the o-o band is matched closely by that in butanol. For DPPC liposomes the matching solvent were ethanol and ether below the T_t and above it, respectively. These observations indicate clearly that the fluorescent probe does not penetrate deeply into the bilayer, but is instead located in the vicinity of the semipolar glycerol backbone of the bilayer (the possibility of attributing the observed pronounced enhancement to small amounts of water that may penetrate into the liposomes was discussed and rejected). This finding attains particular importance in view of the necessity of having information about the approximate location of the probe in order to use it as an effective, informative fluorescent probe. To illustrate this point, let us consider the reported data on the diffusion coefficients of oxygen (Fischkoff and Vanderkooi, 1975) and of pyrene (Vanderkooi et al, 1974; Vanderkooi and Callis, 1974; Galla and Sackmann, 1974; Dorrance and Hunter, 1977). In those studies, as well as in all the other extensive studies involving pyrene as a fluorescent probe, it was assumed that it penetrates deeply into the hydrophobic core of the bilayer. That assignment

was made on the basis of the molecular structure of the probe, an intuitive procedure that was previously suspected to be misleading for some other probes (Yguerabide and Foster, 1981). It so happens that there is a gradient of microviscosity in lipid bilayers with the glycerol region being the most restricted. In the well characterized case of DMPC, the microviscosity decreased by a factor of ~ 70 upon going from the glycerol region to the terminal methyl groups of the fatty acyl chains (Lee et al, 1976). Obviously then it makes a lot of difference whether one assigns the deduced values of the diffusion coefficients to the hydrophobic core or to the glycerol region.

It was further demonstrated that the enhancement effect offers a new method for determining phase transition temperatures of phospholipids and for studying the effects of cholesterol on the structure of their glycerol backbone (Georghiou and Muckhopadhyay, 1981). For sonicated DPPC liposomes a transition temperature of 36.0± 0.4 =°C was determined which is in very good agreement with the values previously obtained by employing the methods of differential scanning calorimetry (Suurkuusk et al, 1976), fluorescence depolarization (Lentz et al, 1976), and Raman spectrosiopy (Gaber and Peticolas, 1977). It was found that small contents of cholesterol (~ 9 mol%) induce an increase in the polarity of the microenvironment of pyrene, whereas contents > 13 mol% induce a decrease in the polarity. In interpreting the data it was noted that an NMR study (Drake et al, 1972) reported that 50 mol% cholesterol induces a pronounced enhancement in the mobility of the

backbone. On the basis of the model proposed by Trauble (1971), according to which the transport of molecules is accomplished through lipid conformational changes, one would then expect thermally-induced structural fluctuations would be facilitated giving use to enhanced penetration of the probe into the bilayer. The data from the enhancement study for 50 mol% were found to be in line with such an interpretation as were those for mole fractions down to 13%. A mole fraction of 9%, on the other hand, was found to diminish the penetration of the probe and to force it toward the polar head groups.

In the present work we have employed this phenomenon for determining the phase transition temperature of the bilayer, the width of the phase transition, and the activation energy for the relocation of the probe in the bilayer for different melittin-to-lipid molar ratios. The results provide an inside on the effects of melittin on the organization of the bilayer.

2. Intramolecular Excimer Formation by PC_3P

There are two processes of excimer formation. One is the intermolecular excimer formation in which an excited molecule interacts with another non-excited, ground-state molecule and form a complex. It is a phenomenon that has been well studied and a good account is found in the book by J.B. Birks (1970). Another process is the intramolecular excimer formation in which two moieties, one excited and the other non-excited, of the same molecule interact to form a complex. The two processes have a different dependence on

temperature. In solvents, intermolecular excimer formation increases as the temperature is lowered whereas intramolecular excimer decreases as the temperature is lowered. In phospholipids, for intermolecular excimer formation, q_e/q_m increases with temperature below T_t while at T_t it decreases dramatically (Galla and Sackmann, 1975). For intramolecular exicimer formulation, however, q_e/q_m increases continuously with increasing the temperature and exhibits a dramatic enhancement at T_t (Zachariasse et al., 1978).

In the present work excimer formation by 1, 3 - bis (1-pyrene) propane, PC_3P, has been used for probing the structure and dynamics of DSPC liposomes. We have employed PC_3P as an intramolecular excimer-forming probe in DSPC for determining the transition temperature, the width of the phase transition, the difference in the free energies of activation between the crystalline and the liquid-crystalline phases, the difference in the entropies of activation between the two phases, and the energies of activation in the crystalline and the liquid-crystalline phases for different melittin-to-lipid molar ratios. Our objective was to obtain information about the nature of the effects of the protein on the bilayer structure and dynamics.

A brief list of references of studies involving intramolecular excimer formation follows: Zachariasse et al,(1980), pointed out that there are two temperature regions for the dependence of the excimer-to-monomer ratio of the fluorescence quantum yields, q_e/q_m, as a function of 1/T, where T is the absolute temperature. The

so-called high-temperature region and the low-temperature region. Excimers formed by PC_3P fall in the low-temperature region for which

$$\frac{q_e}{q_m} = \left(\frac{k_{fe}}{k_{fm}} \right) k_{dm} \tau_{oe}$$

where k_f refers to the radiative rate constant, τ_o to the lifetime of the excimer, k_{dm} to the rate constant for excimer formation and the subscripts e and m refer to excimer and monomer, respectively. The low-temperature region is the one of interest to us in the present work. The photophysics of intramolecular excimer formation was discussed by the following authors: Avouris et al., 1974; Zachariasse et al., 1978; Zachariasse et al., 1980. Schryver et al., 1979, reviewed the field of intramolecular excimer formation and presented a large list of substances that form such excimers. Chandross and Dempster, (1970); Goldenberg et al., (1978); Zachariasse and Kühnle, (1976); Avouris et al., (1974), and Melnick et al., (1981), showed that q_e/q_m is inversely proportional to the viscosity η, except for very low values of n (below 10 cP).

Zachariasse et al., (1978), employed PC_3P in studying the fluidity of micelles. Georgescauld et al., (1979), used the intramolecular forming probe dipyme for studying the fluidity of DMPC, DPPC, DSPC and EPC liposomes. The fluidity of micelles was also studied by Turro et al., (1979), and by Emert et al., (1979). Zachariasse et al., (1980), employed PC_3P in sonicated and non-sonicated liposomes of DMPC and DPPC and determined thermodynamic parameters for excimer formation both below and above T_t. Finally, Melnick et al., (1981), used PC_3P in phospholipids and biological

membranes. The interesting finding of their study was that PC_3P does not report properly the viscosity in the bilayer but it actually reports a much lower value. They concluded that apparently that is the result of the heterogeneous nature of the environment of the bilayer which precludes a direct comparison with homogeneous solvent systems.

The advantage of using intramolecular excimer probes as compared to the intermolecular probes is that low probe concentrations are used in that case, minimizing distortions of the bilayer which may occur in the latter case.

CHAPTER II

MATERIALS AND METHODS

Zone-refined pyrene was obtained from P. Bauric, Philadelphia, while 1, 3- bis (1-pyrene) propane (PC_3P) was obtained from Molecular Probes. Melittin lyophilized and chromatographically pure and distearoyl-phosphatidylcholine (DSPC), chromatogrophically pure, were obtained from Sigma. A sample of melittin obtained from ICN gave identical results with those obtained from Sigma. Scintanalyzed grade dioxane and HCl acid were obtained from Fisher. The measurements were made in Tris buffer, pH7, by using triply distilled water. The 0.01M Tris buffer pH7 was made as follows: First a 0.1M Tris solution was prepared by dissolving 0.605 g of Tris in 50 ml of triply distilled water. Next a 0.1M HCl solution was made by diluting 0.83 ml of concentrated HCl acid to 100 ml with triply distilled water. Then 26 ml of the Tris solution were added to 24 ml of the HCl solution to give 50 ml of 0.1M Tris buffer. This was finally diluted to 500 ml with triply distilled water to yield a 0.01M Tris buffer solution whose pH was checked with a Fisher pH meter.

Fresh samples of liposomes were prepared every time by dissolving 10 mg of lipid in 10 ml 0.01M Tris buffer pH7 to give a 1.25×10^{-3} M solution. The suspension was vigorously stirred for 20 min. and then sonicated for 20 min. using a Heat-Systems-Ultrasonics 20 kHz Model W-375 sonifier equipped with a 0.5 in. tip

at 50% full power. Sonication was made in an Argon atmosphere at 61°C (above the transition temperature). Finally, the sample was centrifuged at 65,000 g for 20 min. using a 50 Ti rotor in a Beckman L3-50 model Ultracentrifuge.

A solution of 10^{-3} M pyrene (M.W. = 202) was prepared by putting 2 mg in 10 ml dioxane. Then 0.04 ml were added in 10 ml liposome to give a 4×10^{-6} solution.

For PC_3P (M.W. = 444) a solution of 10^{-3} M was prepared by putting 2.2 mg in 5 ml dioxane. Then 0.08 ml were added in 10 ml liposome to give a 8×10^{-6} solution. In this way a molar ratio of $1.25 \times 10^{-3}/8 \times 10^{-6} = 156$ between lipid and probe was obtained. For this ratio the probability of intermolecular excimer formation is very small compared with intramolecular excimer formation (Melnick et al, 1981). The pyrene and PC_3P solutions were used for two consecutive days and then fresh samples were prepared.

Fresh samples of melittin were prepared for each measurement by dissolving the desired quantity in 1 ml Tris buffer, pH7. A M.W. of ~ 2800 was used in the calculations. Then, after the liposome was centrifuged, melittin was added in it and it was incubated in the liposome for 30 min. at 61°C. The solutions for the different melittin-to-lipid molar ratios were prepared as follows: 56 mg of melittin were dissolved in 1 ml 0.01M Tris buffer, pH7, and 0.099 ml of that solution were added in 8 ml liposome to give a melittin-to-lipid molar ratio of 1:5. 28 mg of melittin were dissolved in 1 ml 0.01M Tris buffer, pH7, and 0.099 ml of that solution were added in 8 ml liposome to give a molar ratio of 1:10. 14 mg of melittin were

dissolved in 1 ml 0.01M Tris buffer, pH7, and 0.099 ml of it were added in 8 ml liposome to give a ratio of 1:20. 7 mg of melittin were dissolved in 1 ml 0.01M Tris buffer pH7 and 0.099 ml of it were added in 8 ml liposome to give a ratio of 1:40. 7 mg of melittin were dissolved in 1 ml 0.01M Tris buffer pH7 and 0.049 ml of it were added in 8 ml liposome to give a molar ratio of 1:80. Finally 5.6 mg, 4.66 mg, 3.37 mg, 2.8 mg, 1.86 mg and 1.1 mg were dissolved in 1 ml 0.01M Tris buffer pH7 and 0.0495 ml of them were added in 8 ml liposome to give molar ratios of 1:100, 1:120, 1:165, 1:200, 1:300 and 1:500 respectively.

Steady-state fluorometric techniques did not detect any fluorescence from liposomes with melittin which contained no probe (pyrene or PC_3P) at the excitation wavelength of 334 nm with a bandwith of 10 nm. To ascertain that the presence of any residual phospholipase A_2 is not contributing significantly to the observed effects of melittin, we prepared a solution of melittin at a melittin-to-lipid molar ratio of 1:20 in buffer containing 2 mM EDTA. EDTA is known to inactivate the enzyme (Shipolini et al., 1971). No significant change in the results of the enhancement measurements was observed.

The emission bandwith in the steady-state fluorometric measurements was 0.8 nm. For vibronic enhancement measurements use of such a small bandwith is necessary to ensure the accurate determination of the degree of enhancement of the o-o vibronic transition. The enhancement ratio R was measured as the ratio of the fluorescence intensity of the o-o vibronic band at ~ 376 nm to that at ~ 387 nm.

At every temperature the emission monochromator was carefully reset successively at the two fluorescence spectral maxima in order to take into account very small temperature-induced spectral shifts. The spectrofluorometer used, previously described (Georghiou 1975), employs an 1 kW Xe-Hg light source, a sample holder equipped with a Cryo-Tip device for temperature control, two 0.5 m Bausch and Lomb monochromators for selecting the exciting wavelength and for analyzing the emission, a thermoelectrically cooled 9558 QB EMI photomultiplier, a lock-in amplifier, and an X-Y recorder. A block diagram of the spectrofluorometer is shown in Fig. 1.

A nanosecond fluorometer, previously described (Badea and Georghiou, 1976), was used for the nanosecond time-resolved studies. It employs a high pressure light source that provides light pulses at a repetition rate of 10 kHz and in the 200-750 nm wavelength range, a Cryo-Tip device, an Amperex 56 TUVP photomultiplier and an 162 PAR boxcar averager. The excitation filter was a combination of a Corning 7-54 color filter and an 1 cm aqueous solution of saturated $NiSO_4$. A Corning 0-52 color filter was placed before the emission monochromator for rejecting second-order emission in the region of 600 nm. The monochromator employed was a high intensity 0.25 m Bausch and Lomb one with an emission bandwidth of 5 nm. A correction was applied to the spectra for the dependence of the transmission of the 0-52 filter in the wavelength range of 370-405 nm. The transmission was measured by employing a Cary-14 spectrophotometer.

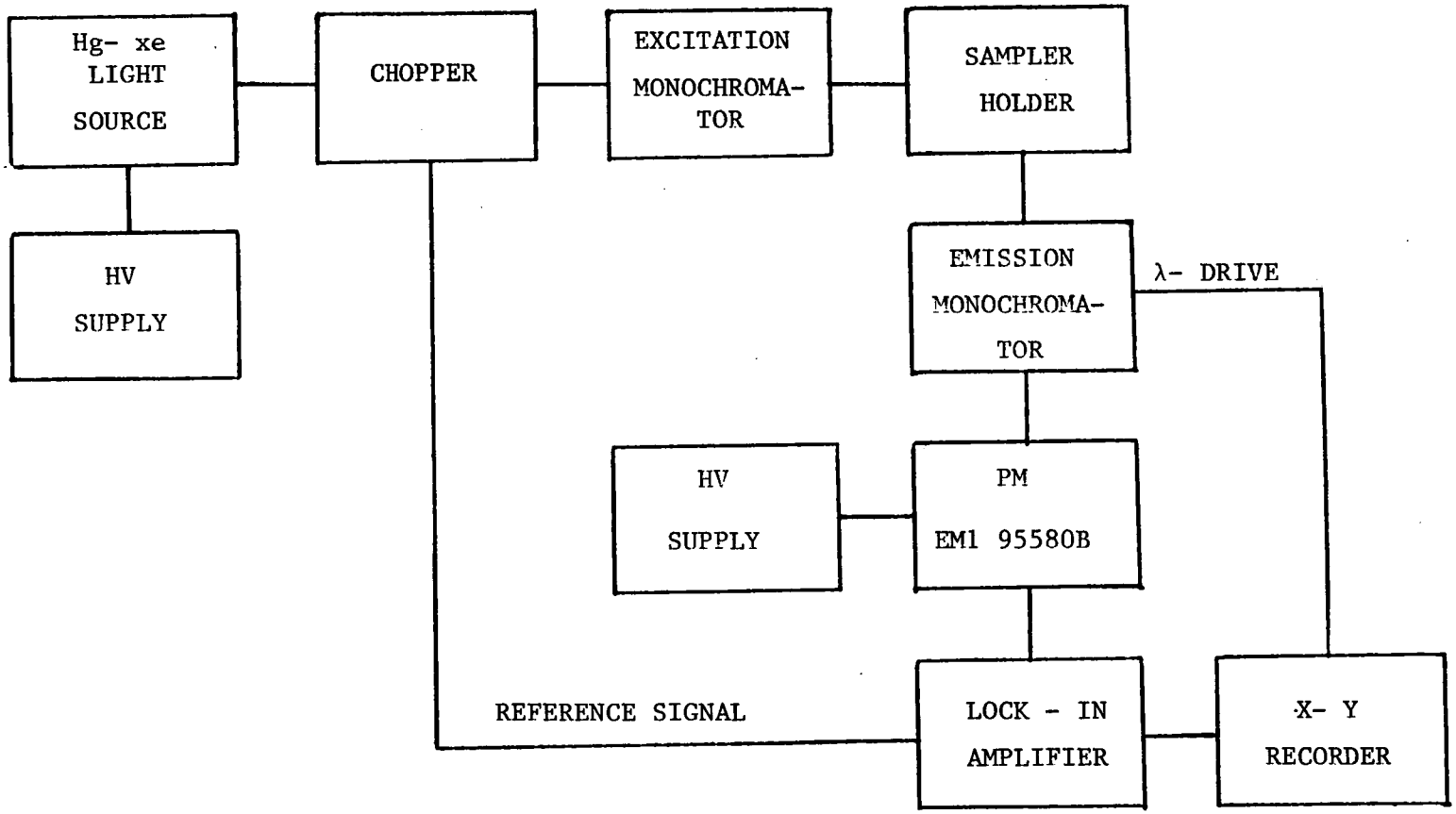


Figure 1. Block diagram of the spectrofluoremeter.

No hysteresis was found when the direction of the temperature was reversed in the titrations involving pyrene or PC_3P.

Also the effect of the oxygen presence was studied. Deoxygenation of samples containing pyrene, but no melittin, by bubbling with N_2 resulted in a substantial increase in the fluorescence intensity. We found, however, that the titrations were not affected by the deoxygenation procedures. For the samples containing PC_3P an increase in the fluorescence intensity of only about 3% was observed in the deoxygenated ones in both of the two peaks (at 480 nm and at 377 nm) which were used to express the excimer-to-monomer ratio of intensities. The titrations in this case also were unaffected upon deoxygenation. In view of these findings, we performed all the measurements in the presence of O_2. This choice was dictated by the difficulty involved in deoxygenating samples containing melittin, for in that case the protein, that has soap-like properties (Haberman, 1972), gave rise to excessive foam formation that resulted in loss of some of the sample.

The temperature of the solutions was measured with a potentiometer by immersing a copper-constantan thermocouple wire directly into the cuvette. All the spectra taken with the steady-state spectrofluorometer were first corrected for the variation of the sensitivity of the photomultiplier-monochromator combination with the emission wavelength.

During titrations with PC_3P we measured the corrected (by multiplying by 1.57) ratio of the peaks at 480 nm to that at 337 nm and took it to be representing the ratio q_e/q_m of the fluorescence

quantum yield of the excimer to that of the monomer. There are two flaws in that assumption. First, the monomer contributes at 480 nm. Second, the peak at 377 nm is very sharp resulting in underestimation of the ratio q_e/q_m. The following approach was followed for remedying these flaws. The spectrum in the liposome at 1°C (Fig. 2) was taken as being representative of the monomer spectrum, in view of the fact that intramolecutive excimer formation is inhibited at low temperatures. That this spectrum was found to be similar to the one taken with 1-methylpyrene at room temperature provided further evidence for the appropriateness of that choice. Then, the corrected spectra at various temperatures (26°C, 35°C, 45°C, 55°C and 68°C) were normalized at the 377 nm peak of the monomer spectrum. By subtracting from the composite spectra, the spectra of the excimers were obtained at the above temperatures. Examples of such spectra are given in Fig. 3 in the absence of melittin and in Fig. 4 in the presence of melittin with a melittin-to-lipid molar ratio of 1:100, at 45°C. We found that the ratio of the areas under the spectra, which represent the ratio q_e/q_m, was virtually independent of the temperature and by a factor of 3.8 higher than that of the ratio of the intensity at 480 nm to that at 377 nm. Therefore, overall the ratio of the intensities was multiplied by 1.57x3.8=5.97 so that it represents the ratio of the corrected quantum yields.

An experiment was performed to exclude the possibility that the probes pyrene and PC_3P interact with melittin and, thus, they may convey information that does not pertain to their microenvironment

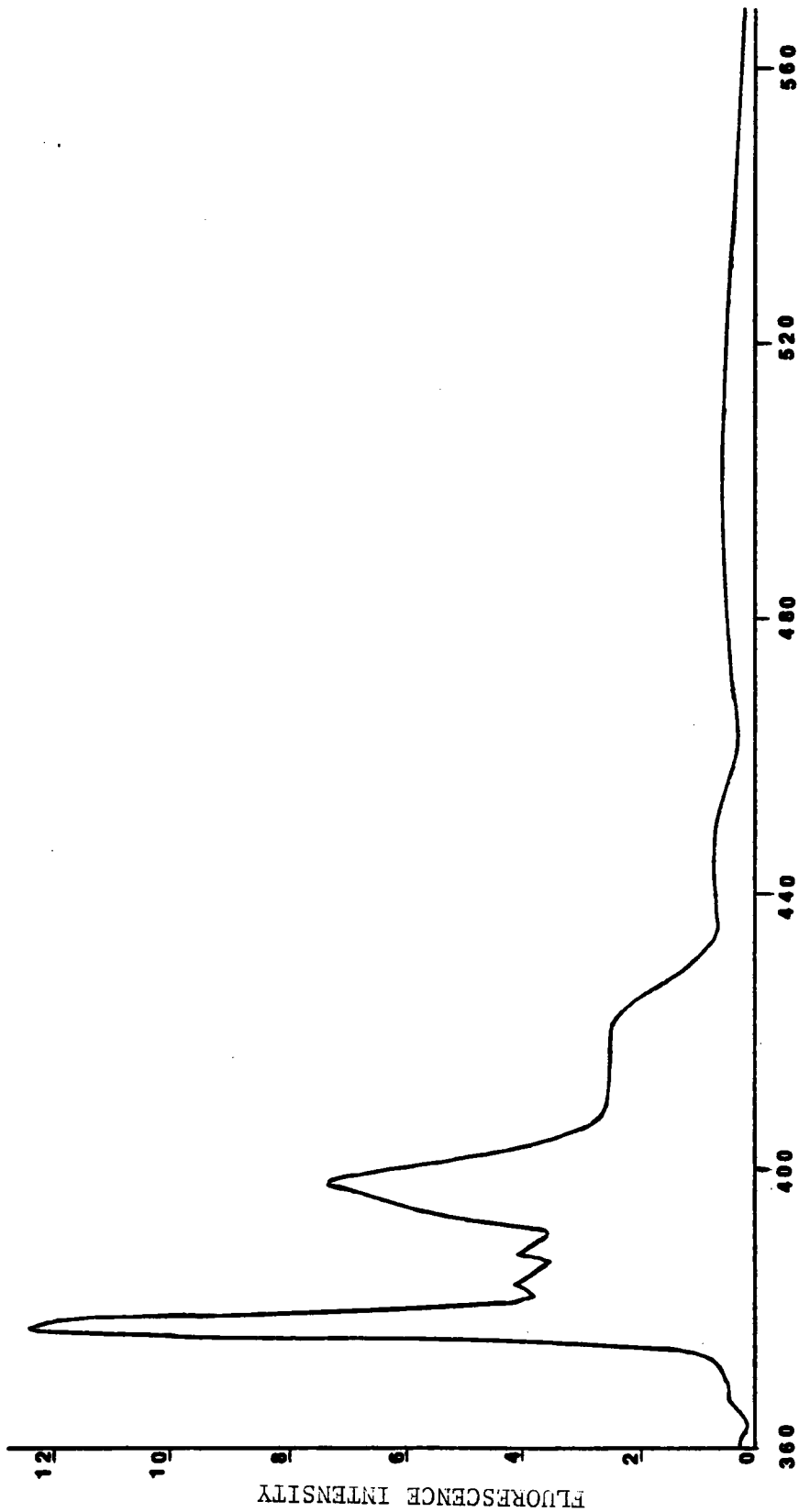


Figure 2. Fluorescence spectrum of PC_3P embedded in DSPC liposomes at 1°C being representative of the monomer spectrum.

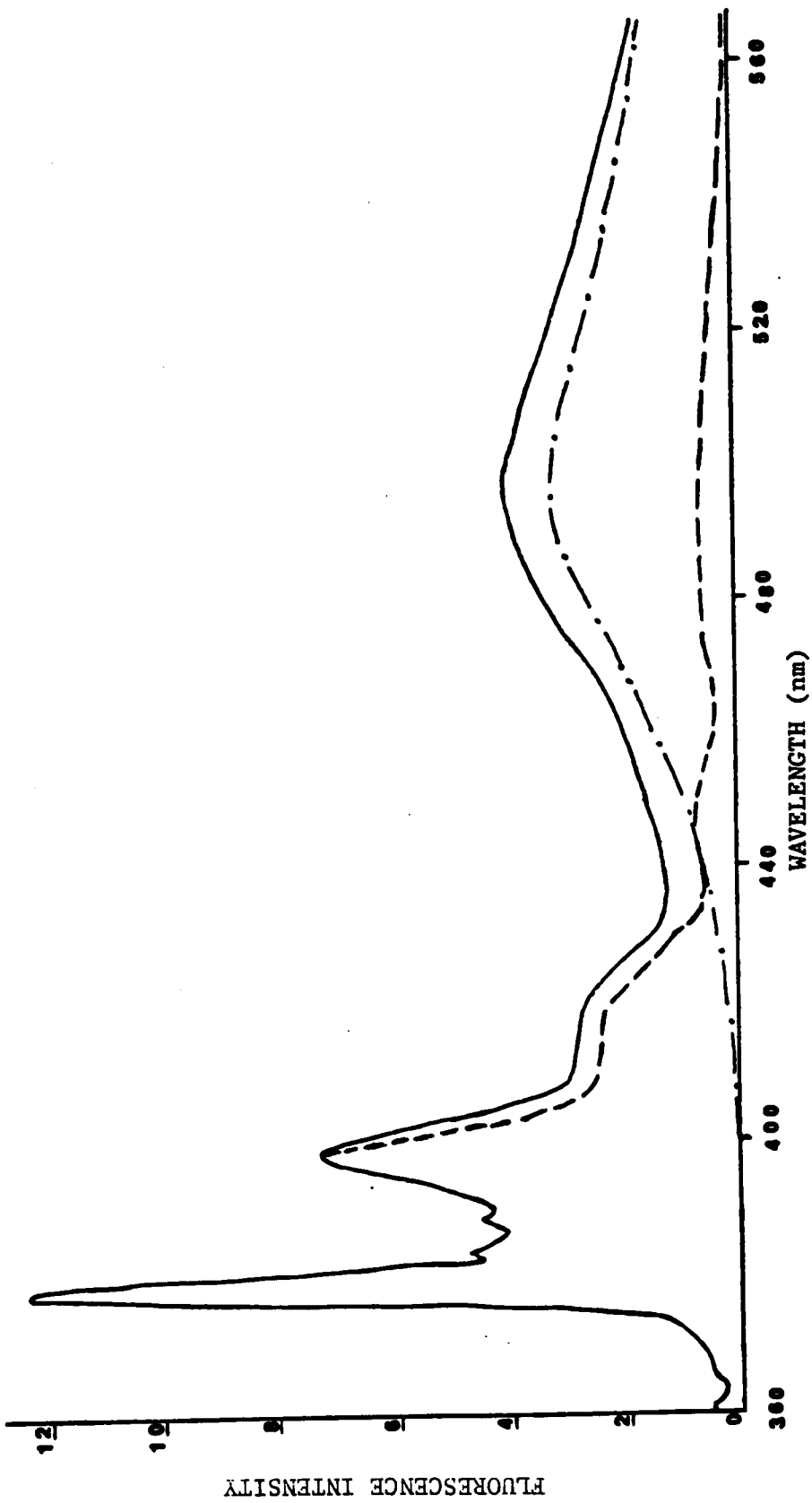


Figure 3. _____ Fluorescence spectrum of PC_3P embedded in DSPC liposomes at 45°C. – – – Fluorescence spectrum of PC_3P in DSPC at 1°C representing the spectrum of the monomer. – · – Fluorescence spectrum of the excimer obtained by subtracting the above two curves.

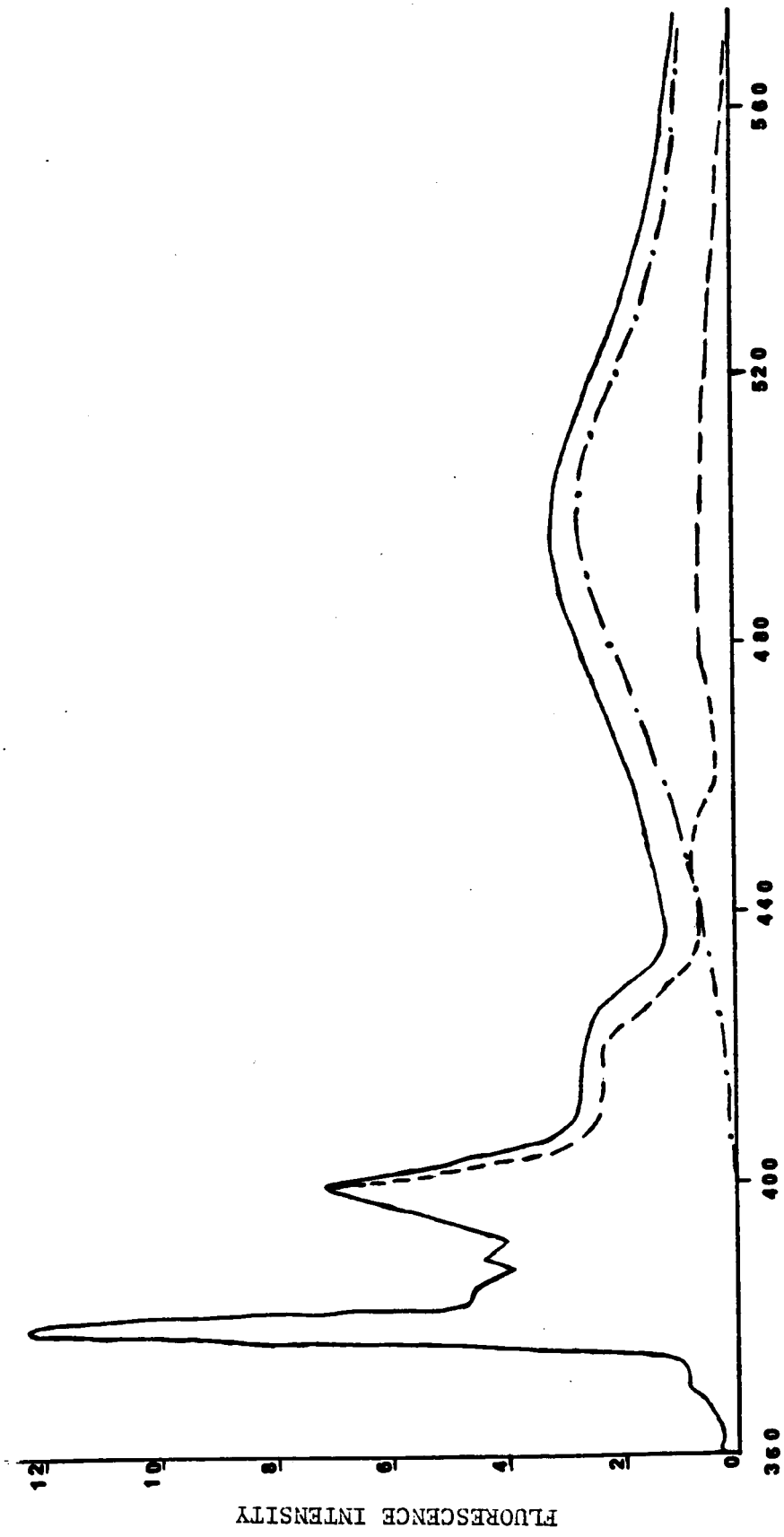


Figure 4. ___Fluorescence spectrum of PC_3P embedded in DSPC liposomes at 45°C in the presence of a melittin-to-lipid molar ratio of 1:100. _ _ _ _ Fluorescence spectrum of PC_3P embedded in DSPC at 1°C representing the spectrum of the monomer. _ · _ fluorescence spectrum of the excimer obtained by subtracting the above two curves.

in the liposome. A solvent mixture consisting of 95% Tris buffer, pH7, and 5% methanol was employed for preparing solutions of pyrene and PC_3P in the absence and in the presence of melittin for a melittin-to-lipid molar ratio corresponding to that used for a melittin-to-lipid molar ratio of 1:40. (7 mg of melittin were dissolved in 1 ml Tris buffer pH7, and then 0.099 ml of it were added in 8 ml solvent). The concentrations of pyrene and PC_3P were the same as those used with the measurements involving DSPC. That solvent mixture was chosen to ensure the solubility of the probes. No substantial changes in the enhancement ratio of the o-o vibronic band of pyrene, in the excimer-forming properties of PC_3P, or in the emission of the tryptophan residue of melittin were detected. It was, therefore, concluded that the probes do not bind to melittin; instead they serve as reporters on their immediate vicinity in the liposome.

CHAPTER III

RESULTS

The enhancement of the weakly allowed o-o vibronic transition in the fluorescence spectrum of the probe pyrene was employed as a method for studying the effect of melittin on the phospholipid. The enhancement ratio R, defined as the ratio of the o-o vibronic band intensity of ~ 376 nm to that of the band at ~ 387 nm, for pyrene in distearoylphosphatidylcholine (DSPC), was measured as a function of temperature and for different melittin-to-lipid molar ratios ranging from 1:5 to 1:500.

The enhancement ratio R was measured as a function of temperature from room temperature up to 78°C. Every experiment was repeated at least once. First, R was measured in a sample containing no melittin. Then, the measurement was repeated in samples containing melittin with a melittin-to-lipid molar ratio 1:5 and 1:10. The results in the absence of melittin are shown in Fig. 5. This type of plot allows the determination of the transition temperature T_t of the phospholipid as was previously demonstrated (Georghiou and Mukhopadhyay, 1981). A value of 52°C was obtained for DSPC, which agrees very well with the value of 51.3°C reported by Lentz et al., (1970), from fluorescence depolarization measurements. The results for the different melittin-to-lipid molar ratios are shown in Figs. 6-11. Some of the graphs have been grouped together and are shown with that in the absence of melittin

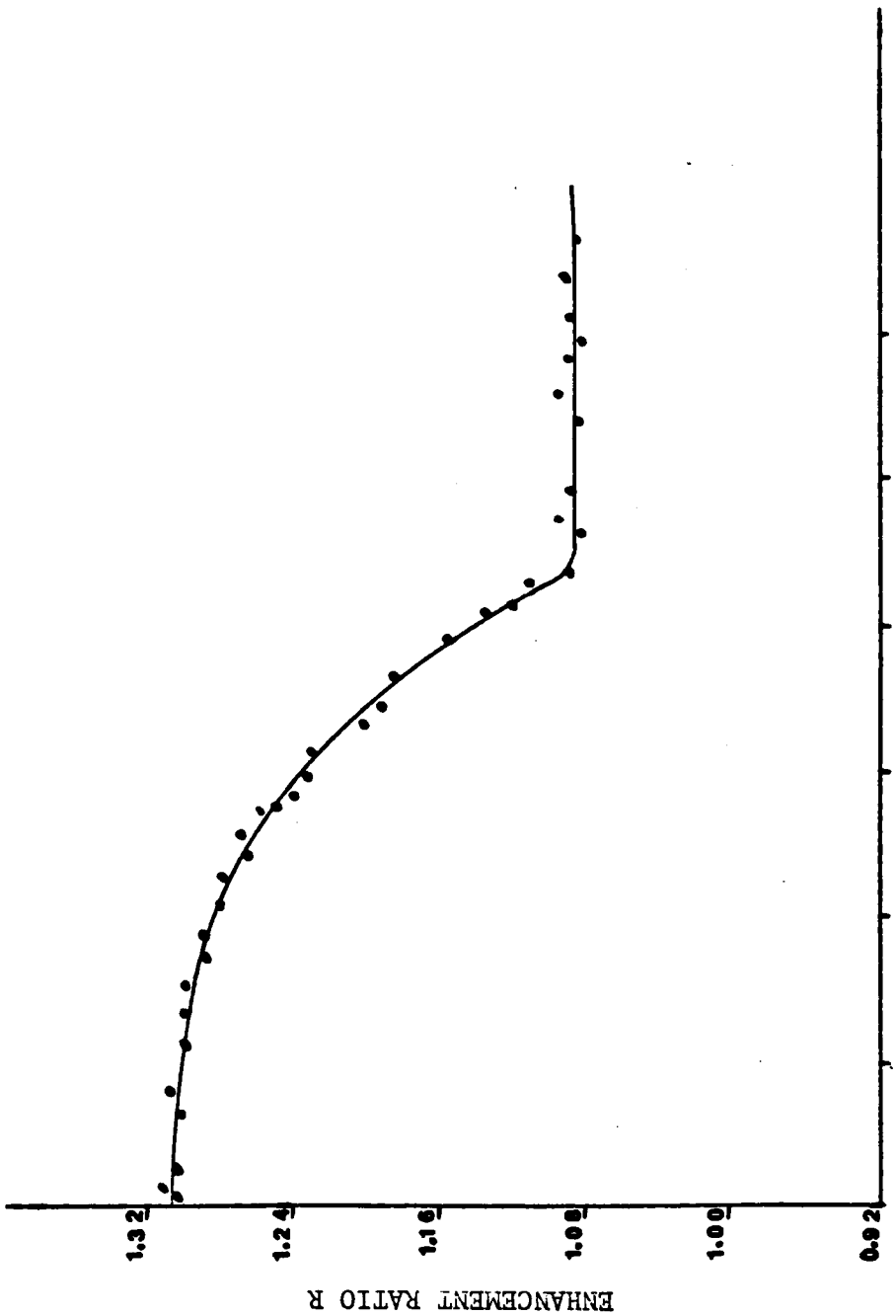


Figure 5. Enhancement of the o-o vibronic transition of pyrene embedded in DSPC bilayer liposomes as a function of temperature.

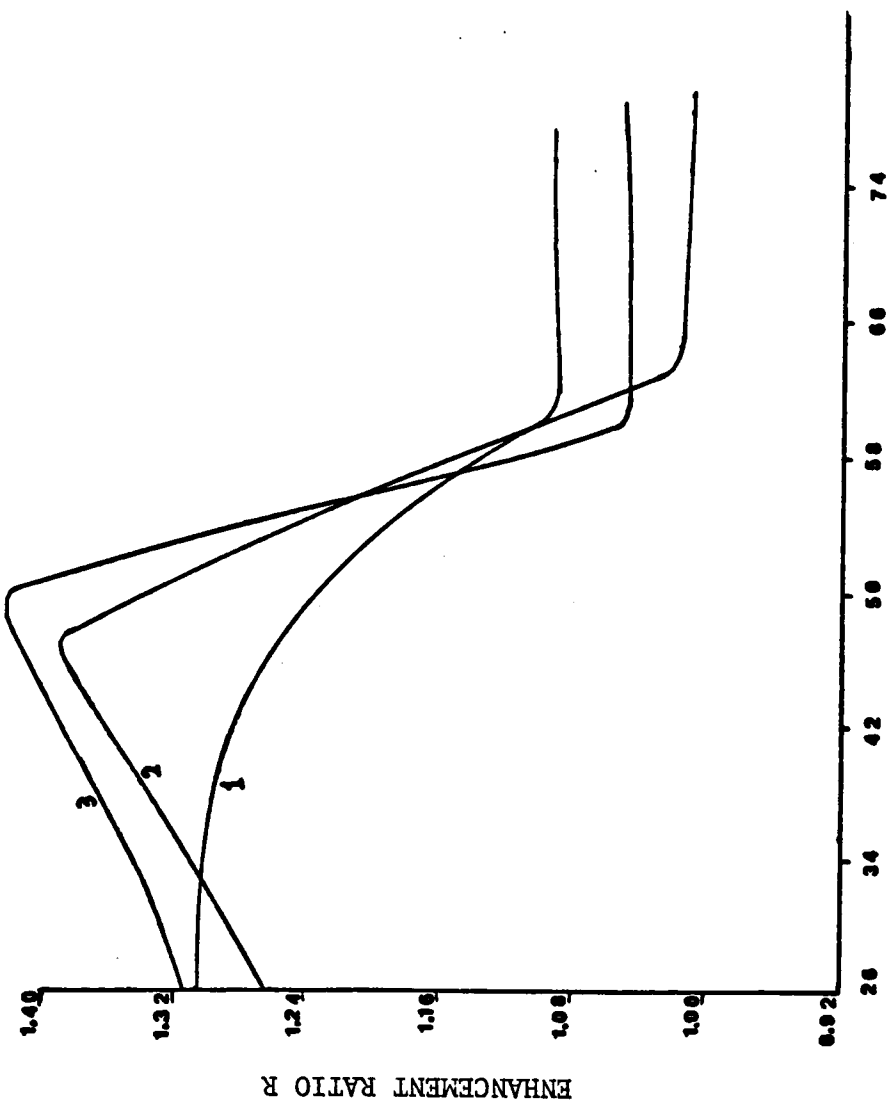


Figure 6. Enhancement of the 0-0 vibronic transition of pyrene embedded in DSPC liposomes as a function of temperature.(1) in the absence of melittin; (2) in the presence of 1:5 melittin-to-lipid molar ratio; and (3) in the presence of 1:10 melittin-to-lipid molar ratio.

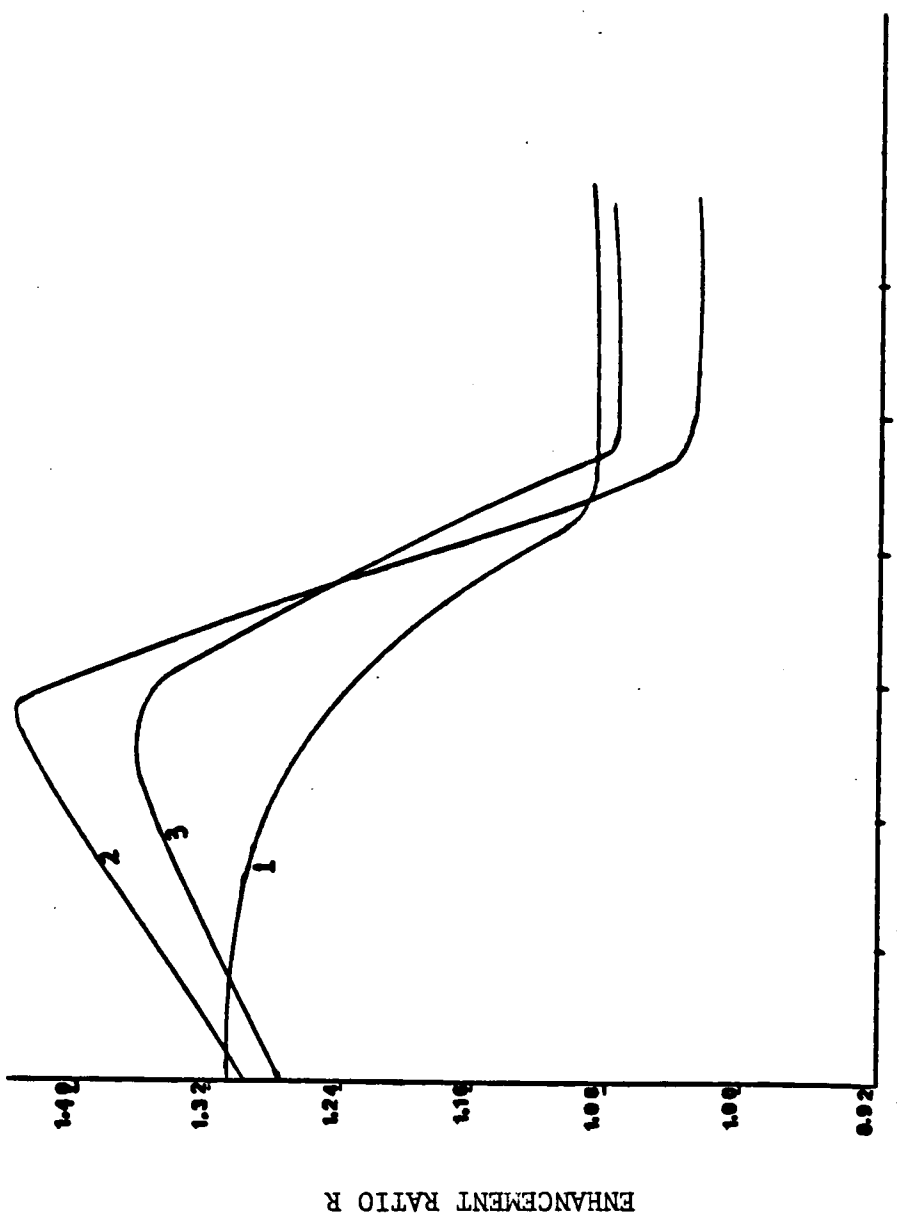


Figure 7. Enhancement of the o-o vibronic transition of pyrene embedded in DSPC liposomes as a function of temperature. (1) In the absence of melittin; (2) in the presence of melittin with 1:20 melittin-to-lipid molar ratio; and (3) in the presence of 1:40 melittin-to-lipid molar ratio.

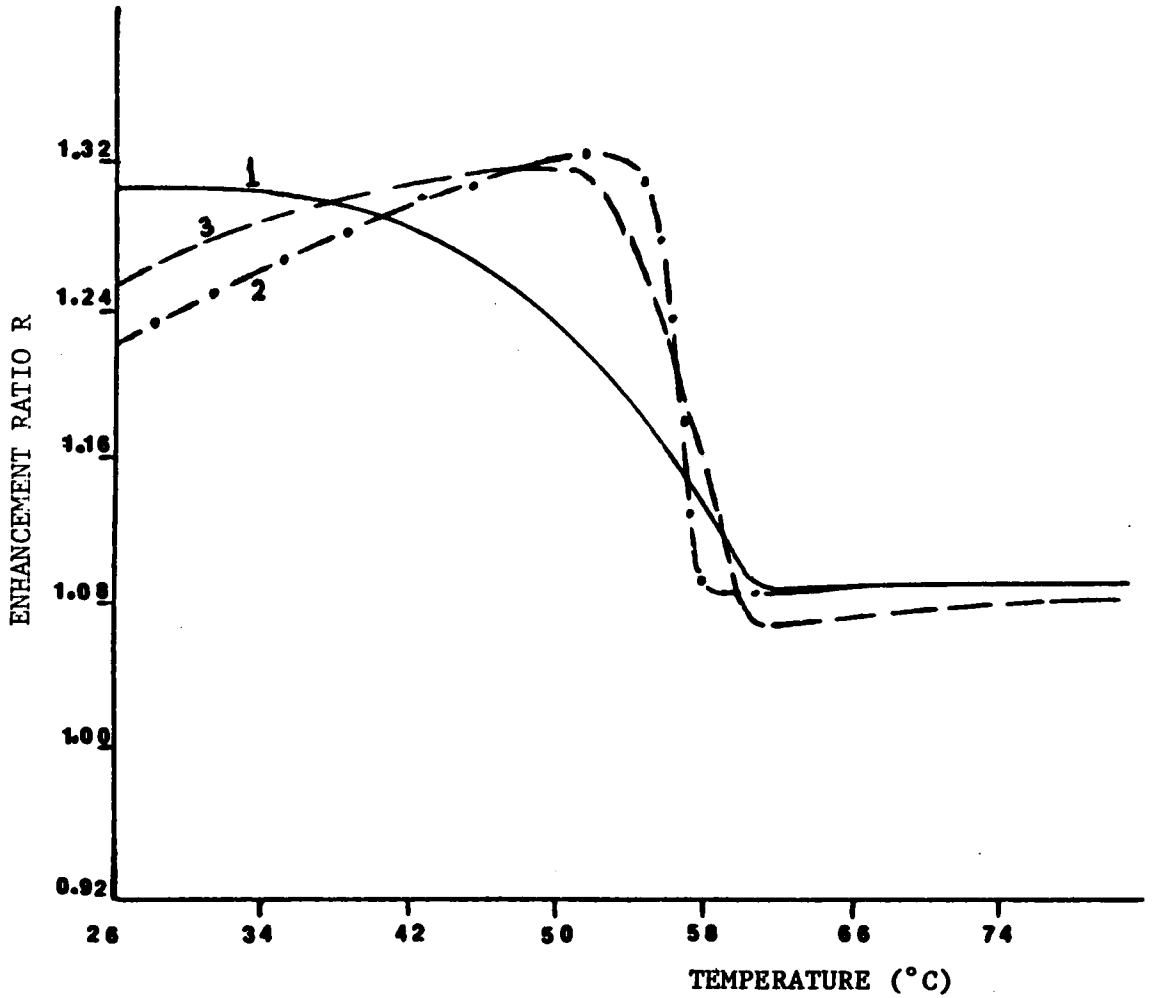


Figure 8. Enhancement of the o-o vibronic transition of pyrene embedded in DSPC liposomes as a function of temperature. (1) In the absence of melittin; (2) in the presence of 1:80 molar ratio; and (3) in the presence of 1:100 melittin-to-lipid molar ratio.

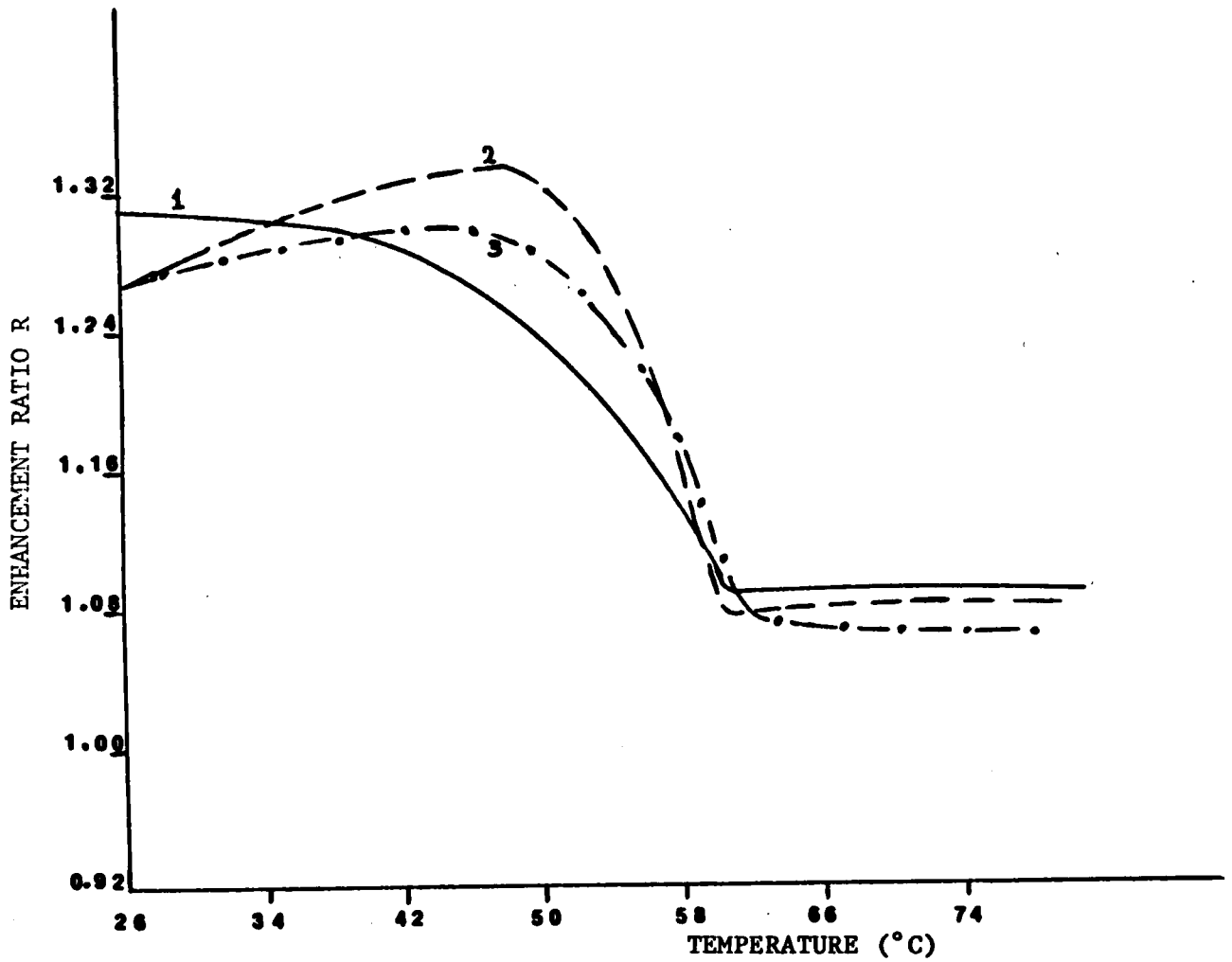


Figure 9. Enhancement of the o-o vibronic transition of pyrene embedded in DSPC liposomes as a function of temperature. (1) In the absence of melittin; (2) in the presence of 1:120 molar ratio; and (3) in the presence of 1:165 melittin-to-lipid molar ratio.

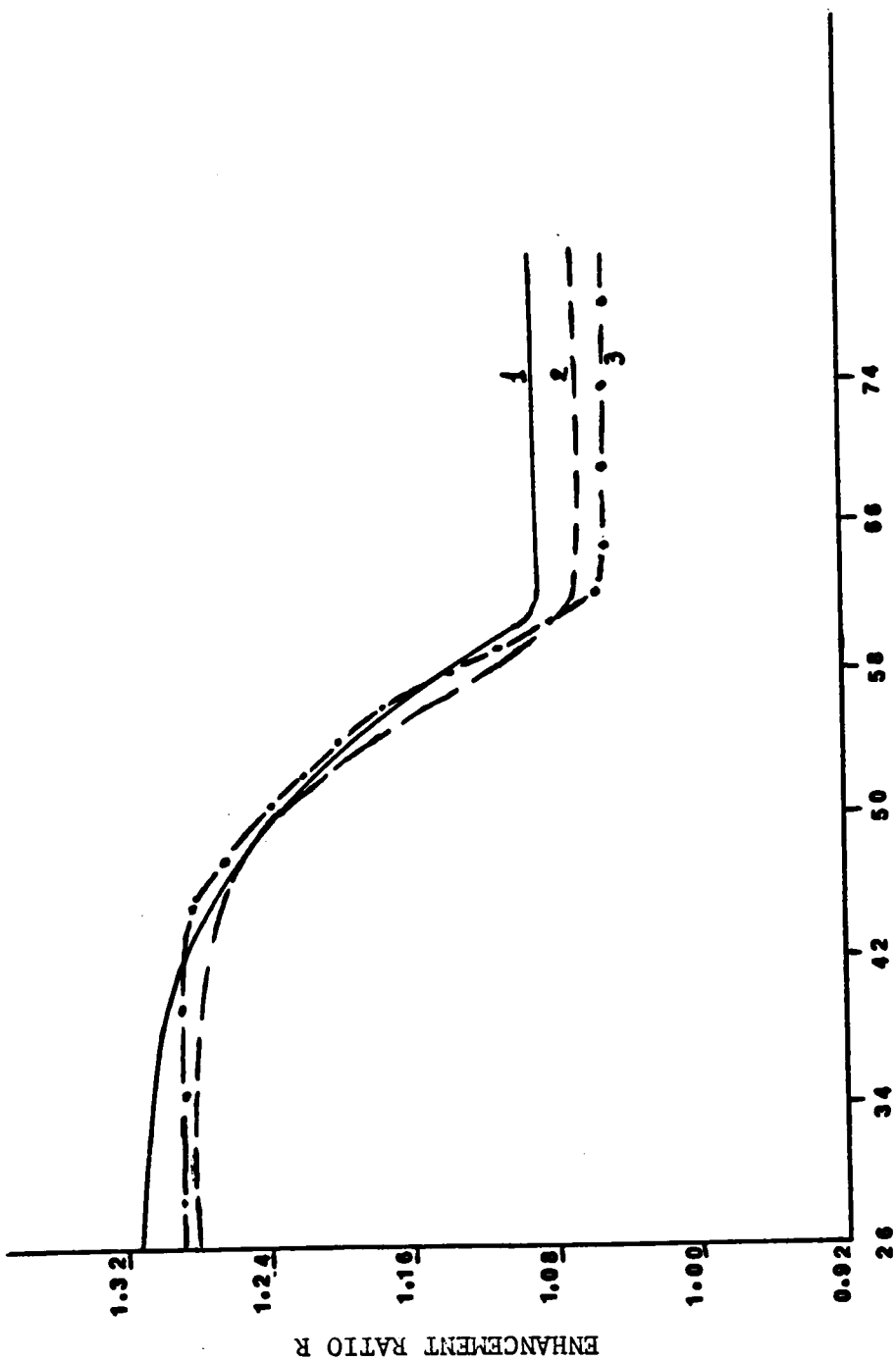


Figure 10. Enhancement of the o-o vibronic transition of pyrene embedded in DSPC liposomes as a function of temperature. (1) In the absence of melittin; (2) in the presence of 1:200 molar ratio; and (3) in the presence of 1:300 melittin-to-lipid molar ratio.

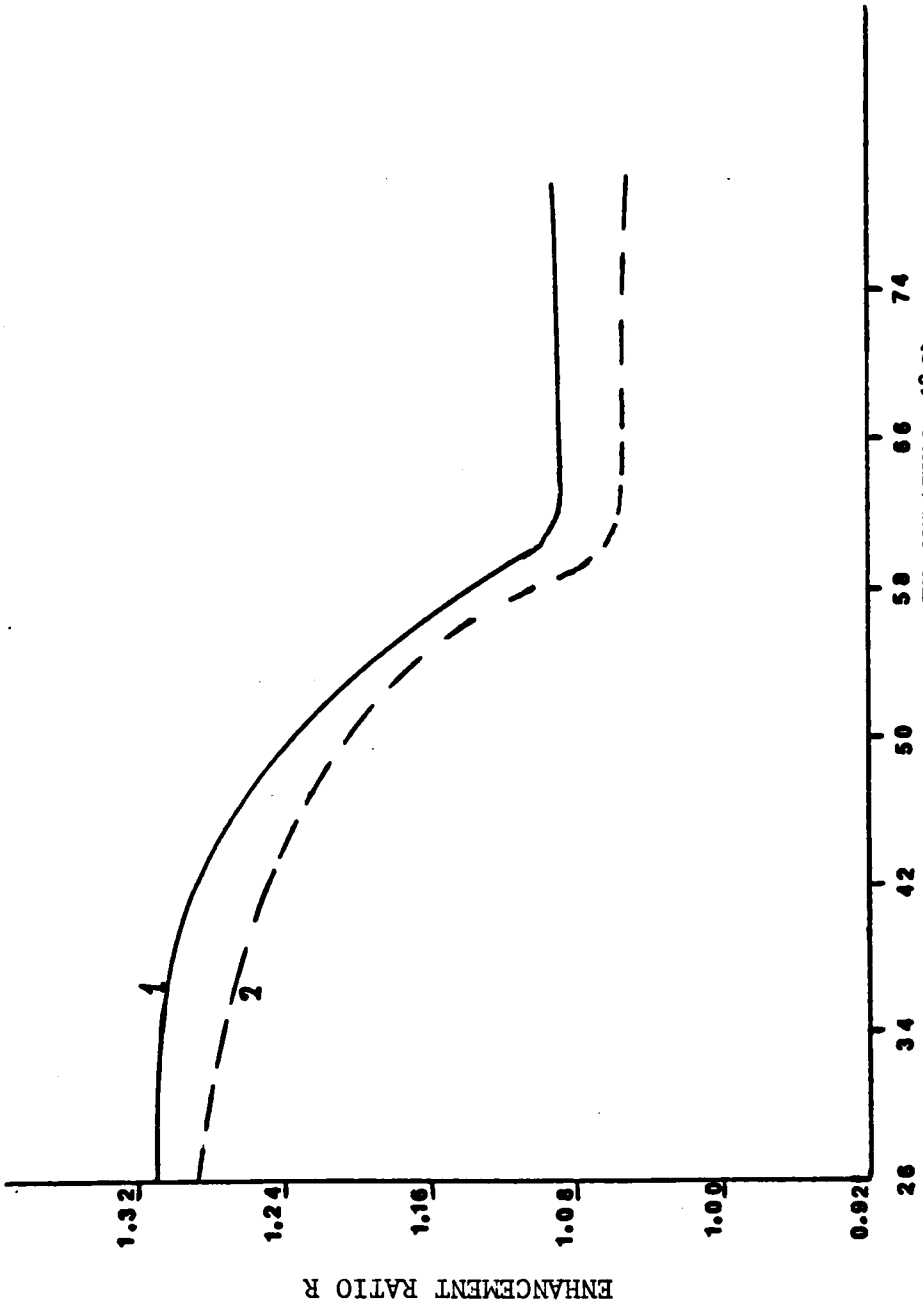


Figure 11. Enhancement of the o-o vibronic transition of pyrene embedded in DSPC liposomes as a function of temperature. (1) In the absence of melittin; and (2) in the presence of 1:500 melittin-to-lipid molar ratio.

for comparison. It can be seen that melittin affects the enhancement profiles in a manner that is dependent on the molar ratio. The most pronounced effect occurs for the ratio of 1:20. The significance of these findings is elaborated in the Discussion. There is also an effect on the transition temperatures T_t. Melittin has been found in all cases to increase T_t by a few degrees as can be seen from Table 1. Melittin also affects the width of the transition, ΔT, as shown in Table 2.

Intramalecular excimer formation is a thermally-activated process that involves a conformational transition leading to a stable conformation. In this kind of excimer formation the excimer-to-monomer ratio of fluorescence quantum yield, q_e/q_m, is related to the rate constants for excimer and monomer emission, the rate constant for excimer formation and dissociation, and the rate constants for excimer and monomer internal quenching. Plots of log (q_e/q_m) against 1/T for molecules forming intramelecular excimers have been observed to be linear. In the so-called high temperature region such plots have a positive slope whereas in the low-temperature region the slope is negative yielding the activation energy for excimer formation. In this case

$$\frac{q_e}{q_m} = \left(\frac{k_{fe}}{k_{fm}} \right) k_{dm} \tau_{oe}$$

where k_f refers to the radiative rate constant, τ_o to the lifetime of the excimer, k_{dm} to the rate constant for excimer formation, and the subscript e and m refer to excimer and monomer, respectively

Table 1. Transition temperatures T_t of DSPC bilayer liposomes for different melittin-to-lipid molar ratios determined from plots of the enhancement ratio R as a function of temperature.

Molar ratio	T_t °C
0	52 ± 0.5
1:500	53.6 ± 0.5
1:300	54 ± 0.6
1:200	55.2 ± 0.5
1:165	55.2 ± 0.7
1:120	54.5 ± 0.6
1:100	56 ± 0.5
1:80	56.4 ± 0.6
1:40	56.4 ± 0.6
1:20	55.6 ± 0.8
1:10	55.4 ± 0.8
1:5	55.2 ± 0.8

Table 2. Width ΔT of the transition of DSPC liposomes for different melittin-to-lipid molar ratios determined from plots of the enhancement ratio R as a function of temperature.*

Molar ratio	ΔT°C
0	22
1:500	20.8
1:300	19.5
1:200	19
1:165	16 ± 0.5
1:120	15 ± 0.5
1:100	12 ± 0.5
1:80	8 ± 0.5
1:40	16 ± 0.5
1:20	16 ± 0.3
1:10	15 ± 0.3
1:5	16 ± 0.3

*The uncertainty in the calculation of ΔT is ± 0.5°C for molar ratios greater than 1:200, whereas it is ± 1°C for lower ratios due to the broadness of the profiles in those cases.

(Zachariasse et al., 1980). This was the case for the intramolecular excimer studies reported in the present work.

First we searched for an isoemissive point in both the free sample and the one containing melittin with a melittin-to-lipid molar ratio 1:40. The existence of such an isoemissive point when the temperature is varied indicates that the variation of q_e/q_m with temperature reflects a variation of k_{dm} and not of the rate constants of deexcitation (Hamilton and Naqvi, 1968). Under the condition, plots of log (q_e/q_m) against 1/T are linear allowing the determination of the activation energy of excimer formation (Melnick et al., 1981). In the present study the temperature was varied from room temperature up to 68°C and the results are shown in Fig. 12 for the free sample and in Fig. 13 for the melittin-containing one. The figures suggest that an isoemissive point exists in both cases near the wavelength of ~ 450 nm.

Titrations were then performed for both the free samples and for those containing different melittin-to-lipid molar ratios. At every temperature the emission monochromator was carefully reset successively at the two fluorescence spectral maxima, at 480 nm for the excimer and at 377 nm for the monomer. The ratio of the fluorescence intensities Ie/Im, corrected with the overall factor 1.57x3.8=5.97 (see Materials and Methods) in order to represent the ratio of corrected quantum yields q_e/q_m, was measured as a function of temperature. We then plotted log (q_e/q_m) against 1/T as shown in Figs 14-18. The results for the free sample and the one containing melittin with a melittin-to-lipid molar ratio of 1:40 have been

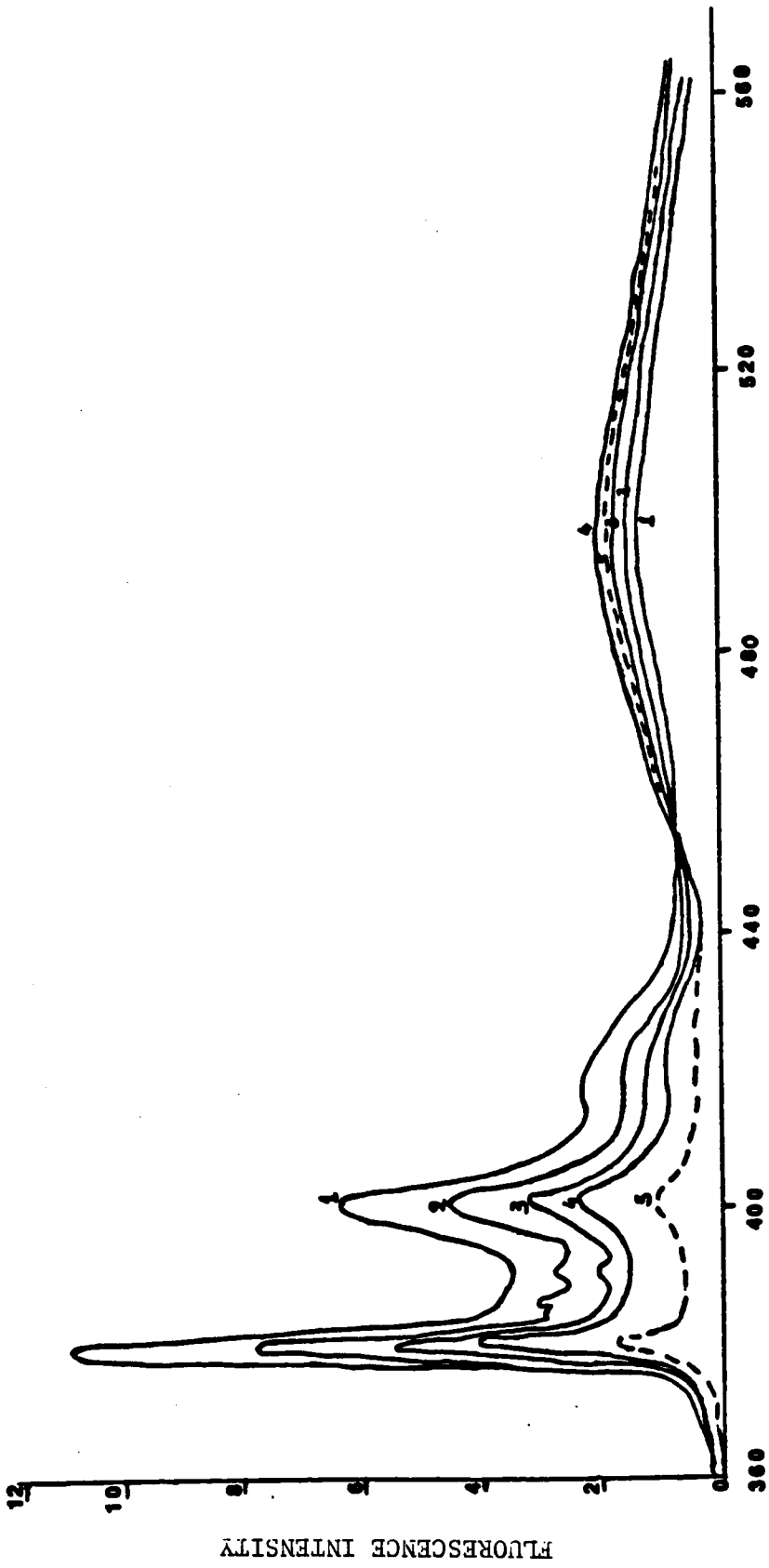


Figure 12. Fluorescence spectra of PC_3P embedded in DSPC liposomes : (1) 27°C; (2) 35°C; (3) 45°C; (4) 55°C; and (5) 65°C.

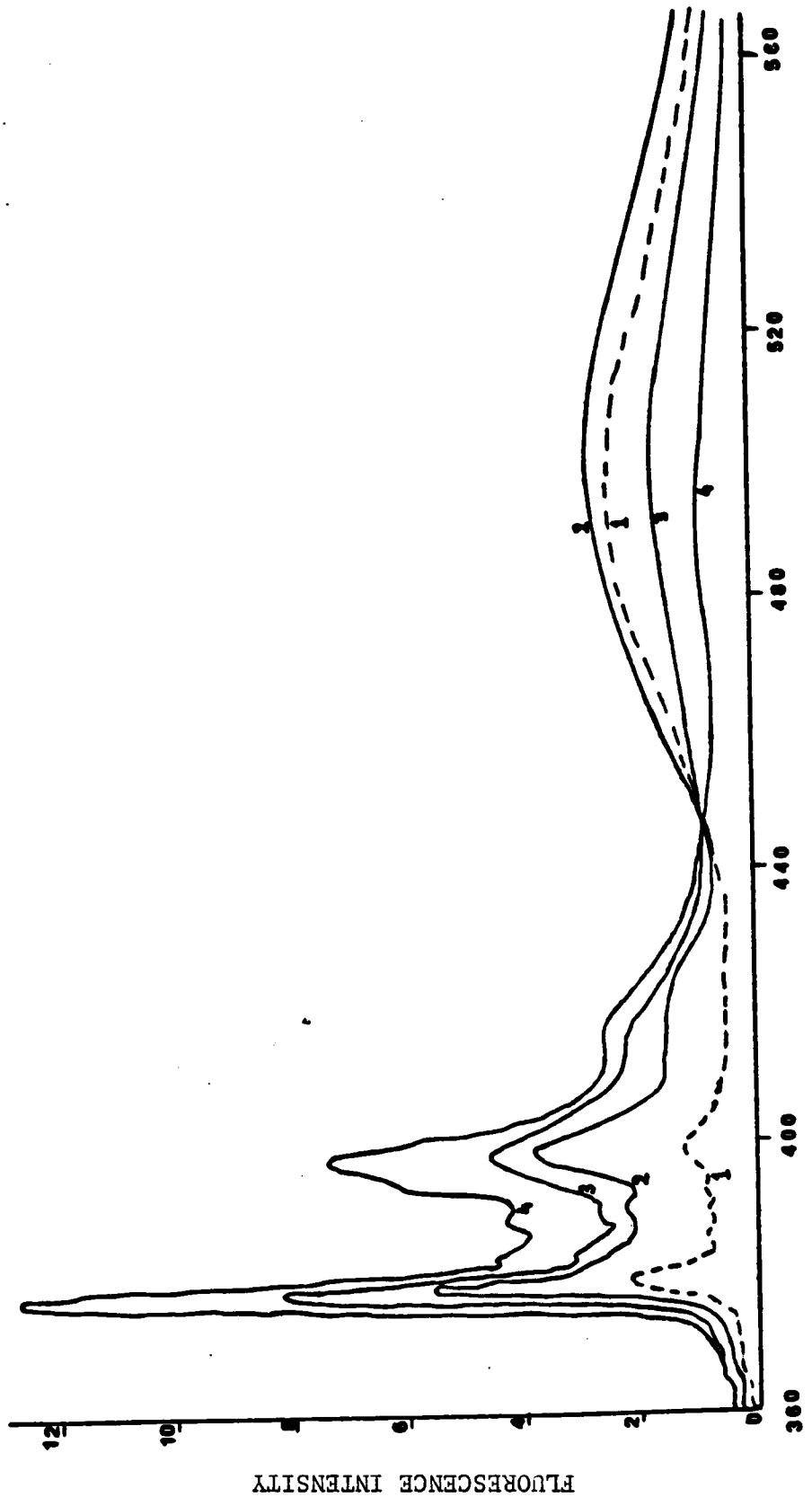


Figure 13. Fluorescence spectra of PC_3P embedded in DSPC bilayer liposomes for a melittin-to-lipid molar ratio of 1:40 : (1) 68°C; (2) 55°C; (3) 45°C; and (4) 30°C.

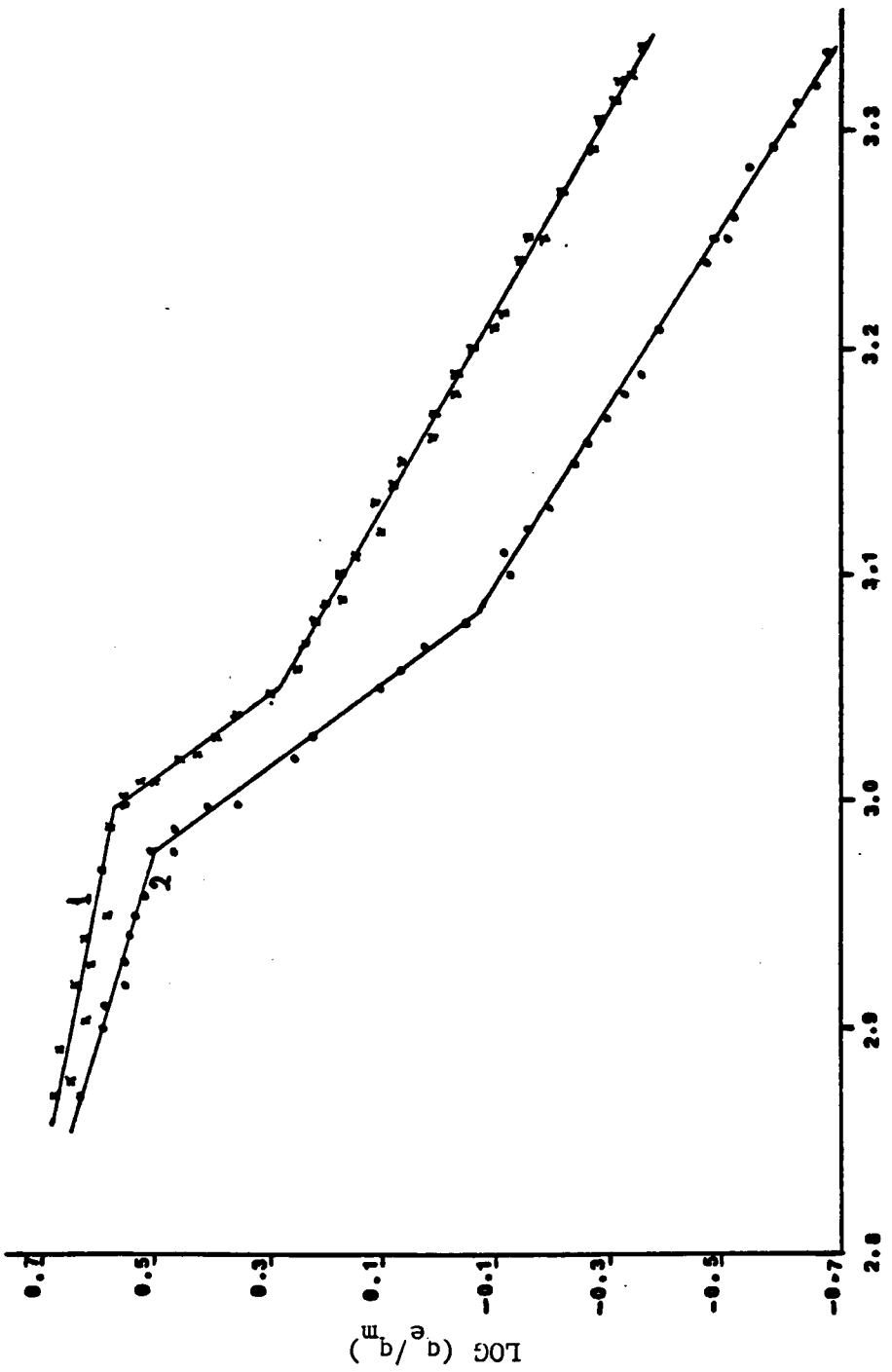


Figure 14. Logarithm of the ratio of the fluorescence quantum yield of the excimer to that of the monomer for PC_3P embedded in DSPC liposomes as a function of 1/temperature. (1) In the absence of melittin; and (2) in the presence of 1:40 melittin-to-lipid molar ratio.

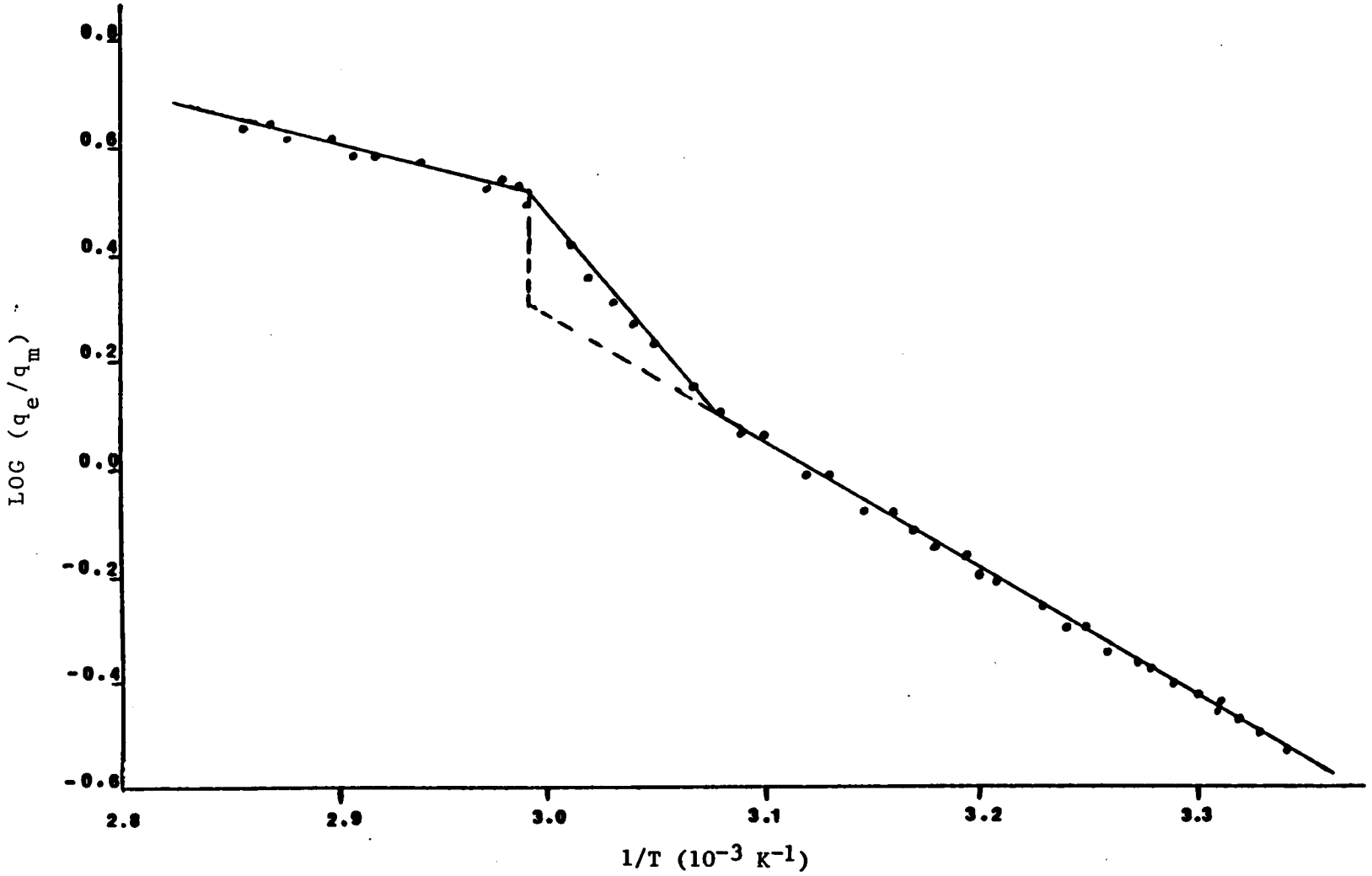


Figure 15. Logarithm of the ratio of the fluorescence quantum yield of the excimer to that of the monomer for PC_3P embedded in DSPC liposomes as a function of 1/temperature in the presence of 1:500 melittin-to-lipid molar ratio.

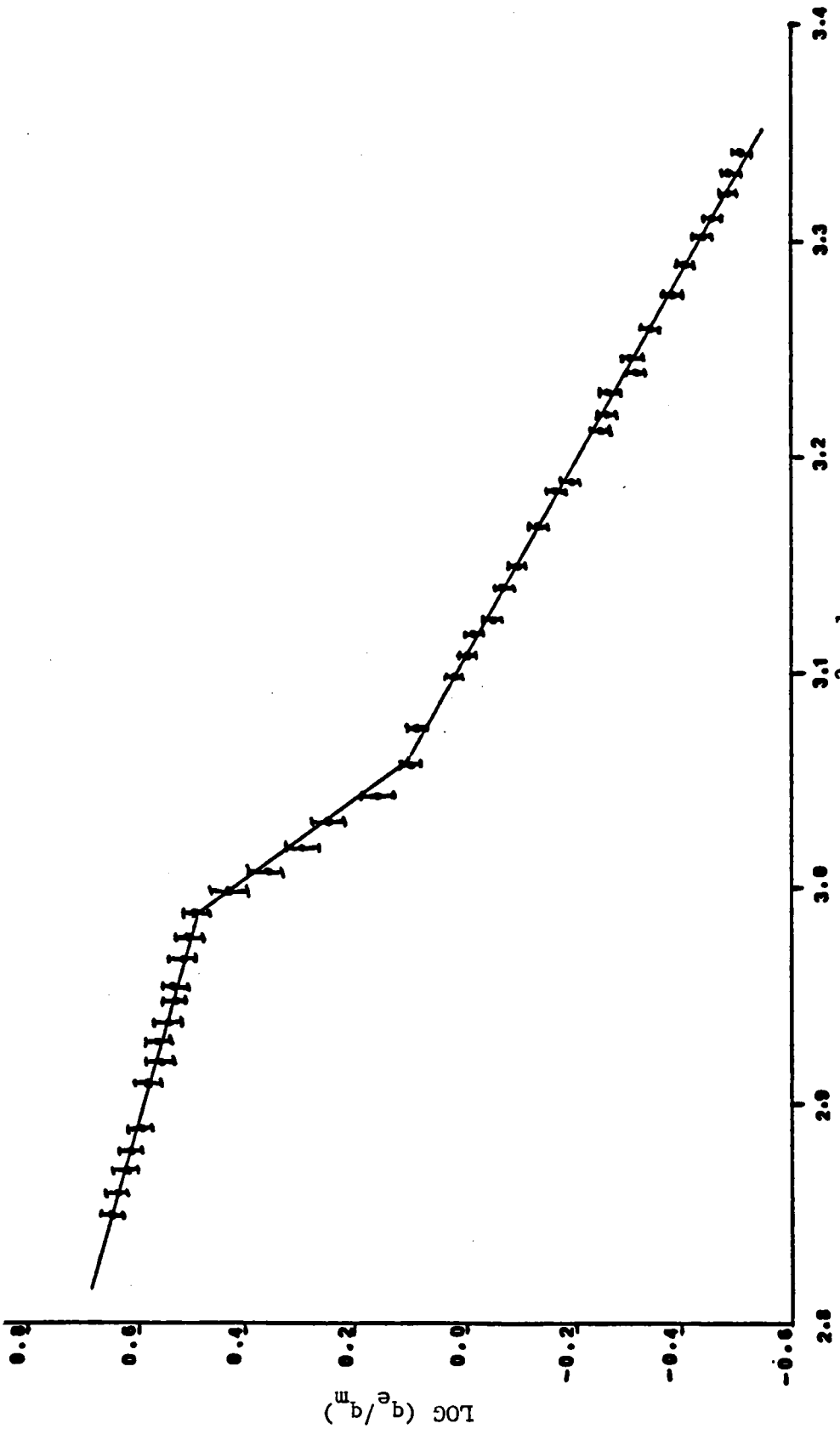


Figure 16. Logarithm of the ratio of the fluorescence quantum yield of the excimer to that of the monomer for PC_3P embedded in DSPC liposomes as a function of 1/temperature in the presence of 1:300 melittin-to-lipid molar ratio.

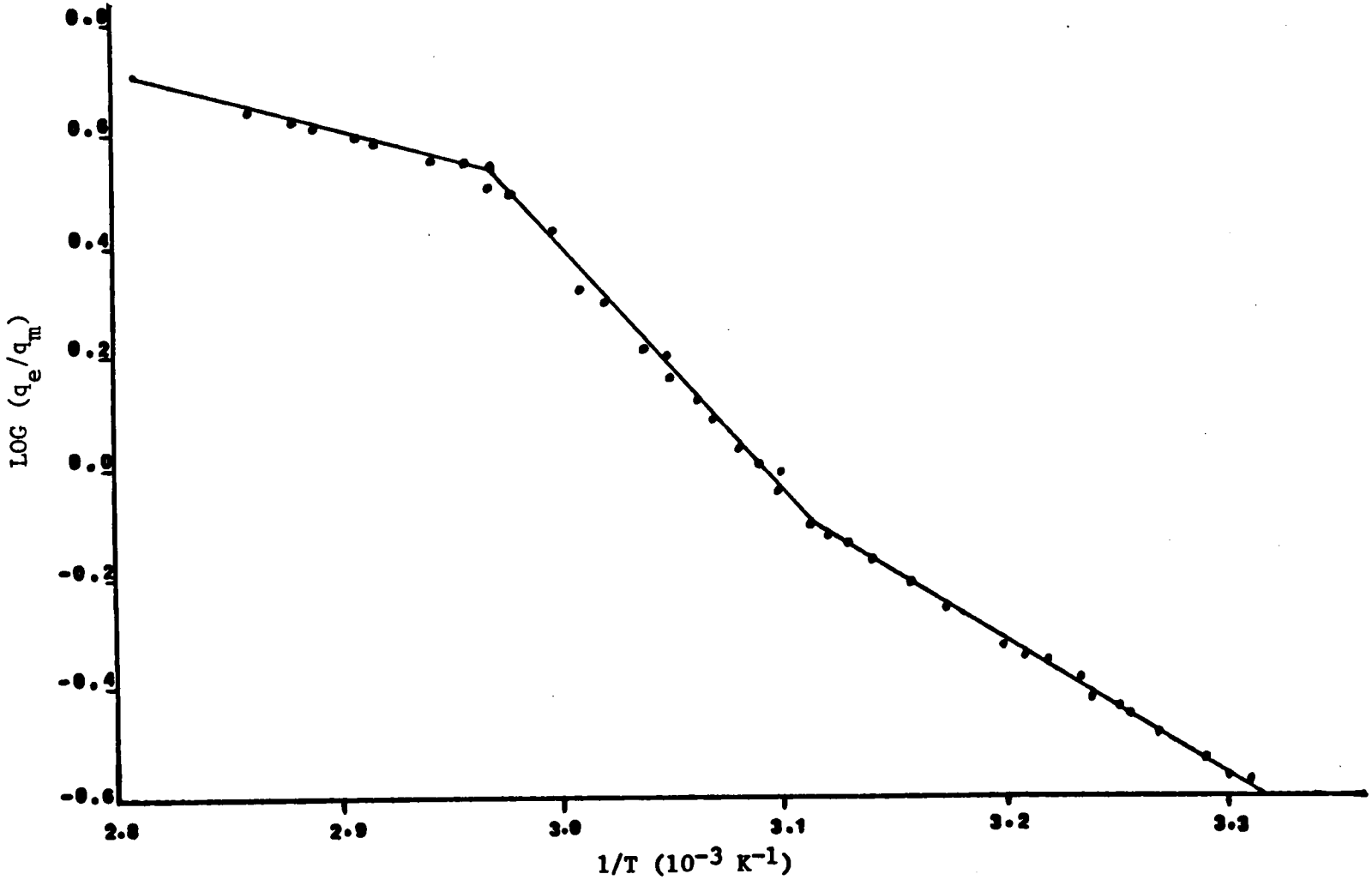


Figure 17. Logarith of the ratio of the fluorescence quantum yield of the excimer to that of the momoner for PC_3P embedded in DSPC liposomes as a function of 1/temperature, in the presence of 1:100 melittin-to-lipid molar ratio.

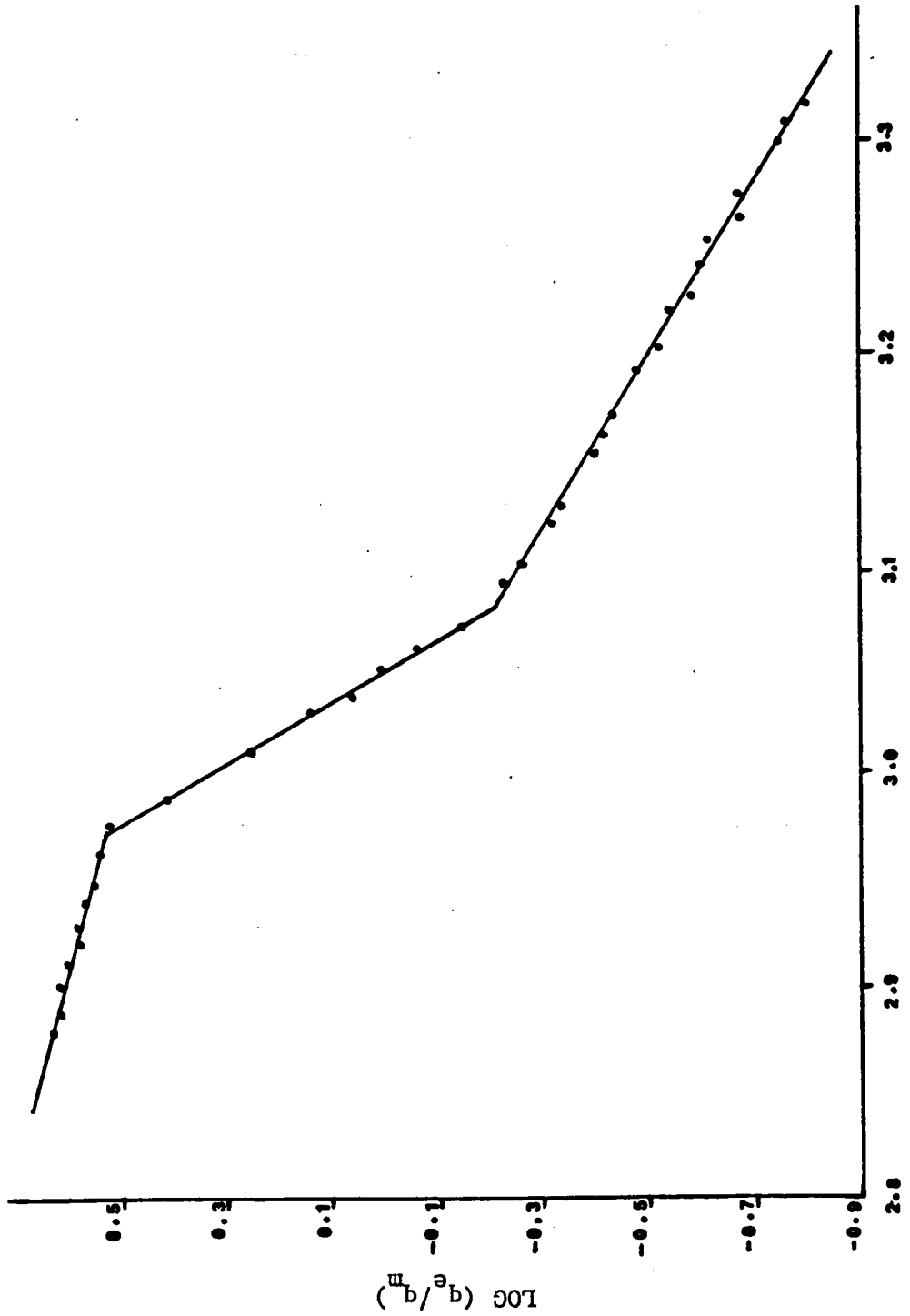


Figure 18. Logarithm of the ratio of the fluorescence quantum yield of the excimer to that of the monomer for PC_3P embedded in DSPC liposomes as a function of 1/temperature in the presence of 1:10 melittin-to-lipid molar ratio.

plotted together for comparison. By employing a linear least-squares computer program, the slopes were then calculated and used to yield the activation energy for the crystalline phase, Ecr, and the liquid-crystalline (fluid) phase, E_{fl}, from

$$\frac{d \log (q_e/q_m)}{d(1/T)} = \frac{E}{2.3R}$$

or E = 2.3x1.987x4.18x (slope) in J/mol. The values of E_{cr} and E_{fl} obtained are shown in Table 3. The rate constant for excimer formation is related to Δ E by an Arrhenius plot

$$k_{dm} = Ae^{-\Delta E/RT}.$$

From the plots of log (q_e/q_m) as a function of 1/T, the discontinuities, Δ_f, determined at the temperature T_f of the onset of the liquid-crystalline state are

$$\Delta_f = \ln (q_e/q_m)_{fl} - \ln (q_e/q_m)_{cr}.$$

Following a procedure similar to that of Zachariasse et al., (1980), we have for the difference of the free energies of activation in the crystalline and the liquid-crystalline phases

$$\Delta G^{\ddagger}_{cr} - \Delta G^{\ddagger}_{fl} = RT_f\Delta_f.$$

Furthermore, the activation entropy differences at T_f can be obtained from

$$T_f(\Delta S^{\ddagger}_{cr} - \Delta S^{\ddagger}_{fl}) = E_{cr} - E_{fl} - (\Delta G^{\ddagger}_{cr} - \Delta G^{\ddagger}_{fl}).$$

These calculations employ the following relation for the viscosity, η, based on the transition state theory (Glasstone et al., 1941)

$$\eta = \frac{hN}{V} e^{\Delta G^{\ddagger}/RT}$$

Table 3. Activation energies for intramolecular excimer formation by PC_3P in DSPC bilayer liposomes for different melittin-to-lipid molar ratios in the crystalline phase, E_{cr}, and in the liquid-crystalline (fluid) phase E_{fl}.

Molar ratio	E_{cr} kcal/mol	E_{cr} kJ/mol	E_{fl} kcal/mol	E_{fl} kJ/mol
0	10.5 ± 0.1	43.9 ± 0.4	3.1 ± 0.2	13.0 ± 0.8
1:500	10.8 ± 0.1	45.2 ± 0.4	4.4 ± 0.3	18.4 ± 1.2
1:300	10.7 ± 0.2	44.8 ± 0.8	4.6 ± 0.3	19.2 ± 1.2
1:100	10.7 ± 0.2	44.8 ± 0.8	5.0 ± 0.4	20.9 ± 1.7
1:40	11.6 ± 0.1	48.3 ± 0.4	5.5 ± 0.2	23.0 ± 0.8
1:10	10.9 ± 0.2	45.4 ± 0.8	4.8 ± 0.4	20.0 ± 1.7

where h is Planck's constant, N is Avogadro's number, V the molecular volume, and R the gas constant. Furthermore, it is assumed that q_e/q_m is proportional to $1/\eta$. This has been shown to be the case for intramolecular excimer formation (except at very low viscosities) by PC_3P as well as for bis (4-biphenylmethyl) ether (Avouris et al., 1974; Zachariasse et al., 1980; Melnick et al., 1981). Therefore,

$$\frac{q_e}{q_m} = K \frac{V}{hN} e^{-\Delta G^{\ddagger}/RT}$$

where K a proportionality constant. From this equation we have for the discontinuity Δf

$$\Delta_f = \ln(q_e/q_m)_{fl} - \ln(q_e/q_m)_{cr} = (\Delta G^{\ddagger}_{cr} - \Delta G^{\ddagger}_{fl})/RT_f$$

or

$$\Delta G^{\ddagger}_{cr} - \Delta G^{\ddagger}_{fl} = \Delta_f RT_f$$

Finally, from the relation

$$\Delta G^{\ddagger} = \Delta H^{\ddagger} - T\Delta S^{\ddagger}$$

and the above equation we have the activation entropy differences at T_f

$$\Delta S^{\ddagger}_{cr} - \Delta S^{\ddagger}_{fl} = [E_{cr} - E_{fl} - (\Delta G^{\ddagger}_{cr} - \Delta G^{\ddagger}_{fl})]/T$$

We illustrate the calculation of the discontinuity value at T_f from log (q_e/q_m) against $1/T$ plots for the sample containing melittin with a melittin-to-lipid molar ratio of 1:500 in Figure 15. a) Obtain the log $(q_e/q_m)_{fl}$ value at $1/T_f$. b) Extrapolate the crystalline-phase straight line up to the $1/T_f$ value and get the log $(q_e/q_m)_{cr}$ at $1/T_f$. c) Find the

$$\log (q_e/q_m)_{fl} - \log (q_e/q_m)_{cr}$$

value from which Δ_f can be obtained

$$\Delta_f = 2.3\ [\log\ (q_e/q_m)_{fl} - \log\ (q_e/q_m)_{cr}].$$

The results of the calculations for the discontinuities Δ_f, the difference of the free energies of activation, $\Delta G^{\ddagger}_{cr} - \Delta G^{\ddagger}_{fl}$, and the difference of the activation entropy, $(\Delta S^{\ddagger}_{cr} - \Delta S^{\ddagger}_{fl})$, are shown in Table 4 for different melittin-to-lipid molar ratios. The transition temperatures, T_t, the temperatures T_f of the onset of the liquid-crystalline phase, and the width of the transition, $T_f - T_{cr}$, (where T_{cr} is the temperature of the onset of the transition) are also listed in Table 4.

The nanosecond fluorometer enables us to observe the formation of intramolecular excimers by PC_3P when bound to DSPC as a function of time on the nanosecond time scale. First, in the free sample of DSPC and at 45°C we recorded the PC_3P spectra at different times relative to the peak of the exciting light pulse which is taken as zero time. Starting at zero nanoseconds and proceeding up to 87 ns we observed the excimer build up progressively. The results for times of o ns, 10.4 ns, 30.4 ns, 39.1 ns, 47.8 ns, 69.6 ns and 87 ns are shown in Fig. 19. All the spectra have been normalized at the second peak at 397 nm. From that figure we can see that, whereas there is very little excimer at short times, as time passes the excimer grows higher with a peak at ~ 480 nm. The measurements were then repeated in samples containing melittin with melittin-to-lipid molar ratios of 1:500, 1:100 and 1:40. The results of those measurements are shown in Figs. 20-22. As can be seen from those

Table 4. Discontinuies Δ_f, differences of free energies of activation $\Delta G^{\ddagger}_{cr} - \Delta G^{\ddagger}_{fl}$, differences of activation entropies $\Delta S^{\ddagger}_{cr} - \Delta S^{\ddagger}_{fl}$, transition temperatures T_t, temperatures of onset of liquid-crystalline phase T_f, and width of transition $T_f - T_{cr}$ (where T_{cr} is the temperature of the onset of transition) for intramolecular excimer formation by PC_3P embedded in DSPC liposomes in the presence of different melittin-to-lipid molar ratios.

Molar ratio	Δ_f	$\Delta G^{\ddagger}_{cr} - \Delta G^{\ddagger}_{fl}$ kJ/mol	$\Delta S^{\ddagger}_{cr} - \Delta S^{\ddagger}_{fl}$ J/mol K	T_t °C	T_f °C	$T_f - T_{cr}$ °C
0	0.39 ± 0.2	1.08 ± 0.06	89.4 ± 3.7	57.5	60.3	6.9
1:500	0.41 ± 0.4	1.13 ± 0.08	76.6 ± 4.6	57.4	60.8	7.9
1:300	0.53 ± 0.3	1.47 ± 0.12	71.7 ± 5.8	57.5	61.4	9.2
1:100	0.62 ± 0.4	1.72 ± 0.12	65.8 ± 7.1	57.3	62.5	12.4
1:40	0.76 ± 0.2	2.12 ± 0.14	68.7 ± 3.7	57.5	63.1	13.6
1:10	1.06 ± 0.4	2.96 ± 0.14	66.7 ± 7.1	57.5	64.2	15.2

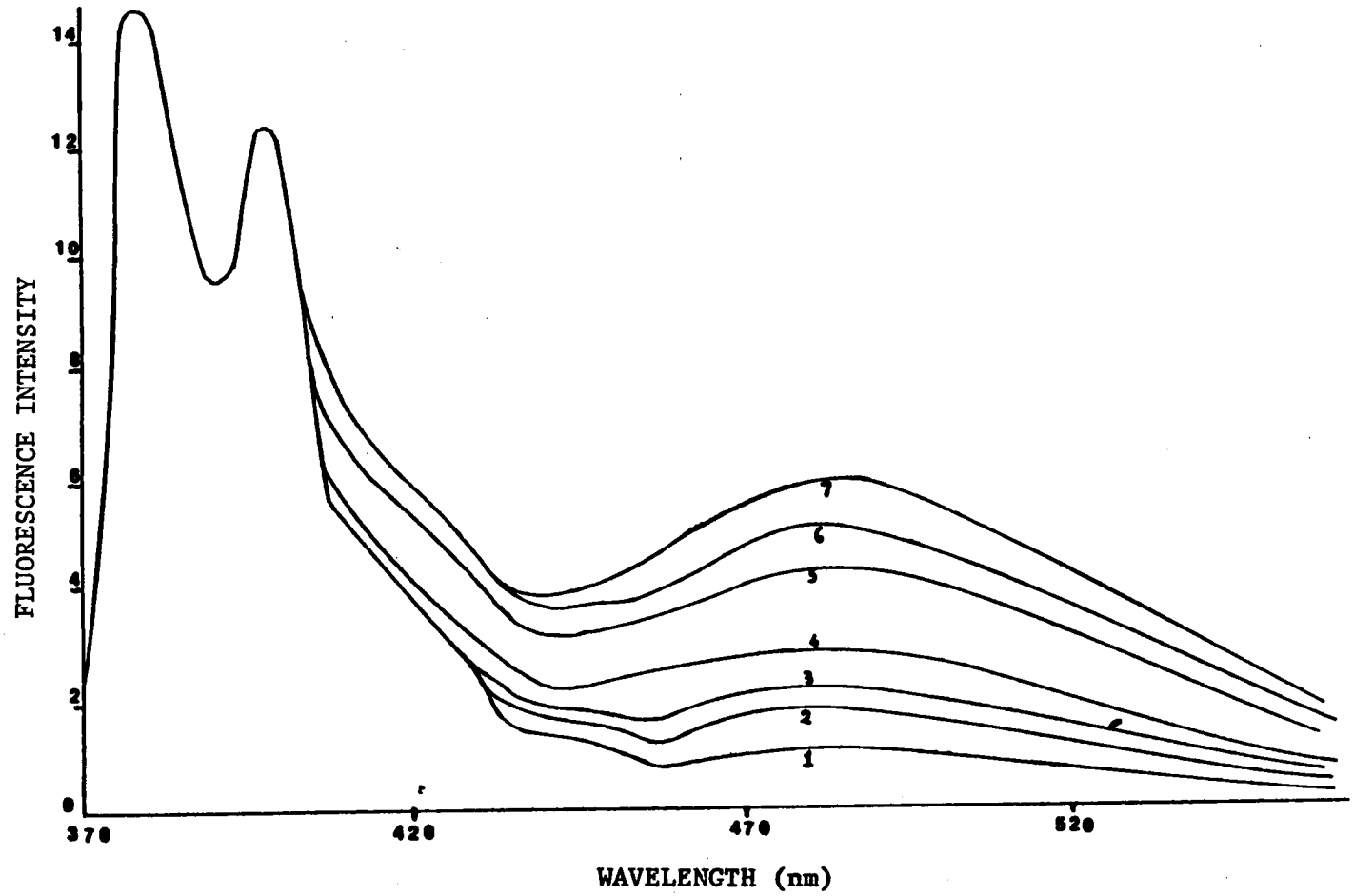


Figure 19. Time-resolved spectra of PC_3P embedded in DSPC liposomes at 45°C, for the following times relative to the peak of the exciting light pulse. (1) 0 ns; (2) 10.4 ns; (3) 30.4 ns; (4) 39.1 ns; (5) 47.8 ns; (6) 69.6 ns; and (7) 87 ns.

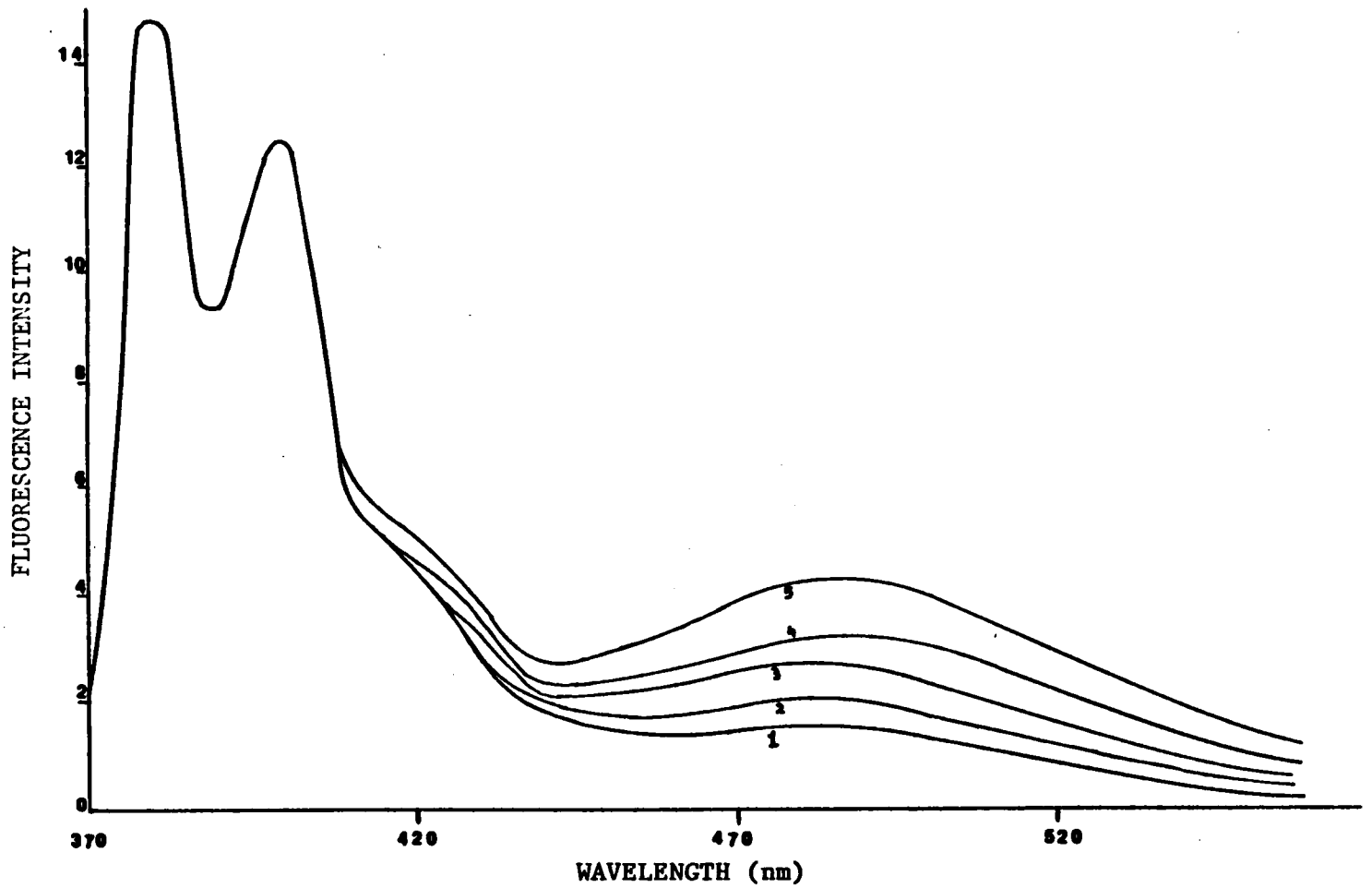


Figure 20. Time-resolved fluorescence spectra of PC_3P embedded in DSPC liposomes in the presence of melittin at a melittin-to-lipid molar ratio of 1:500 at 45°C for the following times. (1) 0 ns; (2) 17.4 ns; (3) 30.4 ns; (4) 47.8 ns; and (5) 79 ns.

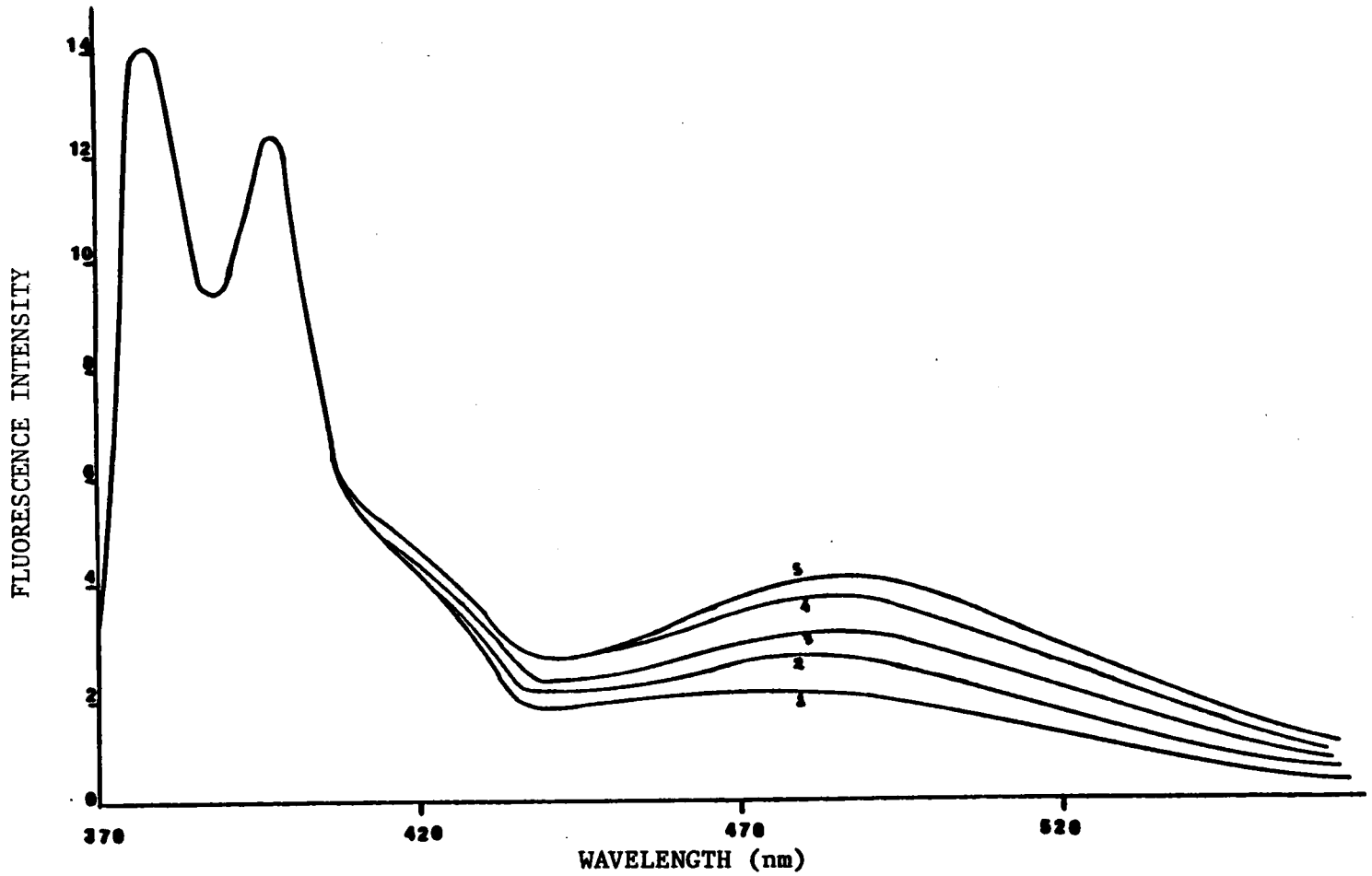


Figure 21. Time-resolved fluorescence spectra of PC_3P embedded in DSPC liposomes in the presence of melittin at a melittin-to-lipid molar ratio of 1:100 at 45°C for the following times. (1) 0 ns; (2) 30.4 ns; (3) 47.8 ns; (4) 69.6 ns; and (5) 117.4 ns.

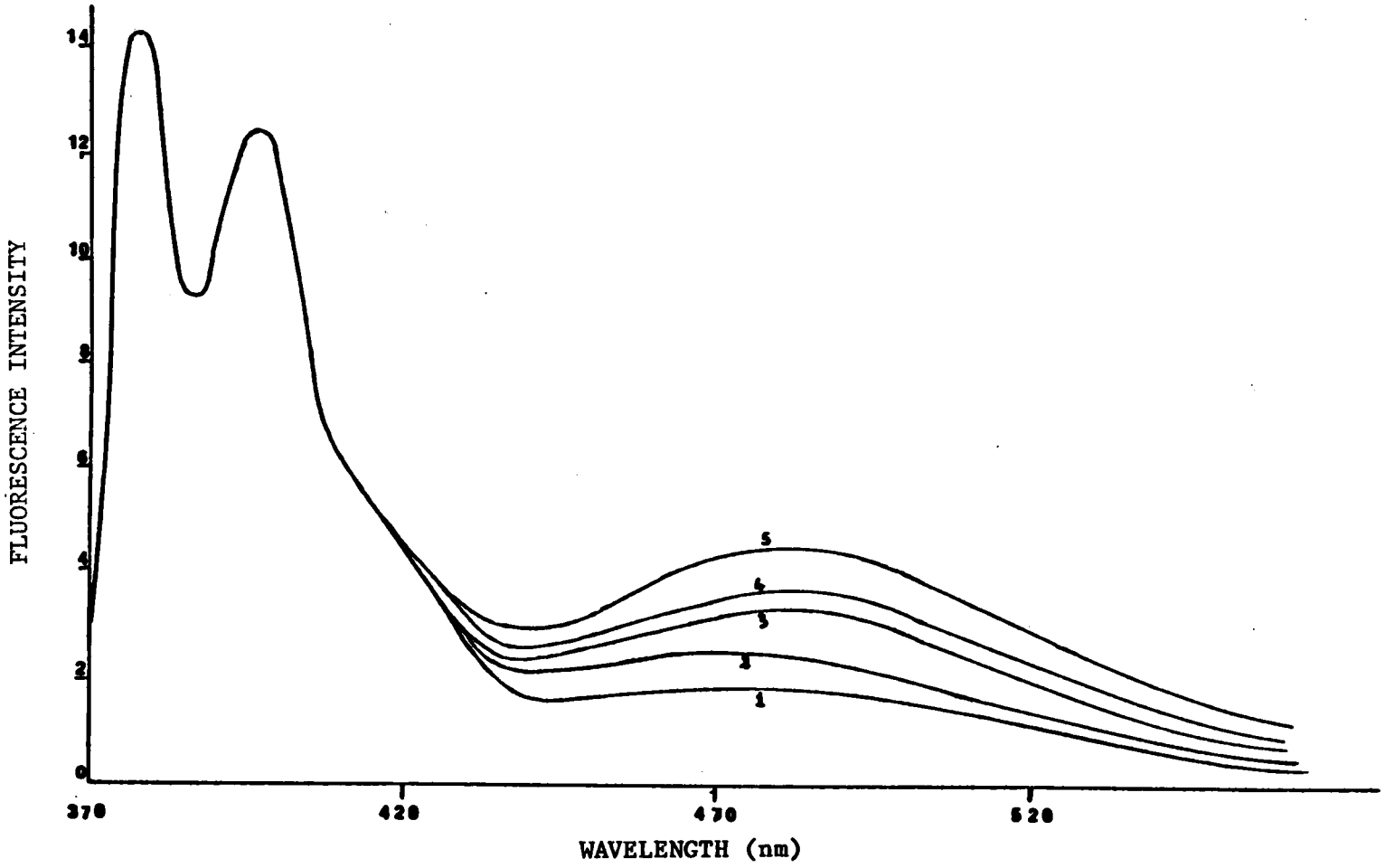


Figure 22. Time-resolved fluorescence spectra of PC_3P embedded in DSPC liposomes in the presence of melittin at a melittin-to-lipid molar ratio of 1:40 at 45°C for the following times. (1) 0 ns; (2) 10.4 ns; (3) 30.4 ns; (4) 39.1 ns; and (5) 69.6 ns.

figures, the presence of melittin in the sample affects the height of excimer at the various times of the measurements.

The next step was to study the intramolecular excimer formation for the free sample and the ones containing melittin, with the same as before molar ratios, at the temperature of 67°C. The normalized spectra of these measurements are shown in Figs. 23-26.

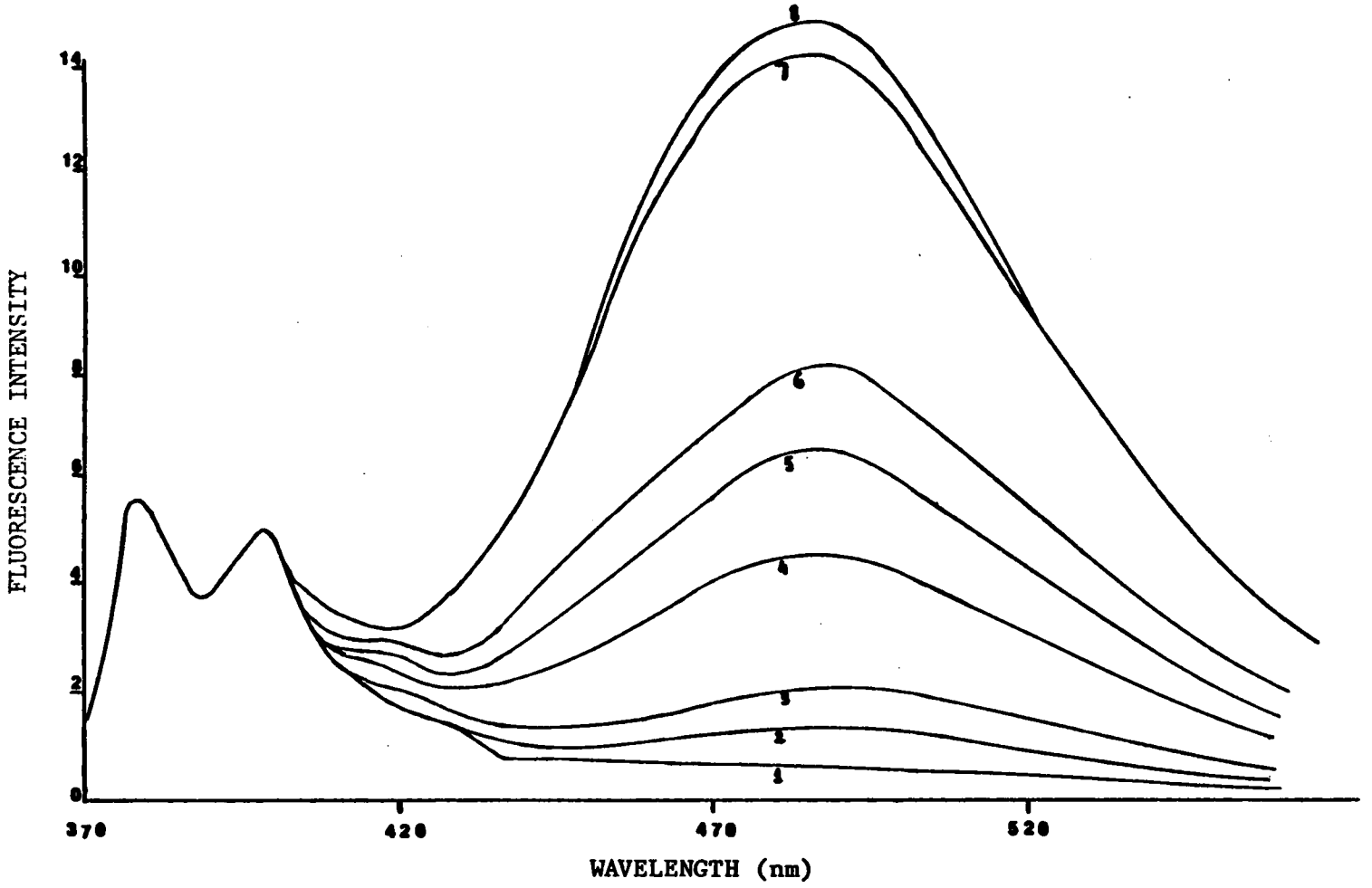


Figure 23. Time-resolved spectra of PC_3P embedded in DSPC liposomes at 67°C, for the following times relative to the peak of the exciting light pulse. (1) 0 ns; (2) 10.4 ns; (3) 17.4 ns; (4) 30.4 ns; (5) 39.1 ns; (6) 47.8 ns; (7) 69.6 ns; and (8) 87 ns.

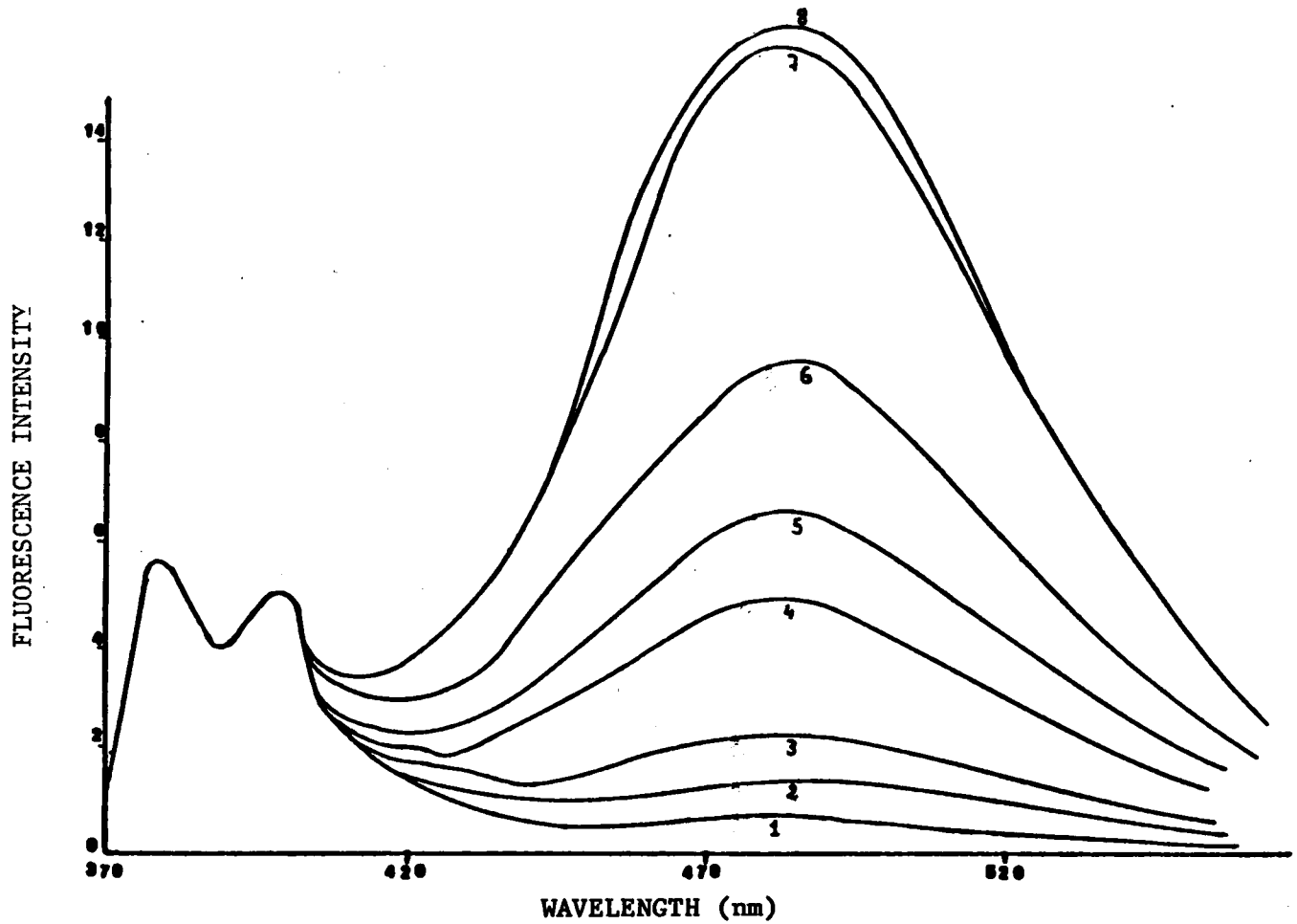


Figure 24. Time-resolved fluorescence spectra of PC_3P embedded in DSPC liposomes in the presence of melittin at a melittin-to-lipid molar ratio of 1:500 at 67°C for the following times. (1) 0 ns; (2) 10.4 ns; (3) 17.4 ns; (4) 30.4 ns; (5) 39.1 ns; (6) 47.8 ns; (7) 69.6 ns; and (8) 87 ns.

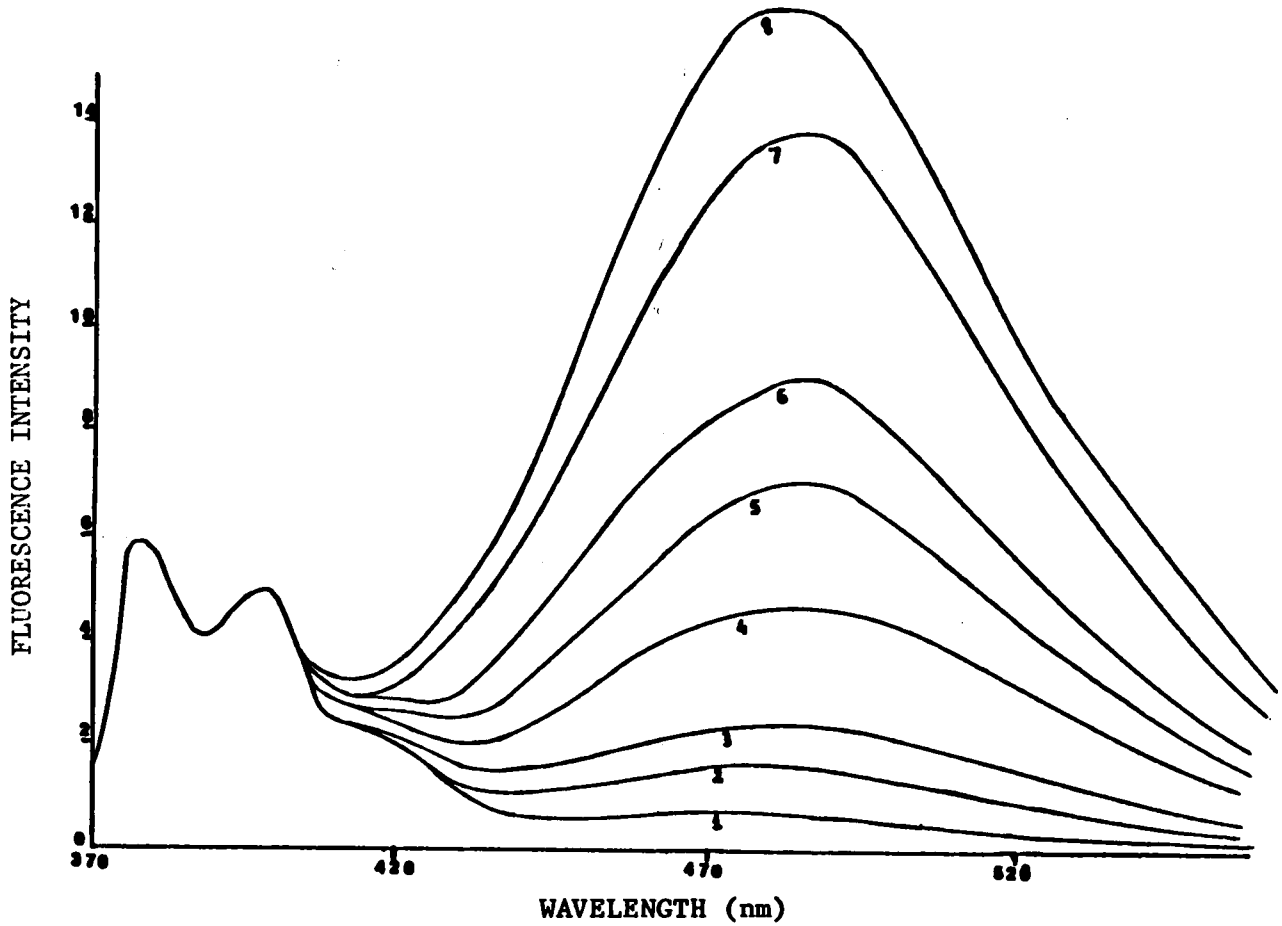


Figure 25. Time-resolved fluorescence spectra of PC_3P embedded in DSPC liposomes in the presence of melittin at a melittin-to-lipid molar ratio of 1:100 at 67°C for the following times. (1) 0 ns; (2) 10.4 ns; (3) 17.4 ns; (4) 30.4 ns; (5) 39.1 ns; (6) 47.8 ns; (7) 69.6 ns; and (8) 87 ns.

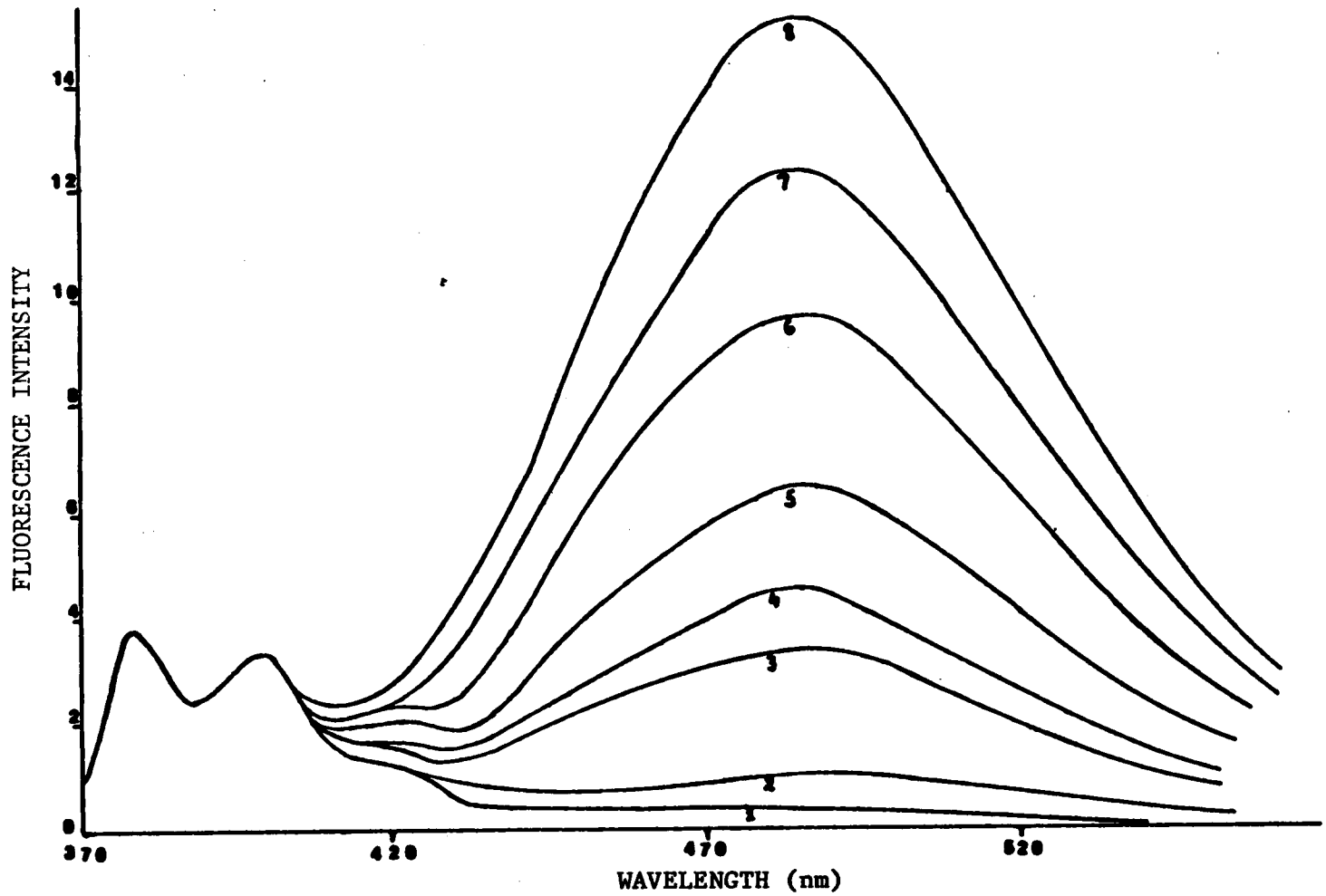


Figure 26. Time-resolved fluorescence spectra of PC_3P embedded in DSPC liposomes in the presence of melittin at a melittin-to-lipid molar ratio of 1:40 at 67°C for the following times. (1) 0 ns; (2) 10.4 ns; (3) 30.6 ns; (4) 39.1 ns; (5) 47.8 ns; (6) 69.6 ns; (7) 87 ns; and (8) 117.4 ns.

CHAPTER IV

DISCUSSION

This work aims at understanding the nature of interaction between melittin and phospholipid membranes. It is known that melittin interacts with membranes causing structural changes in them and that it prepares the way for the enzyme phospholipase A_2 to attack and ultimately lyse the membrane (Habermann, 1972). From previous studies from this laboratory which employed the single tryptophan residue as an intrinsic fluorescence probe, it was found that melittin aggregates when it binds to the membrane, and also that tryptophan is not embedded deeply into the phospholipid membrane.

1. Enhancement of the o-o vibronic transition of pyrene embedded in DSPC liposomes.

The present work was undertaken so that we use further approaches, namely extrinsic fluorescence probes. The first probe we used is pyrene. We have utilized the phenomenon of the enhancement of the o-o vibronic band of pyrene when it interacts with polar groups. Previous work from our laboratory (see Introduction) established the nature of that enhancement. It is a ground-state phenomenon involving complex formation between pyrene and polar groups. That effect was utilized to obtain information about the location of pyrene in the phospholipid membrane. The enhancement ratio in the phospholipids was compared with the enhancement ratios in different solvents. The important finding from those studies was

that pyrene is located in the vicinity of the glycerol backbone and not, as was previously assumed in the literature, in the interior of the bilayer. It was also shown that the location of pyrene depends on the temperature and on the state of the liposome, i.e. as the temperature is increased approaching the transition temperature T_t, pyrene penetrates further into the bilayer. The latter observation was used for obtaining an enhancement profile as a function of temperature which allowed the determination of the transition temperature in an accurate way. The enhancement ratio R was measured as the ratio of the o-o band at ~ 376 nm to that at ~ 387 nm..

In the present study we have used pyrene as a probe when melittin binds to the phospholipid distearoylphosphatidylcholine, (DSPC), at different melittin-to-lipid molar ratios. That lipid was chosen because it does not become turbid upon interaction with melittin. In actual fact, it becomes clearer, as a result of a reduction in the size of the liposome. First, we determined the transition temperature of the liposome in the absence of melittin and found it to be 52 ± 0.5 °C which agrees very well with the value of 51.3 °C reported by Lentz et al (1976). Now looking at Figs. 5-11 we notice that at room temperature, around 26°C, there is a depression in the enhancement ratio R which continues with increasing melittin-to-lipid molar ratio and reaches its lowest value at a molar ratio of 1:80 (Fig. 8). After that molar ratio, R starts increasing slowly and approaches the value for the free sample for the ratio of 1:20 (Fig. 7). The trend is reversed for the ratio of 1:5 (Fig. 6) which exhibits a decrease in R. It is possible however, that at that high

molar ratio the bilayer may be severely disrupted. For a molar ratio of 1:500 (Fig. 11) the enhancement profile is the lowest in the vicinity of T_t for all the ratios studied. For the ratios of 1:200 (Fig. 10) and 1:300 (Fig. 10) the profiles differ only slightly from that for the free sample. At the ratio of 1:165 (Fig. 9) the profile is noticeably higher than that for the free in the vicinity of the transition temperature T_t. This trend continues for higher ratios with the profile reaching its maximum value for the ratio of 1:20 (Fig.7). The profile for the ratio of 1:5 (Fig. 6) exhibits a small decrease relative to those for 1:20 (Fig. 7) and 1:10 (Fig.6), deviating again from the observed trend.

Now, for the high-temperature plateau, starting from low melittin molar ratios, one observes a somewhat lower value as compared to that for the free sample. The plateau level is seen to be raised upon increasing the molar ratio and to be virtually coincident with that for the free sample for a ratio of 1:80. Upon further increasing the ratio, the plateau level drops for the ratios of 1:40 (Fig. 7.), 1:20 (Fig. 7) and 1:5 (Fig. 6). For the ratio of 1:10 (Fig. 6), however, the plateau is somewhat higher than that for 1:20 (Fig. 7). These trends in the dependence of the enhancement ratio R, on the melittin-to-lipid molar ratio are shown in Fig. 27, for 26°C, 47°C, and 66°C.

It should be recalled that R is a measure of the effective polarity of the microenvironment of the probe in the liposome (Georghiou and Mukhopadhyay, 1981). The present observations, therefore, imply that in the presence of high molar ratios of

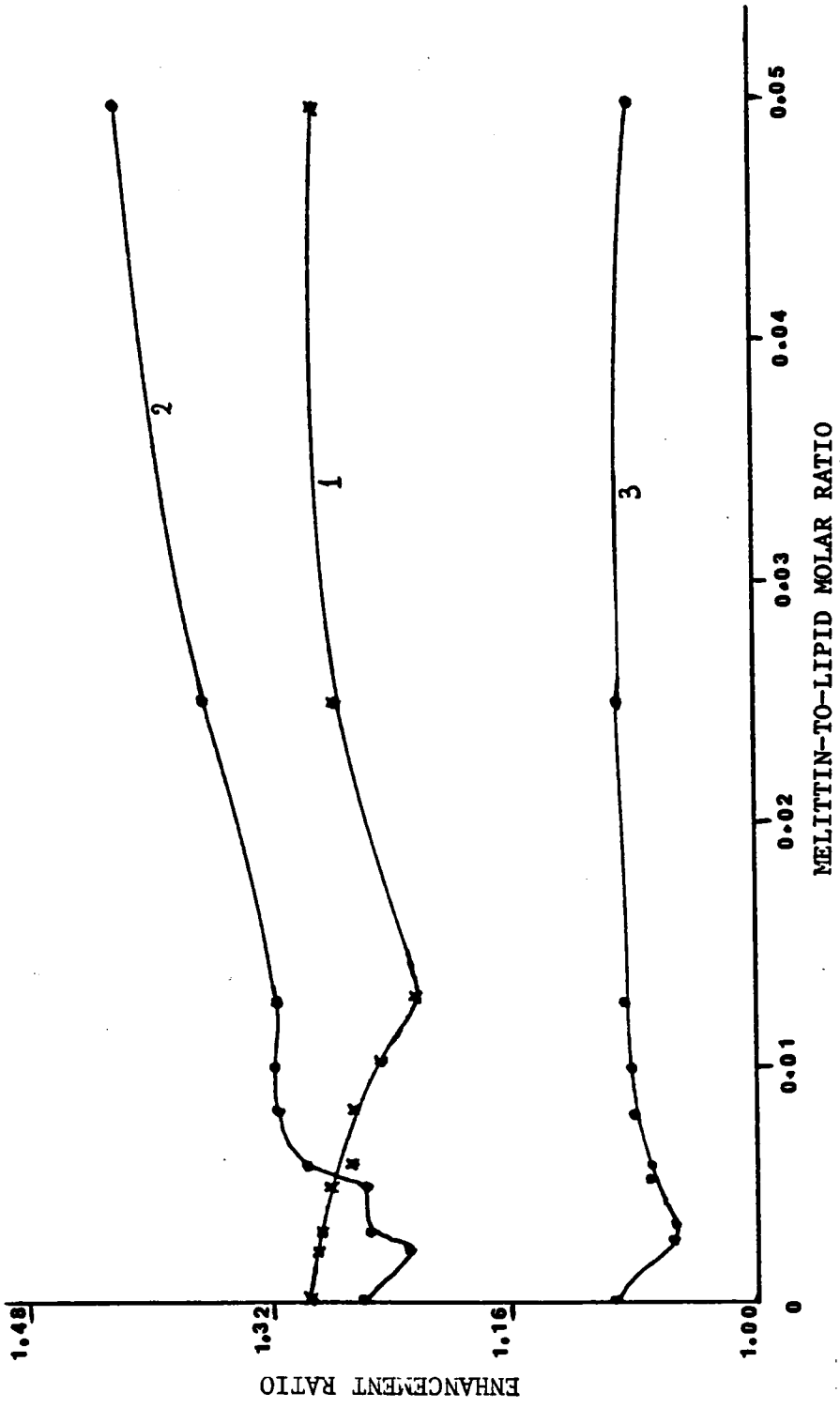


Figure 27. Plot of the enhancement ratio as a function of the melittin-to-lipid molar ratio (expressed as a fraction). (1) for 26°C; (2) for 47°C; and (3) for 66°C.

melittin, e.g. 1:20, the polarity of the microenvironment of pyrene increases. This is interpreted as meaning that pyrene is pushed more toward the direction of the polar head groups. There is, however, another potential interpretation of these data. It could be argued that the location of the probe is not affected by melittin but that the protein changes the structure of the bilayer with a concurrent increase in the ability of water to penetrate into the location of pyrene. That possibility was discussed and discounted for the case of lipid-cholesterol systems (Lianos and Georghiou, 1979). That argument was based on the observation that in binary mixtures of polar solvents in heptane one needs at least 1M of polar solvent for a barely detectable enhancement. Consequently, on the basis of water penetration one would need unsually large amounts of water penetrating into the bilayer to account for the observed enhancement.

We could get an idea as to the scale of polarities involved by comparing the observed range of R values with those of some solvents. Most of the profiles start at room temperatures at an R value of ~ 1.30 which is somewhat lower than that of 1.37 observed in 95% ethanol. Just below T_t, for high molar ratios, e.g. 1:20, R approaches a value of 1.44 which is close to that of 1.50 for pyrene in methanol. In the neighborhood of T_t the R values are comparable to those of 1.19 of pyrene in isopropanol and 1.15 in butanol. Above T_t ,the R values are ~ 1.06 which is close to that of 1.10 in ethyl ether. It should be noted that even above T_t pyrene is not

embedded deeply into the hydrophobic core, as the R value of pyrene in heptane, 0.64, is much lower than any of the observed R values.

The effect of melittin on the phase transition temperature was also investigated in the present study. An increase in T_t by 2-4°C was observed depending on the molar ratio. It should be noted in this respect that there have been two reports in the literature of Raman studies on the effect of melittin on the transition temperature of phospholipids. The first study by Lavialle et al., (1980), found a lowering of the transition temperature of DMPC for a molar ratio of 1:10 by 12°C. This study was on nonsonicated samples. The second study by Verma and Wallach, (1976), showed that for a molar ratio of 1:28 the transition temperature of DMPC was raised by 13°C. This study was done on sonicated samples. It would be rather surprising if these contradicting findings are due to the different methods of sample preparation employed in the two studies. Our data agree with the findings of Verma and Wallach that melittin raises the transition temperature of phospholipids. Referring to the effect of melittin on the width of the transition, (Table 2), it is seen that there is a progressive decrease in the width as the molar ratio increases reaching a minimum value for 1:80. It then increases and attains a value which is lower than that of the free profile (for which there is a rather pronounced uncertainty because of the broad nature of the profile). It should be noted that the width of the transition is a measure of the order in the phospholipid. Thus, the results imply that melittin tends to

reorganize the phospholipid, being more effective in that in the neighborhood of the molar ratio of 1:80.

A plot of log R against 1/T yielded straight lines for temperatures below T_t and for molar ratios > 1:165 (Figs. 28-39). By assuming an Arrhenius form for the enhancement ratio

$$R = Ae^{-\Delta E/RT}$$

(where R in the exponent is the gas constant) we obtained values for the apparent activation energies ΔE (Table 5). It is seen from that table that the values are very low, of the order of thermal energy. We now address the question of assigning physical significance to the activation energy values. Melittin, thermally-aided, is considered to affect the organization of the phospholipid. Pyrene, being in the general vicinity of the glyceral backbone, senses and reports such structural rearrangements. The activation energy ΔE, therefore, can be considered to be the energy required for forcing the probe more outward. This is based on the observation that the profiles for high molar ratios exhibit pronounced enhancement in the temperature region of 36-48°C, implying that the reorganization of the lipid in that temperature range tends to impede the penetration of the probe into the bilayer. We consider that restructuring as involving an increase in the packing density with a concomitant decreease in the fluidity of the bilayer in the presence of melittin. The penetration of the probe can be considered to occur by thermally-induced rotational isomerization of the acyl chains (Trauble, 1971; Marsh, 1974). The energy involved in such a process is ~ RT ≃ 0.8 kcal/mol (Trauble, 1971) which is of the order of

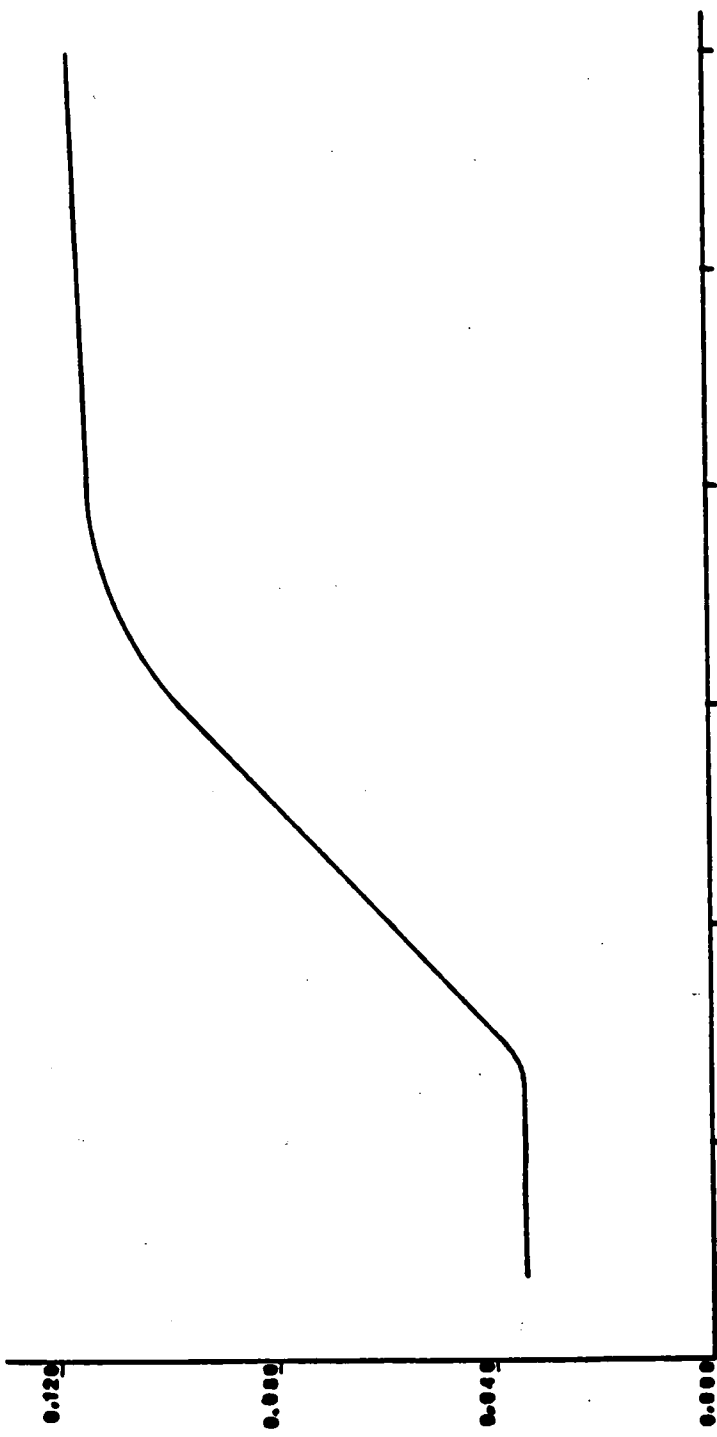


Figure 28. Logarithm of the enhancement ratio of the o-o vibronic transition of pyrene embedded in DSPC liposomes as a function of 1/temperature.

69

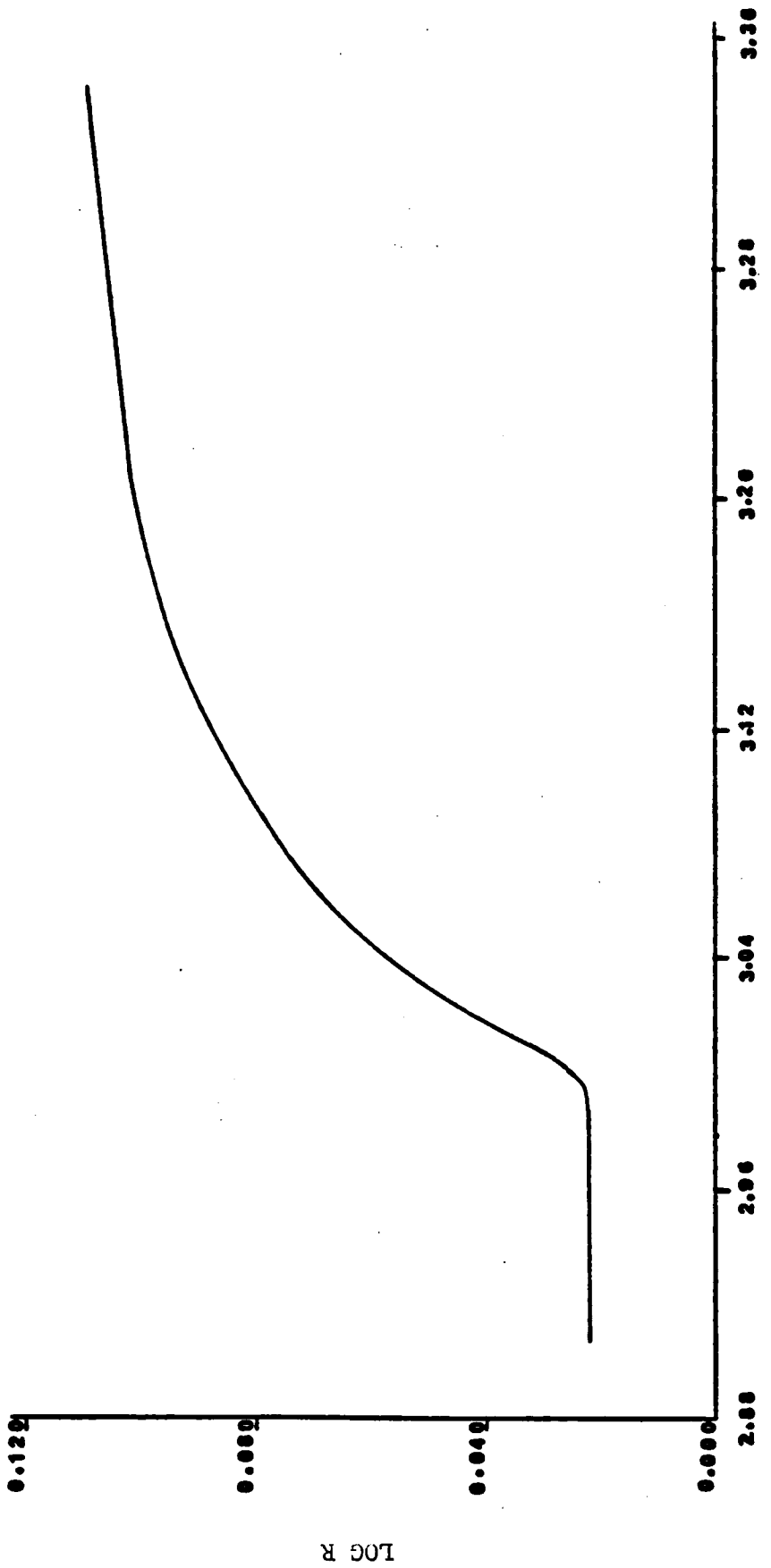


Figure 29. Logarithm of the enhancement ratio of the o-o vibronic transition of pyrene embedded in DSPC liposomes in the presence of 1:500 melittin-to-lipid molar ratio, as a function of 1/temperature.

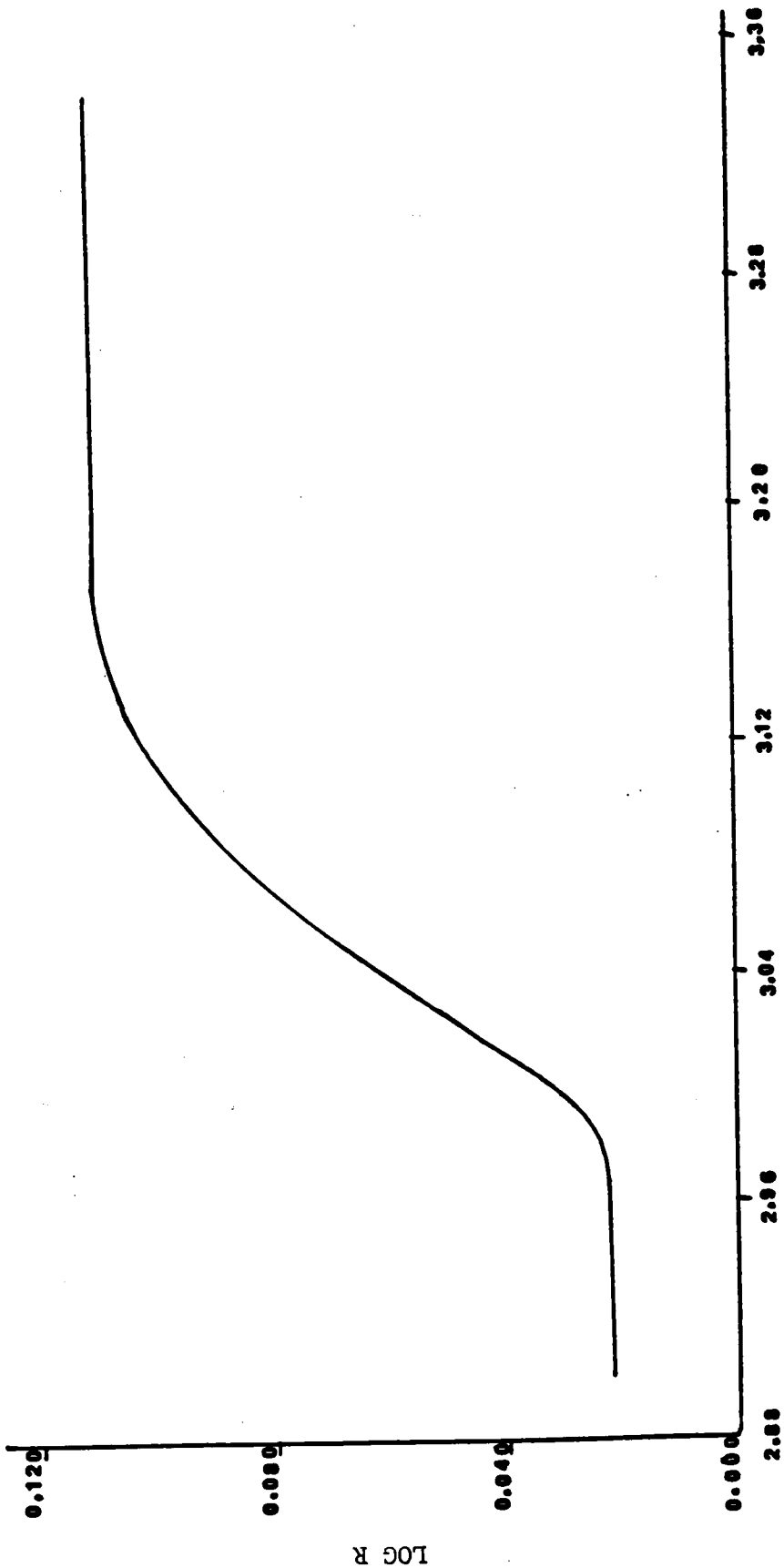


Figure 30. Logarithm of the enhancement ratio of the o-o vibronic transition of pyrene embedded in DSPC liposomes in the presence of 1:300 melittin-to-lipid molar ratio, as a function of 1/temperature.

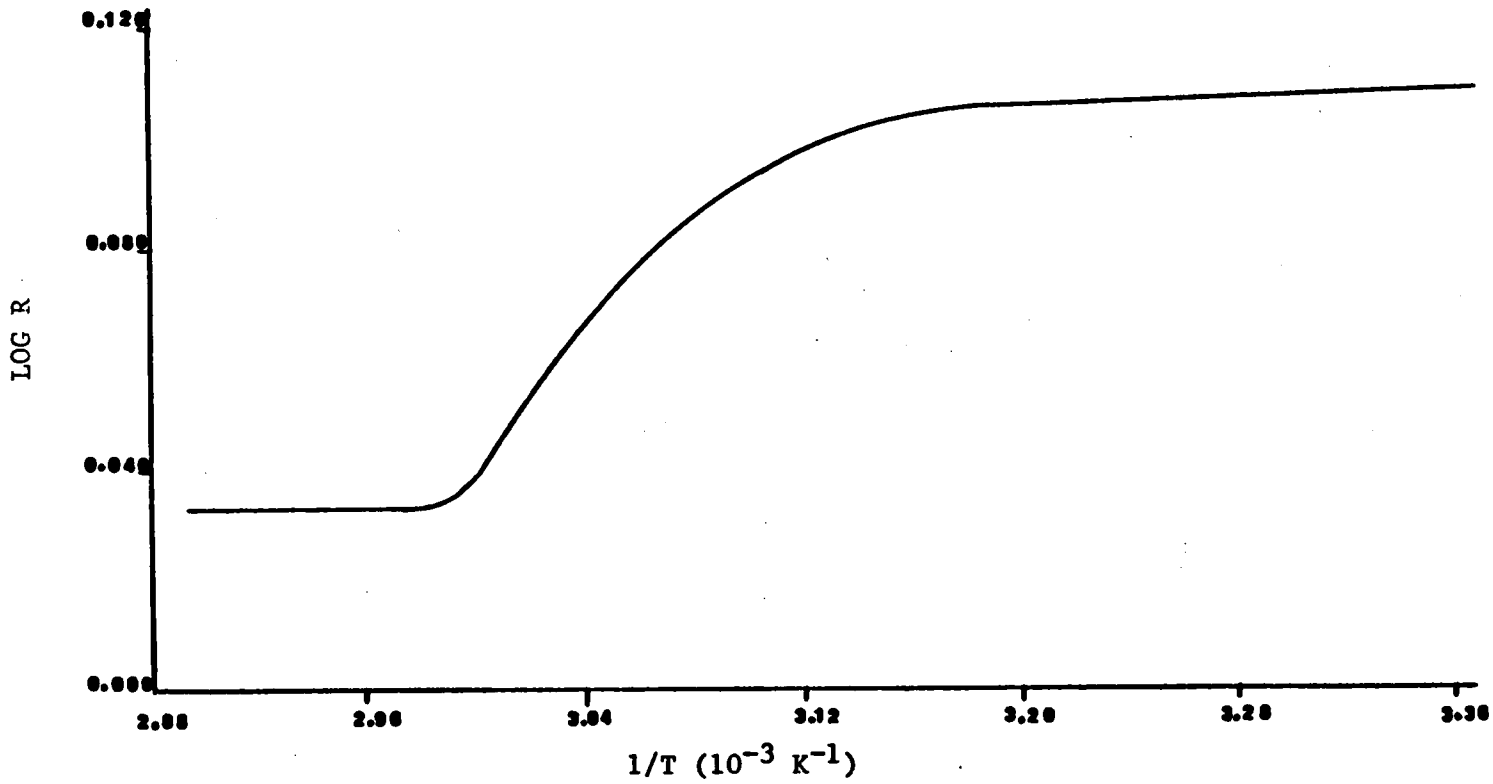


Figure 31. Logarithm of the enhancement ratio of the o-o vibronic transition of pyrene embedded in DSPC liposomes in the presence of 1:200 melittin-to-lipid molar ratio, as a function of 1/temperature.

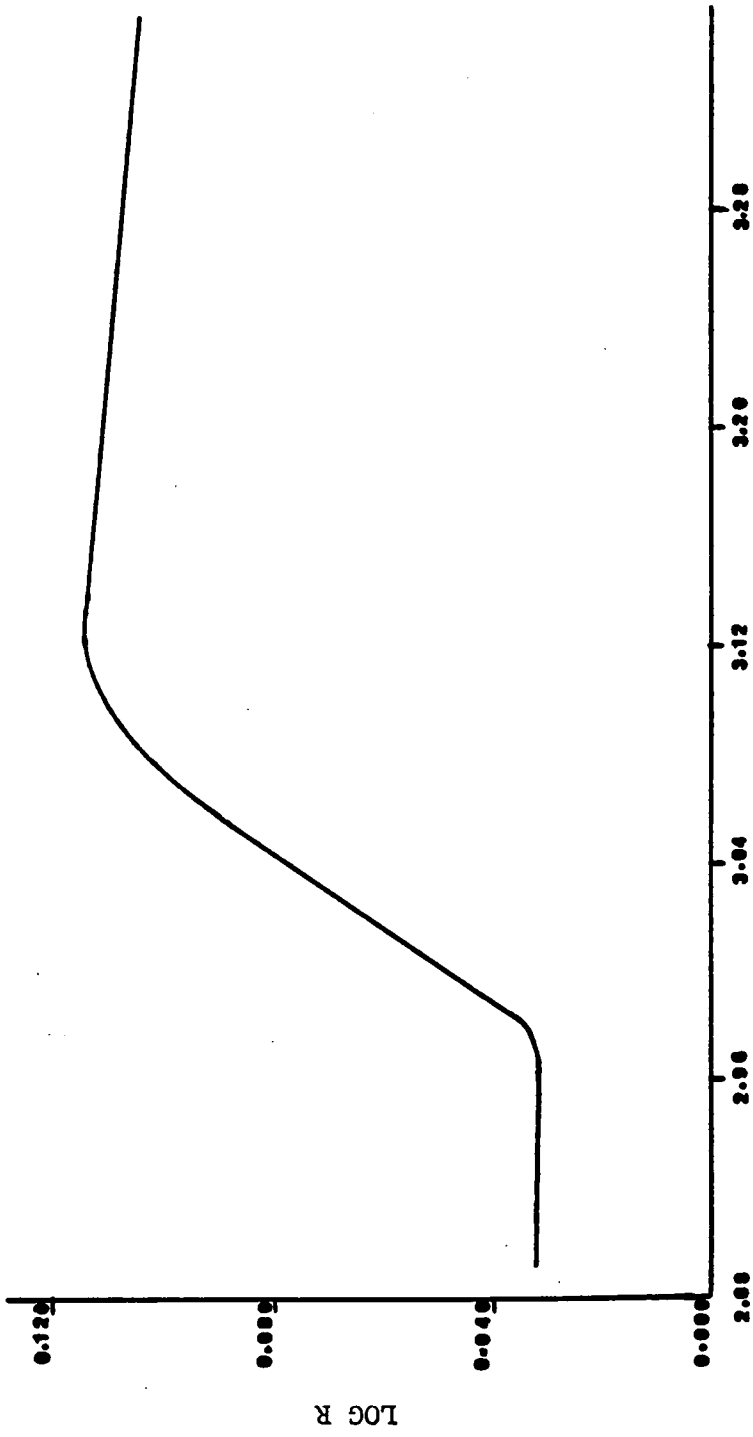


Figure 32. Logarithm of the enhancement ratio of the o-o vibronic transition of pyrene embedded in DSPC liposomes in the presence of 1:165 melittin-to-lipid molar ratio, as a function of 1/temperature.

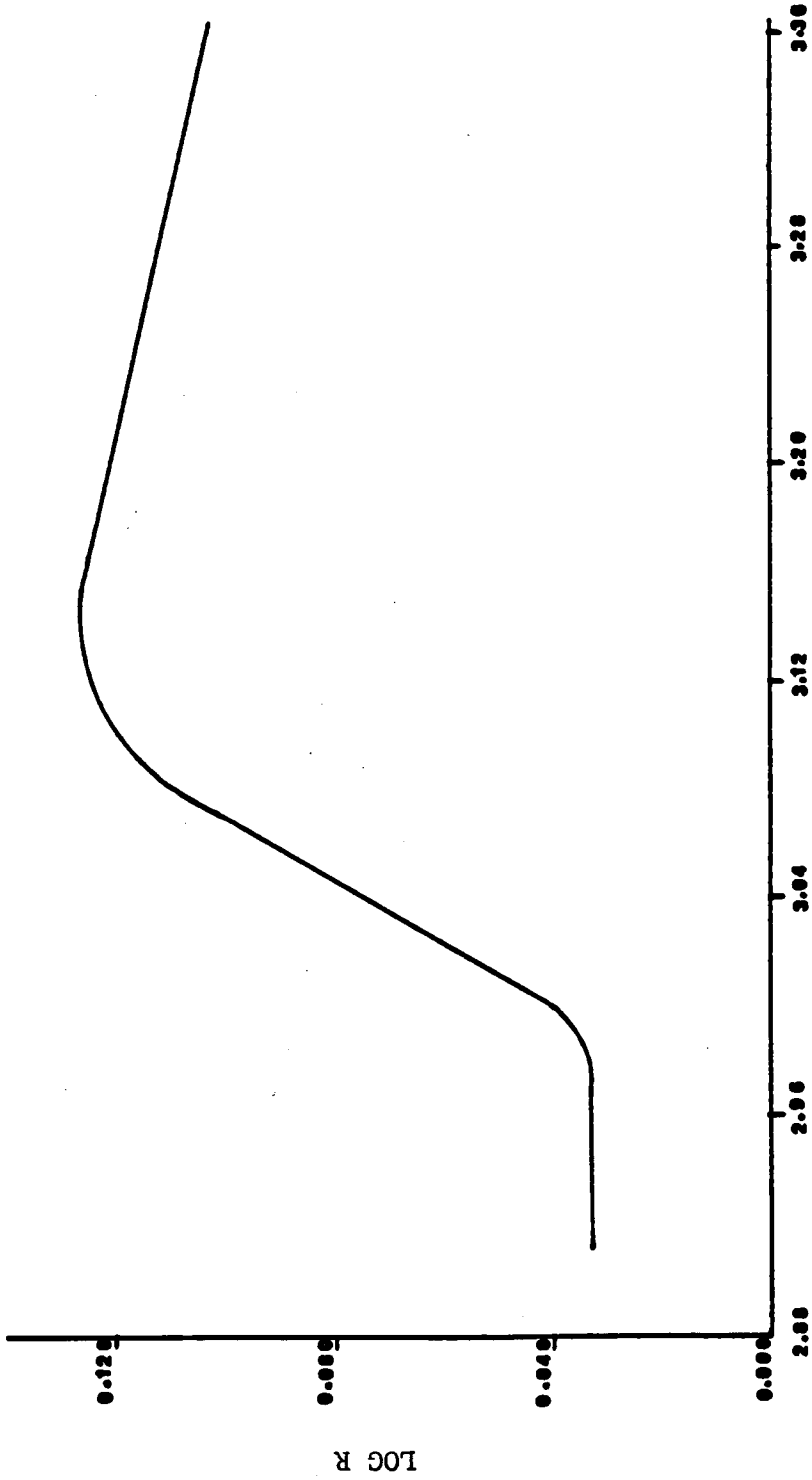


Figure 33. Logarithm of the enhancement ratio of the o-o vibronic transition of pyrene embedded in DSPC liposomes in the presence of 1:120 melittin-to-lipid molar ratio, as a function of 1/temperature.

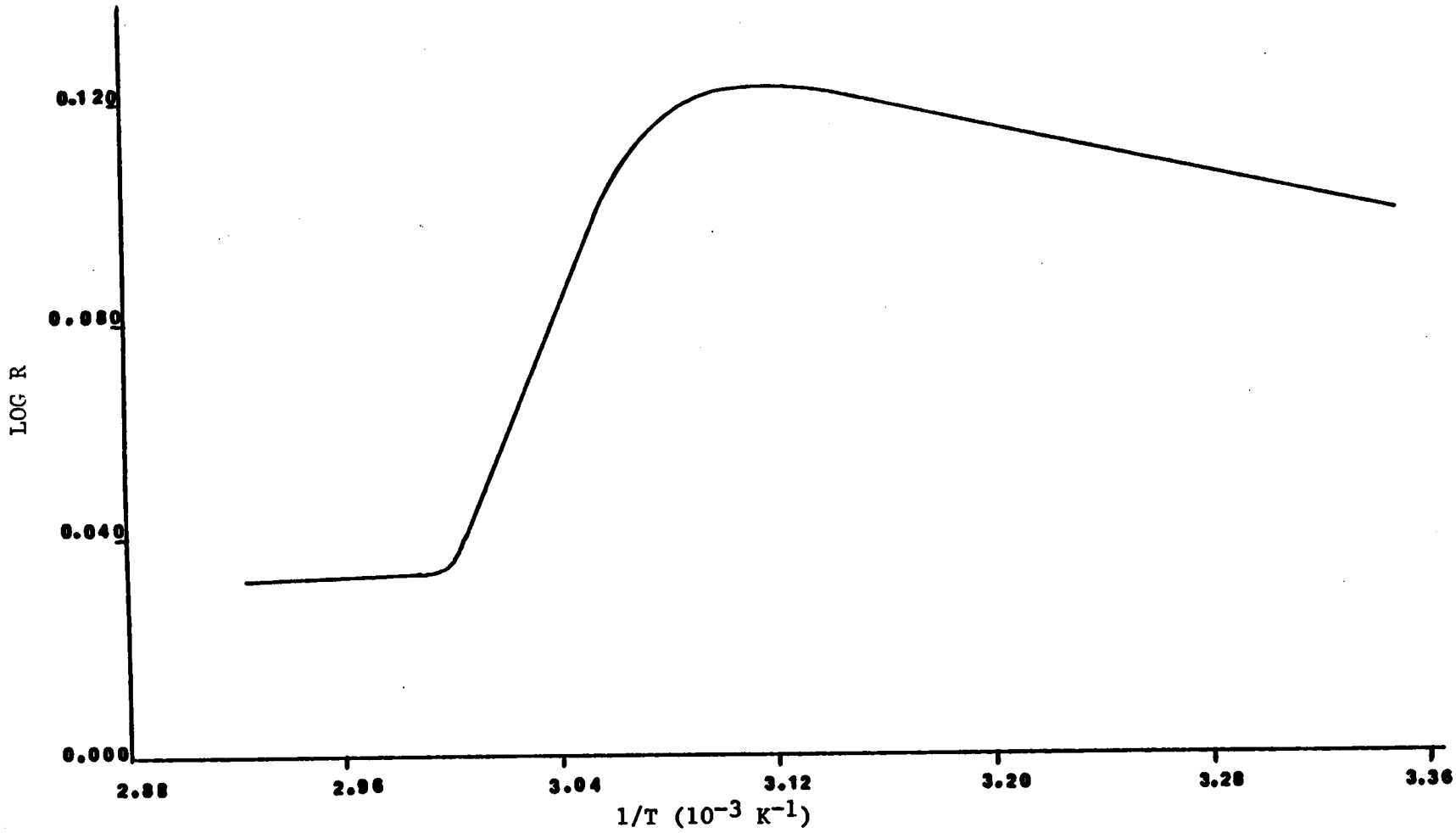


Figure 34. Logarithm of the enhancement ratio of the o-o vibronic transition of pyrene embedded in DSPC liposomes in the presence of 1:100 melittin-to-lipid molar ratio, as a function of 1/temperature.

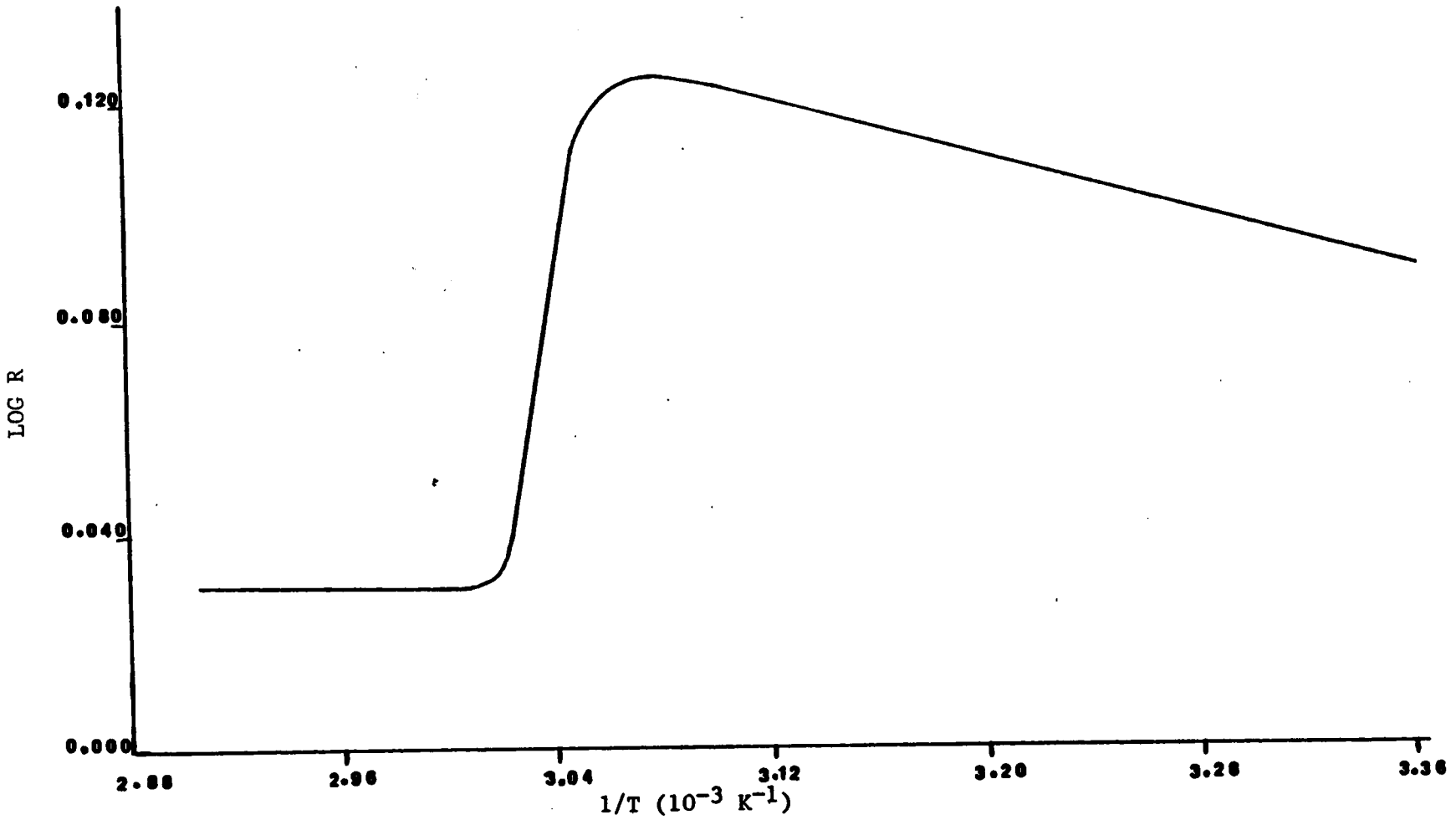


Figure 35. Logarithm of the enhancement ratio of the o-o vibronic transition of pyrene embedded in DSPC liposomes in the presence of 1:80 melittin-to-lipid molar ratio, as a function of 1/temperature.

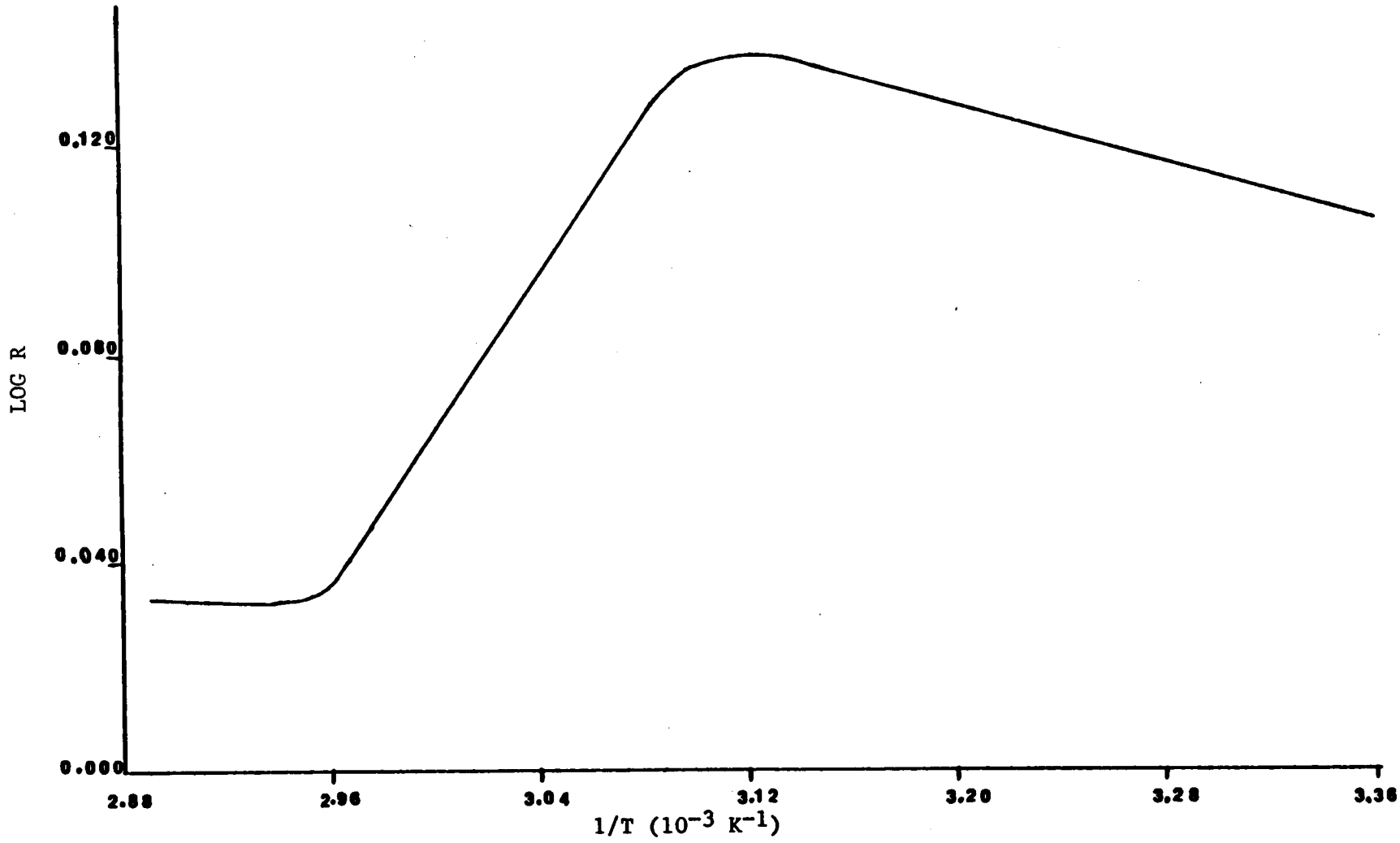


Figure 36. Logarithm of the enhancement ratio of the o-o vibronic transition of pyrene embedded in DSPC liposomes in the presence of 1:40 melittin-to-lipid molar ratio, as a function of 1/temperature.

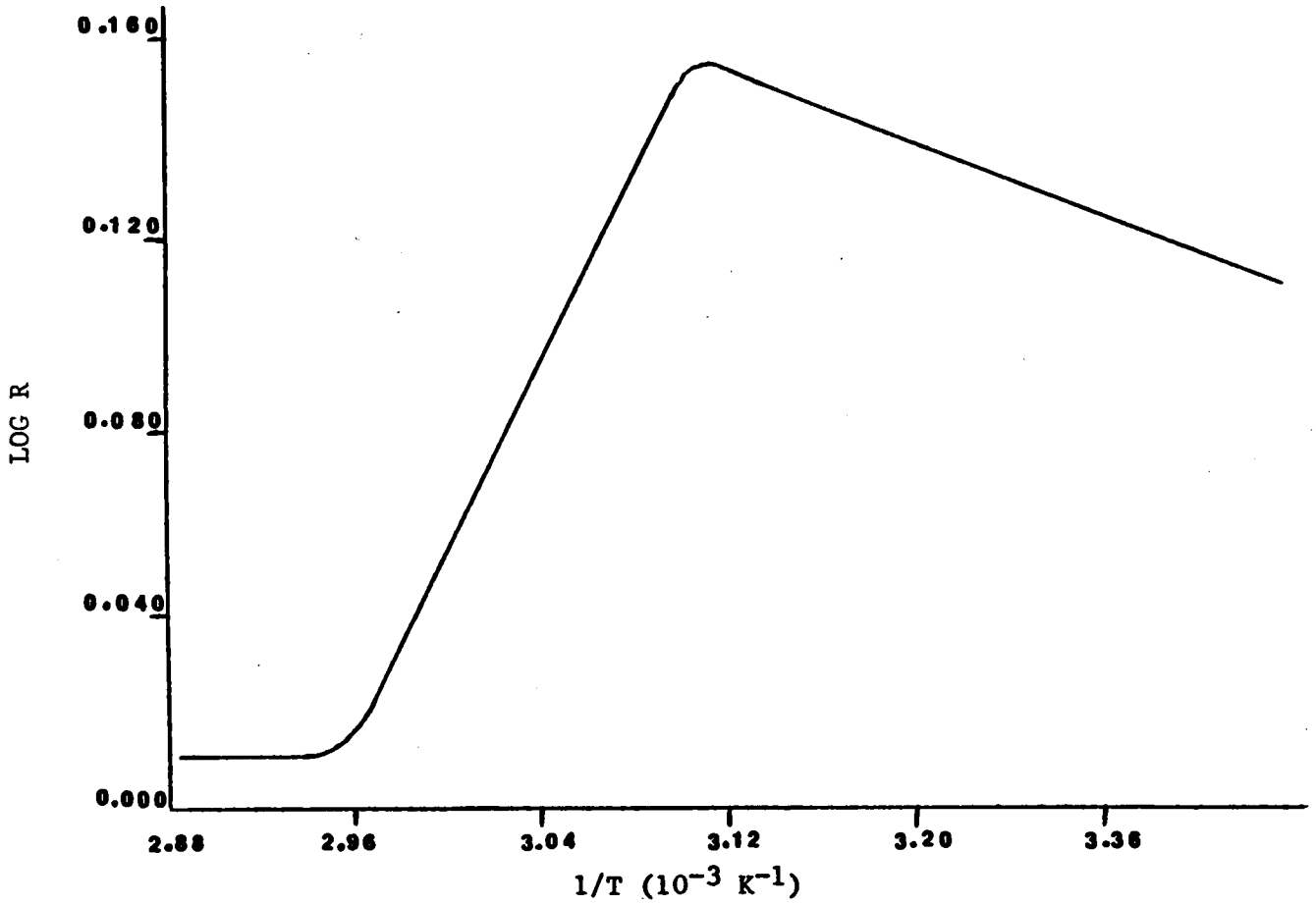


Figure 37. Logarithm of the enhancement ratio of the o-o vibronic transition of pyrene embedded in DSPC liposomes in the presence of 1:20 melittin-to-lipid molar ratio, as a function of 1/temperature.

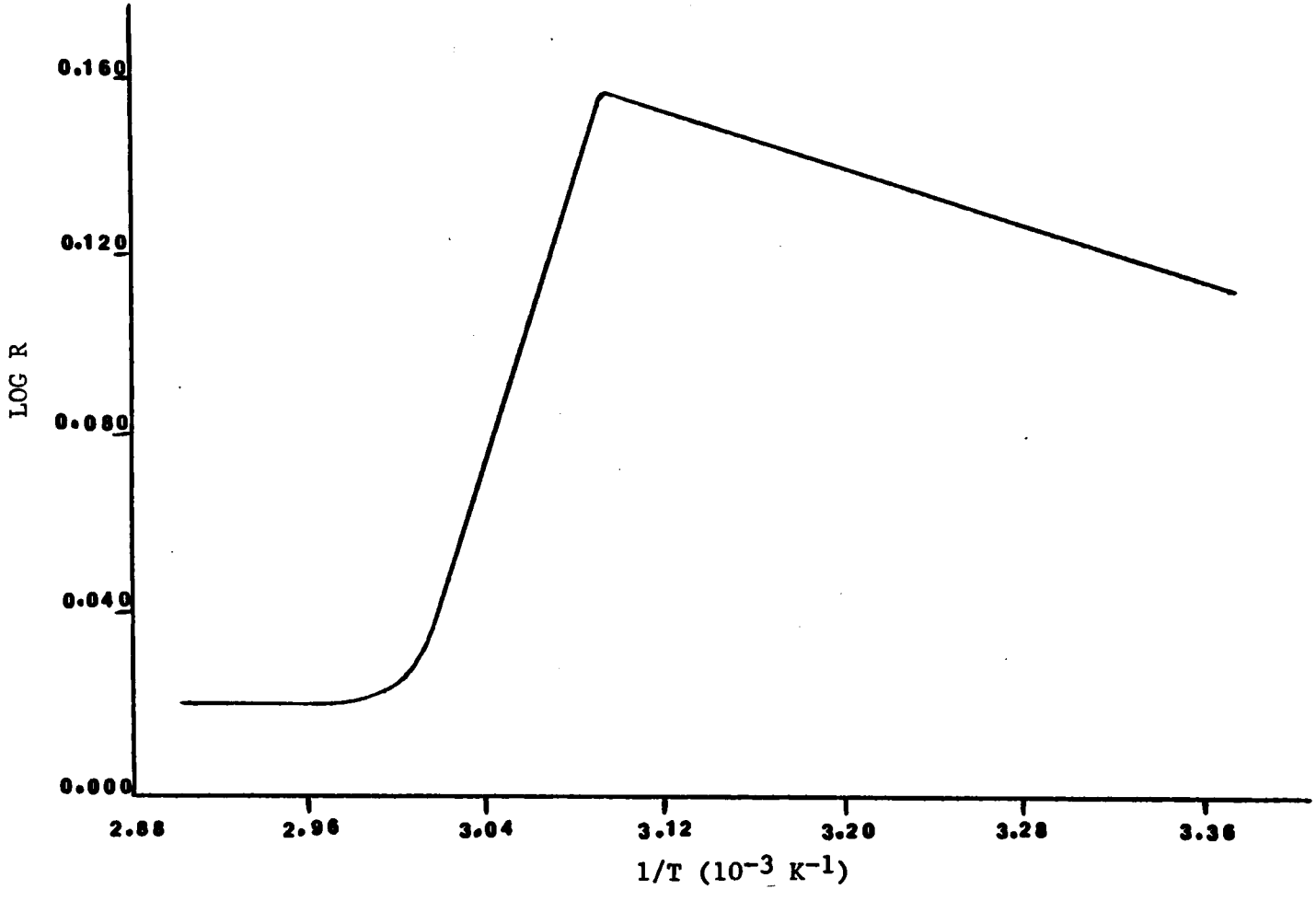


Figure 38. Logarithm of the enhancement ratio of the o-o vibronic transition of pyrene embedded in DSPC liposomes in the presence of 1:10 melittin-to-lipid molar ratio, as a function of 1/temperature.

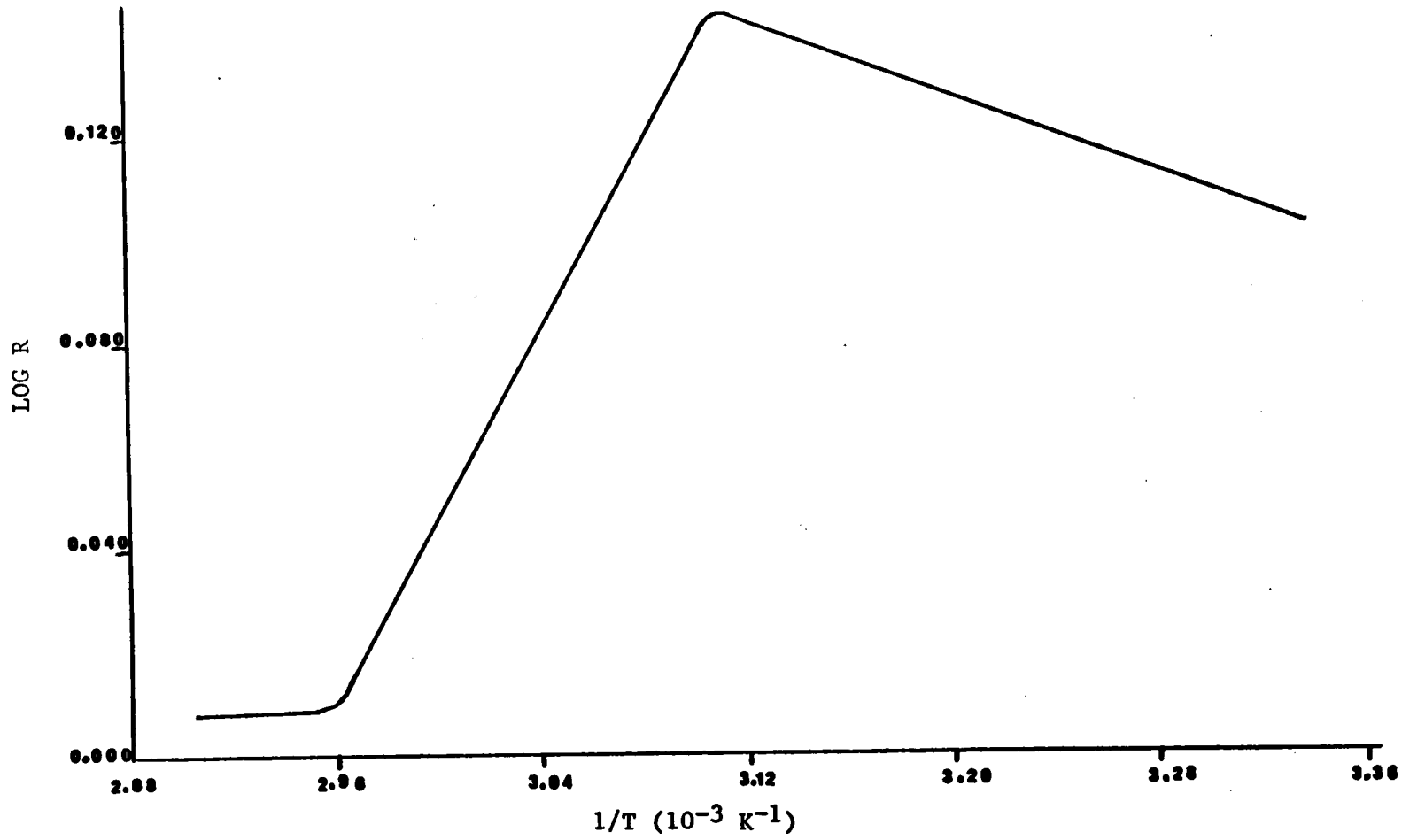


Figure 39. Logarithm of the enhancement ratio of the o-o vibronic transition of pyrene embedded in DSPC liposomes in the presence of 1:5 melittin-to-lipid molar ratio, as a function of 1/temperature.

Table 5. Apparent activation energies obtained from the log R against 1/T plots.*

Molar ratio	Δ E kJ/mol
1:165	0.86
1:20	2.05
1:100	2.12
1:80	2.54
1:40	2.59
1.20	3.79
1:10	2.98
1:5	3.44

*ΔE values for molar ratios smaller than 1:165 were very small.

magnitude of the values of ΔE observed in the present study. Thus melittin may be considered to prevent the formation of thermally-induced structural defects which in its absence aided the penetration of the probe. This interpretation is consistent with the ordering deduced from the observed effects of melittin on the width of the phase transition, and with the immobilization of a spin probe reported by Williams (1972). Alternatively, we may invoke the approach of cluster formation (Freire and Biltonen, 1978). Penetration of solutes according to that framework is aided by an increase in the mismatch between gel and liquid domains as their number increases upon approaching T_t. That model, then, would interpret the effects of melittin as involving a reduction in the probability of formation of such domains.

The effect of melittin apparently becomes effective when T_t is approached where structural defects become more frequent and the fluidity of the bilayer begins to increase. At room temperature, however, as was mentioned above, there is a depression of R up to the molar ratio of 1:80, beyond which R increases toward the value for the free sample. Thus, at temperatures well below T_t, melittin induces some disorder in the lipid. Above T_t, there is virtually no gradient of R, with the level of the plateau being somewhat lower than that for the free sample at high molar ratios, implying again some disordering. We, therefore, conclude that melittin exerts its most pronounced effect as T_t is approached, by increasing the packing density of the glycerol backbone of the bilayer.

The observed increase in the T_t of the bilayer in the presence of melittin (Table 1) is in complete harmony with this interpretation involving structural rearrangements. An alternative interpretation would consider the possibility that the higher T_t reported by the probe in the presence of the protein does not reflect changes in the order and in the fluidity of the bilayer in the vicinity of the glycerol backbone, but instead it reports the melting of a more organized region of the bilayer as sensed by the probe in its new location upon approaching T_t. The magnitude of the observed enhancement, however, would preclude placing the probe very close to the polar head groups; the probe, therefore, should be able to report on the thermal motion of the acyl chains. Experiments are planned involving transfer of excitation energy to determine the actual reduction in the distance between the polar head groups and the probe as T_t is approached.

2. Intramolecular excimer formation by PC_3P

The possibility was considered in the literature (Melnick et al., 1981) that the PC_3P molecules in their ground electronic state may be in a constricted configuration resembling that of the excimer in the bilayer. In order to investigate that possibility, we looked at the fluorescence time-resolved spectra on the ns time scale. Figure 19 shows such spectra for PC_3P at 45°C in the absence of melittin. An interesting conclusion that can be drawn from these results is that the long wavelength emission band of PC_3P is indeed due to an excited-state process with very little contribution from

ground-state complex formation. This inference can be seen from the above Figure at t=o ns (at which the pyrene moieties have a conformation very close to ground-state conformation) which shows that emission at that time at 480 nm is very weak. Interestingly, melittin enhances that emission at t=o ns to some extent (Figs. 20-22) but still the contribution of ground-state complexation is very little. Above T_t, the fraction of excimer-forming PC_3P molecules at t=o ns is even smaller than below T_t (Figs. 23-26). In preleminary measurements we have provided further evidence for the excited-state origin of PC_3P complexation by veryfying the double exponential character of the excimer fluorescence profile as predicted by the kinetic scheme for excimer formation (Birks, 1970).

The following observations regarding the excimer forming properties of PC_3P in DSPC bilayer liposomes in the presence of melittin need to be reconciled and interpreted: (i) the free energy of activation in the crystalline phase is enhanced relative to that in the liquid-crystalline phase; (ii) the entropy of activation in the crystalline phase decreases relative to that in the liquid-crystalline phase; (iii) the width of the transition increases; and (iv) the transition temperature remains practically constant.

As was stated in the Results, for the so-called low temperature limit

$$\frac{q_e}{q_m} = \left(\frac{k_{fe}}{k_{fm}} \right) k_{dm} \tau_{oe}$$

where k_f refers to the radiative rate constant, τ_o to the lifetime of the excimer, k_{dm} to the rate constant for excimer formation and

the subscripts e and m refer to excimer and monomer respectively. If, therefore, the assumption is made that k_{fe}, k_{fm} and τ_{oe} do not change drastically with temperature and upon going from one phase to the other, we can consider the ratio q_e/q_m as being a measure of the rate constant of excimer formation. Preliminary measurements in our laboratory showed that indeed τ_{oe} does not vary very much upon changing the phase of the bilayer. As for the first assumption, it is well established that the radiative rate constant of a wide variety of molecules does not vary strongly with temperature (Birks, 1970). We may, therefore, write by using the Arrhenius equation

$$(q_e/q_m)_{ml} \; / \; (q_e/q_m)_{fr} = \frac{(k_{dm})_{ml}}{(k_{dm})_{fr}} = \frac{A_{ml}}{A_{fr}} \frac{e^{\Delta E_{fr}/RT}}{e^{\Delta Eml/RT}}$$

where the subscripts ml and fr refer to the presence or the absence of melittin, respectively, A is the frequency factor and Δ E the activation energy. Thus for the typical temperature of 40°C in the crystalline phase and a melittin-to-lipid molar ratio of 1:100 we have

$$0.51 = \frac{A_{me}}{A_{fr}} 0.72 \text{ or}$$

$$A_{ml} = 0.71 . A_{fr} .$$

This finding, which is approximately valid for the different molar ratios, implies that $A_{ml} \simeq A_{fr}$. Thus, the frequency factor is not affected appreciably by melittin. Now, according to the transition state theory (Glasstone et al., 1941) the frequency factor is expressed as

$$A = \frac{kT}{h} e^{\Delta S^{\ddagger}/R}$$

where k is Boltzmann's constant, h is Planck's constant, and $\Delta S^{\ddagger}$ is the entropy of activation. Thus

$$\frac{A_{ml}}{A_{fr}} = \frac{e^{\Delta S^{\ddagger}_{ml}/R}}{e^{\Delta S^{\ddagger}_{fr}/R}} \quad \text{or}$$

$$\Delta S^{\ddagger}_{ml} \approx \Delta S^{\ddagger}_{fr} .$$

Therefore, melittin is seen not to affect appreciably the entropy of excimer formation as compared to that in its absence. In other words, the order of the excited-state complex is not very different from that of the two individual moieties from which it originates in the two cases.

Now, above the phase transition, say at 65°C, following the above procedure we have for the same molar ratio of 1:100

$$0.91 = \frac{A_{ml}}{A_{fr}} \frac{e^{\Delta E_{fr}/RT}}{e^{\Delta E_{ml}/RT}} = \frac{A_{ml}}{A_{fr}} \quad 0.059$$

This implies that

$$\frac{A_{ml}}{A_{fr}} = 15.4 = \frac{e^{\Delta S^{\ddagger}_{ml}/R}}{e^{\Delta S^{\ddagger}_{r}/R}}$$

$$\text{or} \quad \Delta S^{\ddagger}_{ml} = \Delta S^{\ddagger}_{fr} + 5.4 \text{ cal/mol.deg}$$

This finding means that melittin induces a large increase in the entropy of excimer formation in the liquid-crystalline phase relative to that in its absence. Thus the order of PC_3P excimers decreases in the presence of the protein. We, therefore, conclude, that the observed decrease in $\Delta S^{\ddagger}_{cr} - \Delta S^{\ddagger}_{fl}$ in the presence of

melittin (Table 4) is due to an increase in $\Delta S^{\ddagger}_{fl}$ in the liquid-crystalline state of the phospholipid. It is of interest to note in this respect that the disordering effect of melittin on liposomes was reported by Sessa et al, (1969), by monitoring the release of solutes and ions.

We now discuss the increase in $\Delta G^{\ddagger}_{cr} - \Delta G^{\ddagger}_{fl}$ in the presence of melittin (Table 4). The above analysis has shown that the excimer is less tightly bound in the liquid-crystalline phase, implying an increase of the fluidity ($1/\eta$, where η is the vicosity) of the environment. In the crystalline phase, however, the protein does not affect appreciably the fluidity. We recall that η is (Glasstone et al 1941)

$$\eta \propto e^{\Delta G^{\ddagger}/RT} .$$

Therefore, a decrease in η implies a decrease in $\Delta G^{\ddagger}$. Thus, $\Delta G^{\ddagger}_{fl}$ is substantially reduced by the presence of melittin. This explains the observed increase in $\Delta G^{\ddagger}_{cr} - \Delta G^{\ddagger}_{fl}$. The observed increase by the protein in the width of the phase transition (Table 4) means that the cooperativity of the lipid has been reduced. That is, the number of lipids that melt at a given temperature has been reduced. Thus, the protein introduces a heterogeneity in the conformations of the bilayer as reported by the PC_3P molecules. In other words, the protein causes a disorder in the bilayer. The above analysis showed that the major effect of the protein occurs in the liquid-crystalline phase in which it disorders the excimer configuration. We, therefore, conclude that the protein exerts its effect on the liquid domains by causing a further disorganization of

the lipid. This inference is in line with that reached from employing pyrene as a fluorescent probe. We saw there that the major increase in the enhancement ratio, R, occurs in the vicinity of T_t at which such domains are being formed.

The large activation energy ΔE_{cr} for excimer formation in the crystalline state as compared to that, ΔE_{fl}, in the liquid-crystalline state (Table 3) implies that the PC_3P molecules are in a less favorable conformation for excimer formation in the former case. Melittin does not appear to affect substantially the PC_3P ground-state conformation in that state, as can be gathered by the fact that ΔE_{cr} is affected only slightly in the presence of the protein. In the liquid-crystalline phase, however, the protein appears to keep PC_3P in a rather unfavorable conformation for excimer formation, as evidenced by the increase in ΔE_{fl}.

We now discuss the fact that PC_3P reports a value of T_t which is higher by about 5°C than that reported by the o-o enhancement of pyrene and by other techniques. In order to answer the question whether the probe reports the T_t of the bilayer distorted by its presence, scattering profiles were obtained in the absence and in the presence of the probe. In both cases a transition temperature of about 50°C was obtained (Fig. 40), implying that the probe does not distort appreciably the bilayer. It is quite plausible that the probe does not penetrate deeply into the bilayer, exhibiting a behavior similar to that of pyrene. In fact, PC_3P, due to its bulky size, may be located further toward the polar head groups which are

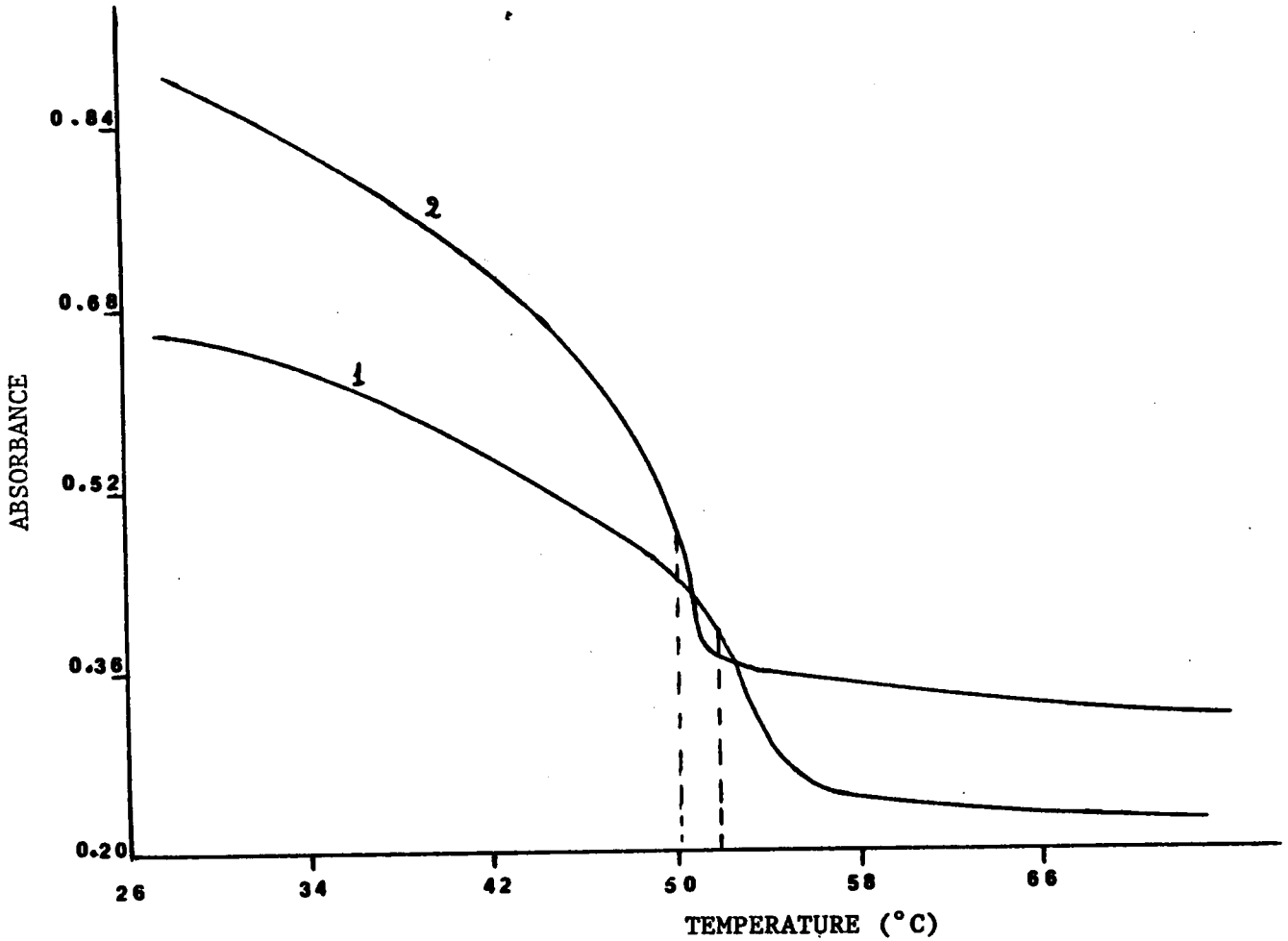


Figure 40. Light scattering measured as absorbance at 360 nm for PC_3P embedded in DSPC liposomes as a function of temperature. (1) In the absence of PC_3P; (2) in the presence of PC_3P.

more highly organized than the acyl chains and which, therefore, presumably melt at a higher temperature. The observed invariance of T_t with the protein-to-lipid molar ratio (Table 4), may simply be an artifact arising from the uncertainty in determining the T_t as a result of the broadness of the transition. A more complex scheme would consider a combination of protein effects on T_t (a raise in T_t, as the pyrene data showed) and a concurrent movement of the probe toward a region of the bilayer possessing a lower fluidity. According to that interpretation, however, one would expect that the activation energy, Δ E, in the equation

$$\frac{q_e}{q_m} \propto A\ e^{-\Delta E/RT}$$

will be changing with the location of the probe and consequently, with T. The very good linearity of the log (q_e/q_m) against 1/T plots, observed in the present work for for all the melittin-to-lipid molar ratios employed, shows that this does not occur and provides evidence against appreciable change in the location of the probe with T.

CHAPTER V

CONCLUSION

The above analysis suggests that melittin induces an increase in the enhancement of the 0-0 vibronic band of pyrene when it is embedded in DSPC liposomes for high melittin-to-lipid molar ratios. Such an increase in the enhancement is taken as meaning that the probe has been dislocated toward the polar head groups as compared with its location in the absence of melittin. This dislocation is the result of structural changes in the liposome, caused by the protein. We could surmise then that the protein reduces the probability of kink formation, which in the absence aids the probe to penetrate into the liposome, and that leads to an increase in the packing density and a decrease in the fluidity of the bilayer. Energy has to be expended in such a dislocation and this is the apparent activation energy which is calculated from the enhancement profiles for the different melittin-to-lipid molar ratios. Melittin seems to be more effective in its ability to cause structural changes in the lipid in the vicinity of the phase transition region.

When PC_3P is embedded in DSPC liposomes its intramolecular excimer-forming ability is affected by the temperature and the presence of the protein. The excimer-to-monomer fluorescence quantum yield, which is a measure of the rate constant of excimer formation, changes with the temperature and the molar ratio. The two aromatic moieties of PC_3P have to overcome a certain potential barrier in

order to approach each other and form the excimer. The activation energy is a measure of this barrier that depends on the lipid phase in which the excimer formation takes place and on the molar ratio in the case of the liquid-crystalline phase. In the crystalline phase the protein seems not to affect substantially the excimer-forming ability of the probe. In the fluid plase it is found to increase the entropy relative to that in its absence which suggests that it causes some disordering of the lipid. So, overall, the protein causes a reduction in the cooperativity of the lipid, or a disorder in it, being more effective in that in the liquid-crystalline phase by acting on the liquid domains which are more abundant there.

In conclusion, the results of the present study reported by both probes show that the protein causes structural changes in the phospholipid that affect its fluidity, being more effective in that respect in the vicinity of the phase transition of the phospholipid.

LIST OF REFERENCES

LIST OF REFERENCES

1. Avouris, P., Kordas, J. and El-Bayoumi, M. (1976) Chem. Phys. Lett. 26, 373.

2. Azzi, A. (1975) Quar. Rev. Biophysics 8, 237.

3. Badea, M. G. and Georghiou, S. (1976) Rev. Sci. Instrum. 47, 314.

4. Birks, J. B. (1970) Photophysics of Aromatic Molecules, John Wiley, New York.

5. Chandross, E. A. and Dempster, C. G. (1970) J. Amer. Soc. 92, 3586.

6. Dawson, C. R., Drake, A. F., Helliwell, J. and Hider, R. C. (1978) Biochim. Biophys. Acta 510, 75.

7. Dorrance, R. C. and Hunter, T. F. (1977) J. Chem. Soc. 73, 1891.

8. Drake, A., Fimer, E. G., Flook, A. G. and Phillips, M. C. (1972) J. Mol. Biol. 63, 265.

9. Dufourcq, J. and Faucon, J. F. (1977) Biochim. Biophys. Acta 467, 1.

10. Eftink, M. R. and Ghiron, C. A. (1976) Proc. Nat. Acad. Sci. U.S. 15, 672.

11. Fischoff, S. and Vanderkooi, J. M. (1975) J. Gen. Physiol. 65, 1975.

12. Freire, E. and Biltonen, R. (1978) Biochim. Biophys. Acta 514, 54.

13. Gaber, B. F. and Peticolas, W. L. (1977) Biochim. Biophys. Acta 465, 260.

14. Galla, H. J. and Sackmann, E. (1974) Biochim. Biophys. Acta 339, 103.

15. Galla, H. J. and Sackmann, E. (1975) J. Am. Chem. Soc. 97, 4114.

16. Georghiou, S. and Mukhopadhyay, A. K. (1981) Biochim. Biophys. Acta 645, 365.

17. Georghiou, S., Thompson, M. and Mukhopadhyay, A. K. (1982a) Third Biophysical Discussion on Protein-Lipid Interactions in Membranes 37, 159.

18. Georghiou, S., Thompson, M. and Mukhopadhyay, A. K. (1982b). Biochim. Biophys. Acta, in press.

19. Georgescauld, D., Desmasez, J. P., Lapouyade, R., Babeau, A., Richard, H. and Winnik, M. (1979) Photochem. Photobiol. 31, 539.

20. Glasstone, S., Laidler, K. J. and Eyring, H. (1941) The Theory of Rate Processes, Mc. Graw-Hill, New York.

21. Goldenberg, M., Emert, J. and Morawetz, H. (1978) J. Amer. Soc. 100, 7171.

22. Habermann, E. (1972) Science 177, 314.

23. Hamilton, T. D. S. and Naqvi, K. R. (1968) Chem. Phys. Lett. 2, 376.

24. Lavialle, F., Levin, I. W. and Mollay, C. (1980) Biochim. Biophy. Acta 600, 62.

25. Lee, A. G., Birdsall, N. J., Metcalfe, J. C., Warren, G. B. and Roberts, G. C. (1976) Proc. Roy. Soc. (London) 193, 253.

26. Lentz, B. R., Barenholz, Y. and Thompson, T. E. (1976) Biochemistry 15, 4521.

27. Lianos, P. and Georghiou, S. (1979) Photochem. Photobiol. 29, 843.

28. Lianos, P., Mukhopadhyay, A. K. and Georghiou, S. (1980) Photochem. Photobiol. 32, 415.

29. Melnick, R., Haspel, H. Goldenberg, M., Greenbaum, L. and Weinstein. S. (1981) Biophys. J. 34, 499.

30. Mollay, C. and Kreil, G. (1974) FEBS Lett. 46, 141.

31. Mollay, C., Kreil, G. and Berger, H. (1976) Biochim. Biophys. Acta 426, 317.

32. Mollay, C. and Kreil, G. (1973) Biochim. Biophys. Acta 316, 196.

33. Nakajima, A. (1971) Bull. Chem. Soc. J pn 44, 3272.

34. Pimentel, G. C. (1957) J. Am. Chem. Soc. 79, 3323.

35. Schryver, F. C. D., Boene, N. and Put, J. (1977) in Advances in Photochemistry 10, p. 359, Interscience - Wiley, New York.

36. Sessa, G., Freer, J. H., Collaccio, G. and Weismann, G. (1969) J. Biol. Chem. 244, 3579.

37. Shipolini, R., Callewaert, G., Cottrell, R., Dooman, S., Vernon, C. and Banks, B. (1971) Eur. J. Biochem. 20, 459.

38. Singer, S. J. and Nicolson, G. L. (1972) Science 175, 720.

39. Suurkuust, J., Lentz, B. R., Barenholtz, Y., Biltonen, R. and Thompson, T. E. (1976) Biochemistry 15, 1393.

40. Trauble, H. (1971) J. Membrane Biol. 4, 193.

41. Turro, N. J., Aikawa, M. and Yekta, A. (1979) J. Am. Chem. Soc. 101, 772.

42. Vanderkooi, J. M., Callis, J. and Chamce B. (1974) Histochem. J. 6, 301.

43. Vanderkooi, J. M. and Callis, J. B. (1974) Biochemistry 13, 4000.

44. Verma, S. P. and Wallach, D. F. H. (1976) Biochim. Biophys. Acta 426, 616.

45. Verma, S. P., Wallach, D. F. H. and Smith, I. C. P. (1974) Biochem. Biophys. Acta 345, 129.

46. Williams, J. C. and Bell, R. M. (1972) Biochim. Biophys. Acta 288, 255.

47. Yguerabide, J. and Foster, M. C. (1981) Molecular Biology, Biochemistry and Biophysics 31, 199.

48. Yunes, R., Goldhammer, A. R., Garner, W. K. and Cordes, E. H. (1977) Arch. Biochem. Biophys. 183, 105.

49. Zachariasse, K. A., Kuhnle, W. and Weller, A. (1978) Chem. Phys. Lett. 59, 379.

50. Zachariasse, K. and Kuhnle, W. (1975) Zeits. Phys. Chem. News Folge 101, 267.

51. Zachariasse, K. A., Kuhnle, W. and Weller, A. (1980) Chem. Phys. Lett. 73, 6.

VITA

George N. Georgiades was born in Kyrenia, Cyprus, on the 13th of November, 1938. He attended elementary school and high school in Kyrenia. In 1957 he moved to Athens, Greece, where he took university courses in the Department of Physics of the Athen's University. He graduated in 1962. Then, he went back to Cyprus where he was teaching physics and Chemistry in high school in Nicosia until 1968. At that year, he received a scholarship by the Cyprus's Government and went back to Athens where for two years took courses on Education and Problems on Teaching. He, then, went back to Cyprus where he continued teaching physics in high school until 1980. In 1980 he was admitted to the Graduate School of the University of Tennessee and was awarded a Teaching Assistantship in the Department of Physics. He worked in the Laboratory of Biophysics and Chemical Physics under the supervision of Dr. S. Georghiou. He received his Master's degree with a major in Physics in August 1982.